University of Calgary

PRISM Repository **https://prism.ucalgary.ca**

The Vault Open Theses and Dissertations

2014-03-13

Geochemical and Isotopic Investigations of Lake Sediments From the Athabasca Oil Sands Region

Stanners, Fiona Mary

Stanners, F. M. (2014). Geochemical and Isotopic Investigations of Lake Sediments From the Athabasca Oil Sands Region (Master's thesis, University of Calgary, Calgary, Canada). Retrieved from https://prism.ucalgary.ca. doi:10.11575/PRISM/26277

http://hdl.handle.net/11023/1388

Downloaded from PRISM Repository, University of Calgary

UNIVERSITY OF CALGARY

Geochemical and Isotopic Investigations of Lake Sediments From the Athabasca Oil Sands Region

by

Fiona Mary Stanners

A THESIS

SUBMITTED TO THE FACULTY OF GRADUATE STUDIES

IN PARTIAL FULFILLMENT OF THE REQUIREMENT FOR THE

DEGREE OF MASTER OF SCIENCE

DEPARTMENT OF GEOSCIENCE

CALGARY, ALBERTA

February, 2014

© Fiona Stanners 2014

Abstract

The Athabasca oil sands region (AOSR) is one of the largest unconventional oil reserves globally, and is projected to become increasingly important as conventional oil resources are depleted. This has lead to increasing concerns about the impact of industrial emissions on surrounding ecosystems.

Four sediment cores from three lakes in northeastern Alberta and northwestern Saskatchewan were analyzed to assess the type and quantity of organic matter (OM) in sediments, and whether there had been any impact from industrial emissions originating in the AOSR on lake sediment geochemistry.

Analyses showed that sediments in all three lakes are organic-rich, and the OM is dominantly derived from authochthonous primary production of phytoplankton and bacteria. Stable N and S isotope analyses of sediments, deposited between 1850 and 2010 showed no clear impact from industrial emissions in the AOSR.

Acknowledgements

I have many people to thank for their input and support in the completion of this MSc thesis. First must be my supervisors, Dr. Bernhard Mayer and Dr. Hamed Sanei, whose insights and guidance throughout every stage of the project were integral to its success. Many thanks to the members of the Applied Geochemistry Group and to the staff of the Isotope Science Laboratory and the Geological Survey of Canada laboratory, in particular Jesusa Overend-Pontoy and Steve Taylor. I thank the researchers involved in the CORES project for providing my samples, and graciously offering me their insights on my data. In particular, thanks to Dr. Jason Ahad and Dr. Jesse Carrie; your patience with my unending emails and questions is greatly appreciated! I am grateful for the financial support provided by the AGG, the RAP bursary from the GSC, and the Graduate Studies Faculties and the Geoscience Department of the University of Calgary.

To the family and friends who graciously lent an ear whenever I needed to rant, or provided a hug when I needed one of those, thank you, thank you. Chris, I couldn't have asked for a better comrade-in-arms with whom to tackle this whole graduate research business. Mike, your jokes keep me smiling and your faith in me keeps me motivated. Jess, thank you for your contributions to maintaining my sanity; the sushi dates are much appreciated. Love you all.

Dedication

I dedicate this thesis to my parents, Duncan and Jan. You have inspired me to keep learning, and to keep working hard. I can't imagine where I would be without your unending love, patience and support.

Table of Contents

List of Abbreviations

AIR – atmospheric air, international reference standard for stable N isotopes

ALE – Alberta Lake E, sampled for this study. ALE1 refers to the core collected from ALE

AOSR – Athabasca oil sands region

AVS – acid-volatile sulfur (sulfur fraction)

BBL – billion barrels

BSR – bacterial sulfate reduction

CDT – Canyon Diablo troilite, international reference standard for stable S isotopes

CRS – chromium reducible sulfur (sulfur fraction)

DIC – dissolved inorganic carbon

GSC – Geological Survey of Canada

HI – hydrogen index (Rock-Eval)

MinC – mineral carbon (Rock-Eval)

OIRE6 – oxygen index by Rock-Eval 6 (Rock-Eval)

OM – organic matter

PC – pyrolysable carbon (Rock-Eval)

PDB – Peedee belemnite, international reference standard for stable C isotopes

RC – residual carbon (Rock-Eval)

RSD – relative standard deviation, reported in %, equal to ((S.D./mean)*100)

S1, S2 (S2a, S2b), S3 – fractions of OM determined by pyrolysis (Rock-Eval)

SL10M – Saskatchewan Lake 10M, sampled for this study. SL10M1 refers to the core collected from SL10M

SL10W – Saskatchewan Lake 10W, sampled for this study. SL10W1 and SL10W2 refer to the cores collected from SL10W

S_{org} – organic sulfur (sulfur fraction)

TOC – total organic carbon (Rock-Eval)

Tmax – temperature of “peak” of S2 fraction produced by pyrolysis (Rock-Eval)

WCSB – Western Canadian Sedimentary Basin

List of Tables

List of Figures

CHAPTER ONE: INTRODUCTION

Canada possesses the third largest proven reserves of crude oil in the world following Saudi Arabia and Venezuela (Alberta Energy, 2013a). Of these reserves, 98% are located in Alberta, consisting of an estimated 1800 billion barrels in-situ; approximately 170 billion barrels contained in unconventional (heavy; gravity <10 API) oil sands deposits and 1.5 billion barrels of conventional oil (Alberta Energy, 2013a; Alberta Government, 2013a). Alberta's oil sands are currently producing from three regions; largest to smallest, these are Athabasca, Cold Lake and Peace River (Figure 1.1) (Alberta Government, 2013a; ERCB, 2013).

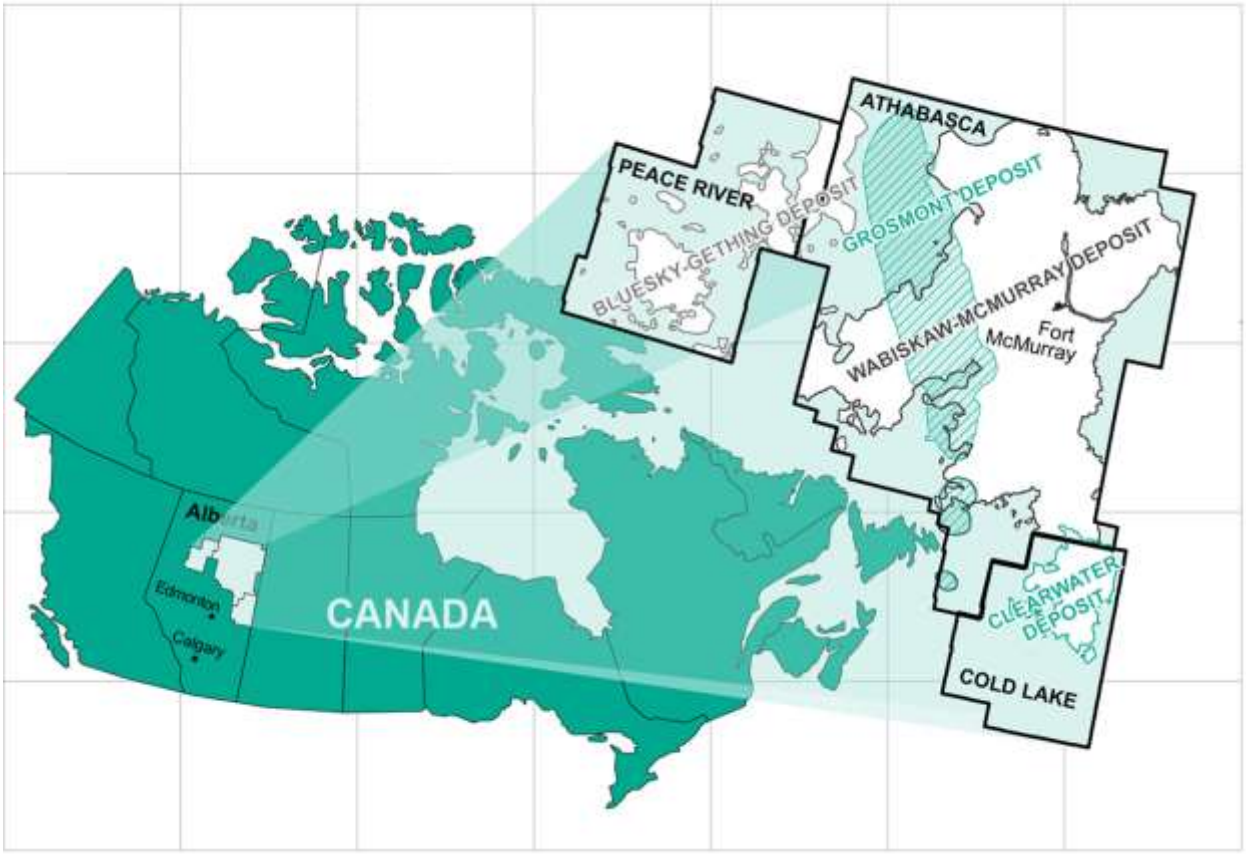

Figure 1.1: Map of the locations of major Alberta oil sands deposits, including the Athabasca Oil Sands Region. Formation names refer to the producing formation in each of the major oil sands areas: Peace River, Athabasca and Cold Lake (modified from ERCB, 2013).

1.1 Alberta's Oil Sands: History, and Environmental Concerns

The first oil sands project initiated/operated by Suncor began production in 1967 at a rate of ~45000 barrels per day (Suncor, 2013). Since that time, the rate of production from all projects extracting crude bitumen from Alberta's oil sands deposits has increased nearly continuously to nearly 2 million barrels per day in 2012 (Figure 1.2) and is projected to increase to a rate of over 3.5 million barrels per day by 2021 (ERCB, 2013). In January of 2013, there were 127 projects operating in the Alberta oil sands. Of these, five extract bitumen from shallow deposits by mining while the remainder use in-situ technologies eg. cyclic steam stimulation (CSS) or steam-assisted gravity drainage (SAGD), where oil sands deposits are too deeply buried for mining (Alberta Energy, 2013b). It is estimated that 133 billion dollars were invested in oil sands development between 2001 and 2011, and given the projected increase in oil sands development and production in the future, it is clear that this resource is of considerable importance to the province of Alberta, and to Canada's present and future economy (Alberta Government, 2013a; ERCB, 2013).

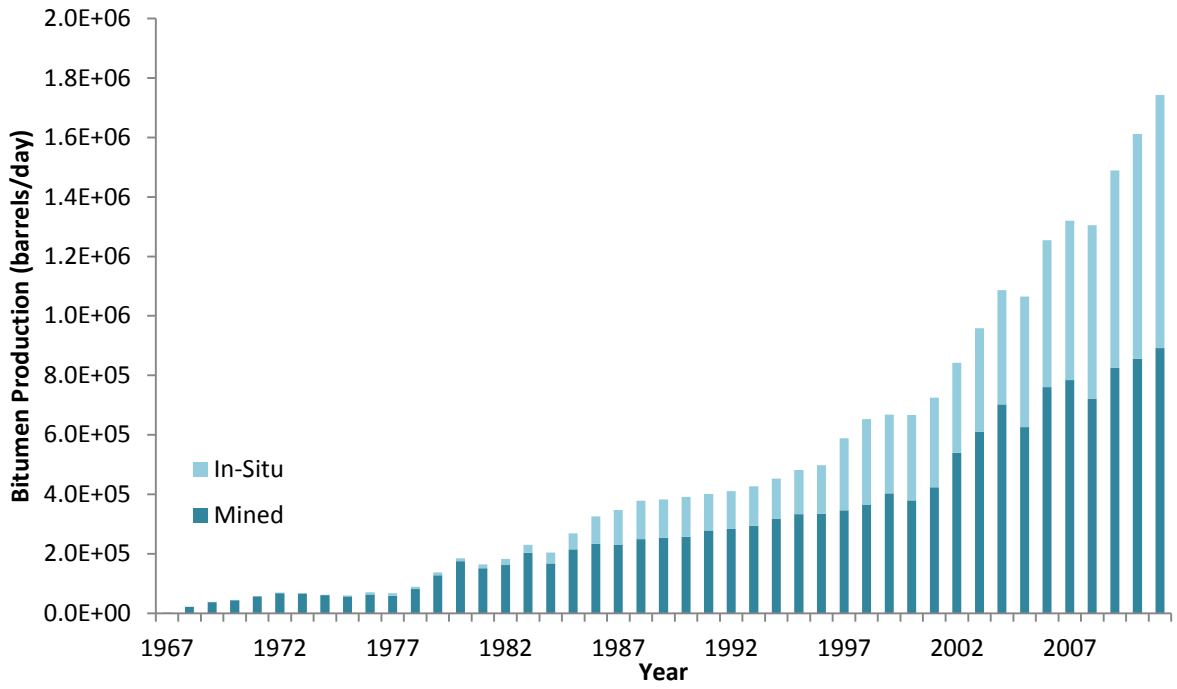

Figure 1.2: Increasing production of bitumen by mining and in-situ production from Alberta's oil sands deposits from 1967 to 2011 (compiled from ERCB, 2013).

Bitumen extracted from the Alberta oil sands undergoes treatment referred to as upgrading, which adds hydrogen and removes contaminants including heavy metals, salt, oxygen, nitrogen and sulfur in order to convert crude bitumen into more valuable and more easily-refined synthetic crude (Alberta Energy, 2013c). Production processes, including mining and upgrading in the oil sands region, emit a number of substances to the atmosphere which are of concern in terms of health and environmental impact. These include greenhouse gases, ozone, fine particulate matter, NO_x, SO_2 and H_2S. Therefore, air quality in the area is now monitored constantly (Alberta Government, 2013c). Recent scientific studies have traced the fate and impact of emissions of these and other contaminants (metals, PAHs) in surrounding ecosystems. Scientific studies thus far have investigated atmospheric deposition of NO_3^-, NH_4^+ and SO_4^{2-} (Proemse et al., 2013) as well as N and S deposition and uptake in a variety of

receptors including lichens (Proemse and Mayer, 2013; Landis et al., 2013), conifer needles (Jaques and Legge, 2013; Proemse and Mayer, 2013), and rivers (Kelly et al., 2009).

Polycyclic aromatic hydrocarbons (PAHs) are a class of compounds which are produced by incomplete combustion of materials such as coal, oil, garbage and lumber (Nagpal, 1993). PAHs may be naturally-occurring as a result of forest fires, or they may have an anthropogenic origin such as from smelters, combustion of coal or other fossil fuels (Nagpal, 1993). Prolonged exposure to certain PAHs is associated with increased risk of cancer in animals and in humans (ATSDR, 2011). Thus the accumulation of PAHs in air, water and soil is understandably concerning and should be monitored in the vicinity of emission sources. It has been shown that development of the oil sands has released PAHs into the Athabasca River via loading of the snowpack with airborne PAH compounds (Kelly et al., 2009). Kurek et al. (2012) measured levels of PAHs in six lakes surrounding the Athabasca oil sands region, including Namur Lake, located 90km from the site of oil sands development (Figure 1.3). Kurek et al. (2012) found that PAH concentrations and fluxes in sediments in all six lakes had increased markedly, since development of the Alberta Oil Sands began in 1967. These lakes showed recent (post-2010) concentrations of PAHs in the lake sediments of 1000 to 10000μg/kg; an increase from pre-1970 concentrations of generally less than 1000μg/kg (Kurek et al., 2012). A study of lakes in the United States from 1970 to 2001 (Van Metre and Mahler, 2005) reported mean values of PAHs in lake sediments in heavily urbanized areas of around 9000μg/kg and lightly urbanized areas of around 700μg/kg compared to concentrations of around 300μg/kg in “reference” lakes, taken to represent background concentrations of PAHs. While Kurek et al. (2012) noted that populations of zooplankton had yet to be conclusively impacted by increased levels of PAH loading in lakes relative to pre-developmental levels, the study called for more rigorous studies to establish background PAH concentrations in lake sediments, and for future monitoring to assess the impact of PAH and other emissions derived from oil sands development.

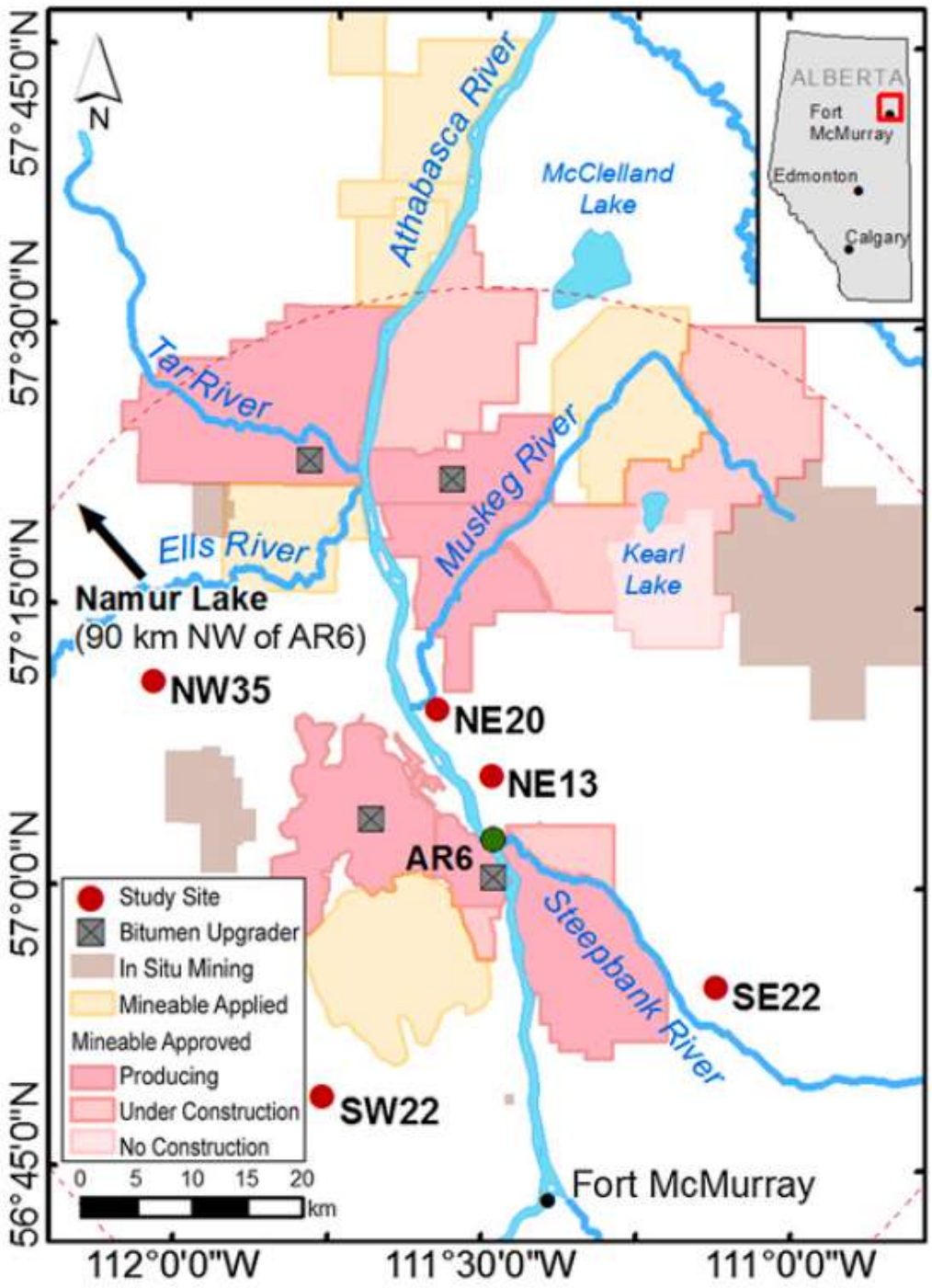

Figure 1.3: Study sites used by Kurek et al. (2012) for analysis of PAH contents of lake sediments from 1967 to 2011 (from Kurek et al., 2012).

Another recent scientific study by Jautzy et al. (2013) used PAHs in lake sediments from two lakes (Figure 1.4), one of which was also analyzed in this study (ALE), to evaluate the impact of airborne contaminants from mining operations in the AOSR on surrounding boreal ecosystems. Although concentrations of PAHs were below the government-defined guidelines, the study reported a marked increase in PAH fluxes over the last 10-15 years, postulated to be a result of increasing levels of anthropogenic activity in the region related to bitumen mining. Analyses of $\delta^{13}C$ values of individual PAH compounds indicated that the observed increases in PAH fluxes in sediments from both lakes resulted from contributions of petroleum-generated PAHs rather than from natural sources.

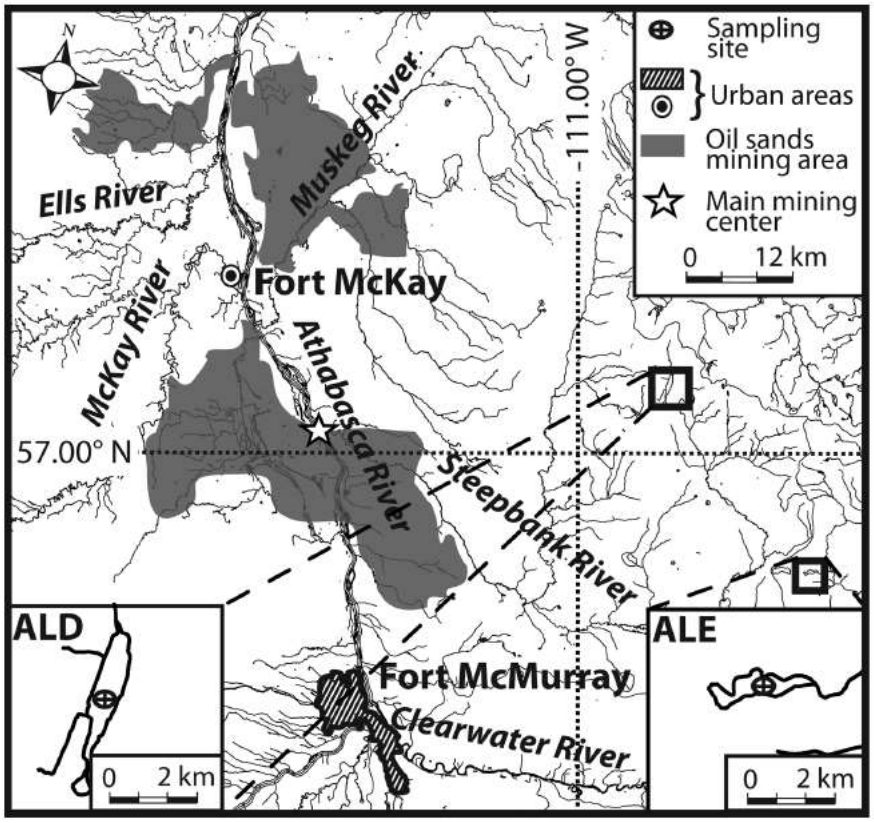

Figure 1.4: Study sites used by Jautzy et al. (2013) for analysis of PAH contents of lake sediments from ~1920 to 2011 (from Jautzy et al., 2013).

Increases in N and S contents of lakes and lake sediments outside the AOSR resulting from contamination by anthropogenic activities have been documented (Mayer et al., 2007; Allen, 2004; Smith et al., 1999; Vitousek et al., 1997), and negative impacts on lake ecosystems as a result of anthropogenic loading of N and S have also been reported. Input of excess quantities of reactive nitrogen may result in eutrophication (Smith et al., 1999), while another concern related to anthropogenic emissions of S and N is acidification of lakes through acid rain (Vitousek et al., 1997; Battarbee et al., 1990). Acid rain may also have adverse effects on terrestrial ecosystems (Allen, 2004).

Monitoring of concentrations of N and S-containing gases in the atmosphere has been conducted at a variety of sites around Alberta since 1986. While there is no apparent increase in either NO_x or SO_2 reflected in data gathered from a variety of monitoring stations around the AOSR (Figure 1.5), a 2008 report by Alberta Environment asserts that atmospheric concentrations of NO_x (Figure 1.6) and SO_x, including SO_2 (Figure 1.7) derived from oil sands activities are increasing as a result of increasing development, and are projected to keep on increasing through 2015 (Alberta Environment, 2008). This report apportioned the annual industrial emissions of atmospheric NO_x and SO_2 to various industries around Alberta, and indicated that oil sands development is currently and will continue to be a significant contributor of NO_x and SO_2 to the atmosphere (Figure 1.6, Figure 1.7).

Relative to an average concentration of SO_2 in the air of 1.3 ppb over all sampled intervals from all the above-mentioned sampling sites around the AOSR, remote locations have ambient concentrations between 0.01 and 0.12 ppb (Treissman et al., 2003; Harrison, 1990), while urban areas of Canada have ambient concentrations ranging from 1 to 10 ppb (CASA, 2003). Concentrations of NO_x averaged 13.0 ppb over all sampled intervals from all the above-mentioned sampling sites around the AOSR, relative to concentrations of around 0.2 ppb measured in the air at remote sites (Kelly et al.,

1980) and concentrations averaging around 100 ppb in urban areas (Houston) (Zhang et al., 2004). Studies of both remote and urban areas noted significant diurnal variations in concentrations of NO_x.

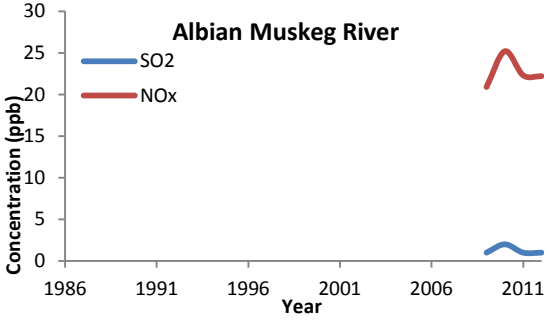
Albian Muskeg River
SO2
NOx
Concentration (ppb)
Year
0
5
10
15
20
25
30
1986
1991
1996
2001
2006
2011

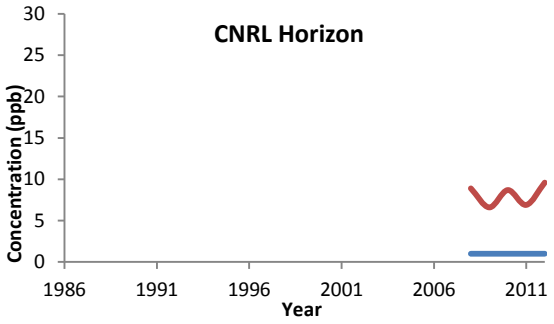
CNRL Horizon
Concentration (ppb)
Year
0
5
10
15
20
25
30
1986
1991
1996
2001
2006
2011

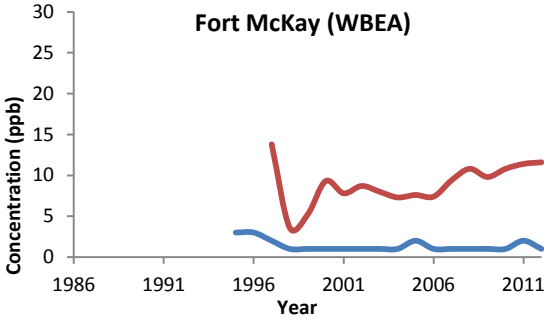
Fort McKay (WBEA)
Concentration (ppb)
Year
0
5
10
15
20
25
30
1986
1991
1996
2001
2006
2011


CNRL Horizon
Albian Muskeg River
Fort McKay (WBEA)
Syncrude UE
Syncrude Upgrader
ALE
Fort McMurray-
Athabasca River
AB
SK
SL10W
SL10M

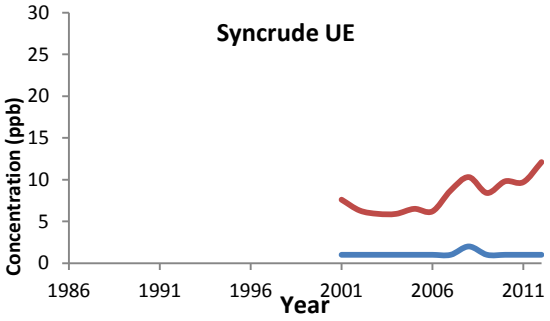
Syncrude UE
Concentration (ppb)
Year
0
5
10
15
20
25
30
1986
1991
1996
2001
2006
2011

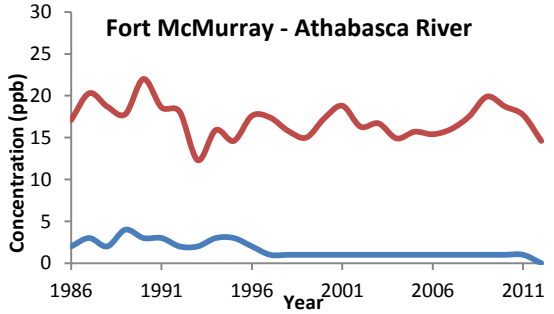
Fort McMurray - Athabasca River
Concentration (ppb)
Year
0
5
10
15
20
25
30
1986
1991
1996
2001
2006
2011

Figure 1.5: Average annual concentrations of SO_2 and NO_x measured at various monitoring stations around the AOSR. Lake study site locations for this study and the location of the upgrader taken to represent the "center" of the industrial emissions are included for reference (compiled from data accessed from the CASA Data Warehouse, 2013).

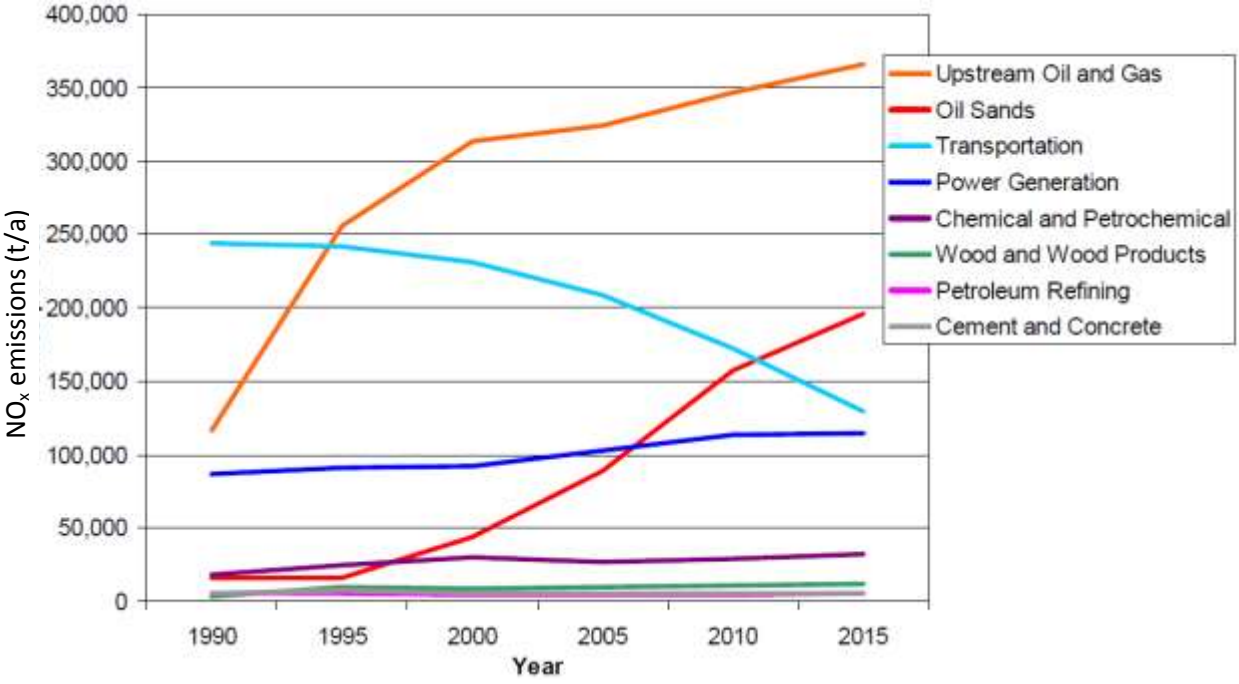

Figure 1.6: Alberta NO_x emissions attributed to various industrial sources from 1990, projected to 2015 (from Alberta Environment, 2008).

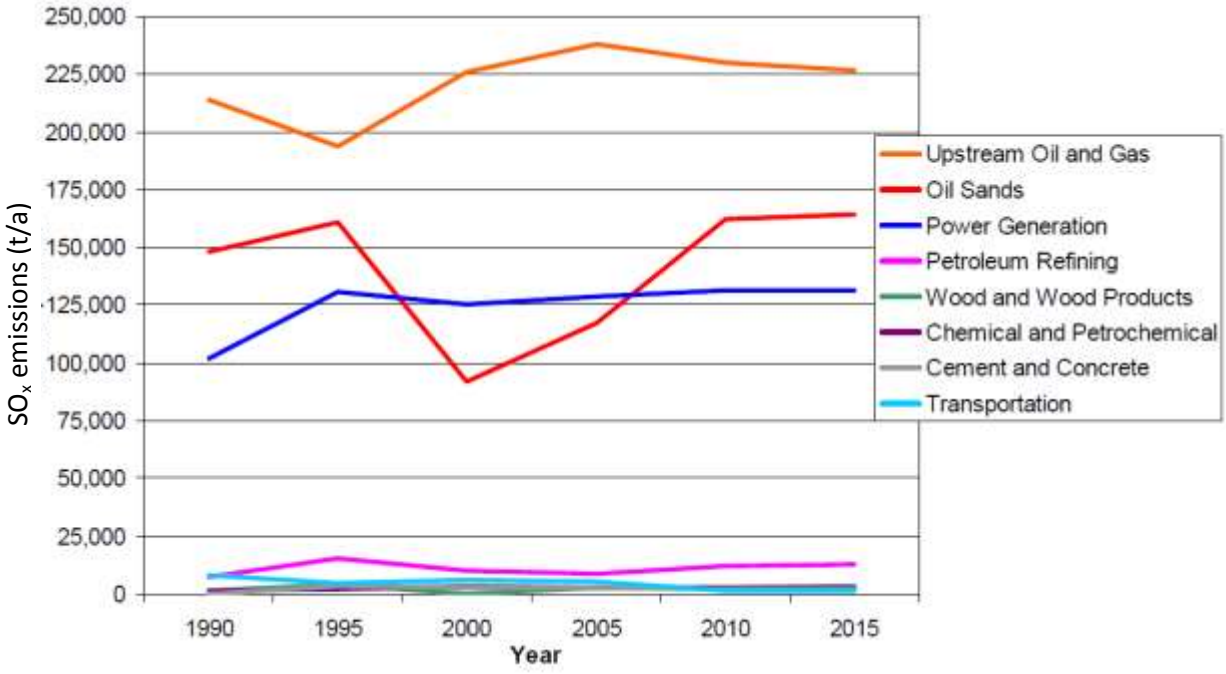

Figure 1.7: Alberta SO_x emissions attributed to various industrial sources from 1990, projected to 2015. Decrease in oil sands emissions between 1995 and 2010 is attributed to the development of sulfur-capture technology (from Alberta Environment, 2008).

Stable isotopes have previously been used to trace anthropogenic input of nitrogen and sulfur to lakes in other parts of the world. A coherent decrease in $\delta^{15}N$ of total N of ~1 to 5‰ was observed in a variety of sediment cores from remote lakes throughout the northern hemisphere (Holtgrieve et al., 2011). The trend appears to have begun around the year 1900, and was postulated to have been a result of the addition of reactive nitrogen to the atmosphere by emissions derived from the burning of fossil fuels which occurred with industrialization (Holtgrieve et al., 2011). A study of lake sediments in the vicinity of a Quebec smelter by Mayer et al. (2007), reported a decrease in $\delta^{34}S$ in sediments deposited after the start-up of the smelter. It was suggested that the trend resulted from the release of anthropogenically-derived SO_2 into the atmosphere during smelting which contributed to an increase in

the concentration of SO_4^{2-} in lake water. The increase in the amount of available dissolved S resulted in enhanced isotope fractionation effects during sulfate reduction by sulfur-reducing bacteria (SRB), which caused a preferential accumulation of ^{32}S in the sediments and resulted in the decreasing trend in $\delta^{34}S$ observed in sediments deposited after the start-up of smelting operations in the area. Prior to this study of three Alberta and Saskatchewan lakes, stable isotope techniques using N and S had been used for tracing N and S emissions from source to sink in forests and soils, but not in lake sediments.

Proemse and Mayer (2013) characterized the isotopic compositions of N and S compounds emitted from stacks in the AOSR and in atmospheric deposition in their vicinity. The study made the following conclusions about the potential use of stable isotopes as tracers in the AOSR:

1) Although deposition rates of sulfate in the vicinity of the AOSR are elevated relative to background rates, the isotopic signature of sulfur in SO_4^{2-}deposited close to operations in the AOSR was not distinct from the background values of atmospheric deposition, and thus does not constitute an appropriate tracer of S in industrial emissions.
2) Deposition rates of both NO_3^- and NH_4^+ are elevated relative to background rates near the main industrial emitters in the AOSR (<30km). Nitrogen stable isotope values ($\delta^{15}N$) were variable but tended to be more ^{15}N enriched in deposition in the vicinity of industrial operations versus more distant sites representing “background” deposition, and could potentially be used as a qualitative tracer for NO_3^- and NH_4^+ emitted from industrial sources.
3) $\Delta^{17}O$ and $\delta^{18}O$ values in NO_3^- and $\delta^{18}O$ values in SO_4^{2-}were isotopically distinct from those representing background atmospheric deposition, and could be used as quantitative tracers for elucidating the fate of NO_3^- and SO_4^{2-} derived from industrial emissions in the AOSR.

1.2 Study Objectives

Given that stable isotope techniques using N and S have successfully been used elsewhere in lake sediments to assess impact from industrial emissions, and given that emissions from the AOSR have been isotopically characterized, the overall purpose of this study was to determine whether there is any evidence for impact of industrial emissions in the contents and isotopic compositions of N and S in lake sediments of lakes at various distances from the main industrial emission sources in the AOSR.

To attain this goal, sediment cores from three different lakes located at distances between 97 and 143km from the main anthropogenic emission sources were analyzed to pursue the following sub-objectives:

1) Test whether lake sediment deposits are analogous among the three lakes, using organic petrology, geochemical parameters and stable isotope analyses;
2) Determine the temporal distribution of sediment in the core to determine whether segments deposited prior to the onset of industrial activity and after are sufficiently represented to assess anthropogenic impact;
3) Compare and contrast pre and post-industrial signals in the contents and isotope values of N and S to test for impact from industrial emissions.

CHAPTER TWO: BACKGROUND

2.1 Lake Sediment Constituents

Lake sediment components fall into one of three categories based on their origins, as proposed by Schnurrenberger et al. (2003). These are:

1. Clastic sediment, composed of transported mineral/rock grains
2. Chemical sediment, composed of inorganic minerals precipitated from the water column during or after deposition
3. Biogenic sediment, which refers to particles with a biological origin

Clastic sediments include clay, silt and sand particles. Chemical sediment includes evaporites, carbonate precipitates such as calcite or siderite or authigenic pyrites. Biogenic sediment is the class which is of primary interest in this study; this class comprises any components which are original parts of organisms' (plant or animal) "bodies" including fossiliferous material, carbonaceous debris derived from allochthonous plant matter which is washed into the lake, and from autochthonous production by aquatic macrophytes, phytoplankton, or bacterial mats.

Components of sediments may be separated physically or chemically for analysis, depending upon the particular goals of a study.

Because aquatic sediments accumulate chronologically and are less subject to erosion relative to terrestrially-deposited sediment sequences, these can preserve records of proxies relating to past climatic or environmental conditions, changes and events (Meyers, 1997; Frey, 1988). The study of lake sediments in order to reconstruct the historical ecological systems in which the lakes exist is called palaeolimnology. Dated lake sediments may be analyzed for a variety of parameters, which can be interpreted to characterize the climate and ecological conditions under which these sediments were deposited. Studies of trace elements, have been used to establish the fate of anthropogenically-derived

contaminants around industrial sites (eg. Mayer et al., 2007; Donahue et al., 2006; Sanei et al., 2000; Carignan et al., 1994). Stable isotope and geochemical studies of organic matter and biomarkers preserved in lake sediments can provide information about sources of OM, nutrient loading, rates of primary production, pH and redox conditions, etc. which may be further extrapolated to descriptions of climate and ecological conditions, and anthropogenic modifications of either of these (eg. Leng et al., 2005; Meyers and Teranes, 2001; Ariztegui et al., 1996; Gu et al., 1996). As these data are proxies only, it is typical for studies to utilize more than one parameter to support hypotheses about climate/ecological conditions or changes.

2.2 Stable Isotopes and Fractionation Effects

Stable isotope ratios of C, N and S are expressed relative to international standards, rather than as absolute values (Table 2.1). Isotope values of biological and geological materials are typically reported using the δ notation, which is reported in units of permil (‰) as shown in equation 1:

$$\delta\ [‰] = \left(\frac{R_x - R_s}{R_s}\right) 1000 \qquad [1]$$

Where Rx is the ratio of heavy to light isotopes of the sample, and Rs is the ratio of heavy to light isotopes of a standard (Kendall and Caldwell, 1998; Fogel and Cifuentes, 1993).

Table 2.1: Stable isotope ratios of carbon, nitrogen and sulfur and internationally accepted standards against which C, N and S isotope ratios are reported.

Element	Heavy:Light Isotopes	International Standard
Carbon	^{13}C:^{12}C	Peedee Belemnite (PDB)
Nitrogen	^{15}N:^{14}N	Atmospheric Air (AIR)
Sulfur	^{34}S:^{32}S	Canyon Diablo Troilite (CDT)

Biological or chemical processes are often associated with isotope fractionation effects during which either the heavy or the light isotope of an element is consistently concentrated either in the product or in the substrate/reactant. Fractionation effects may be expressed as a fractionation factor (α), calculated by equation 2:

$$\alpha = \frac{R_p}{R_s} \qquad [2]$$

Where R_p is the stable isotope ratio of the product in ‰, and R_s is the stable isotope ratio of the substrate (reactant) in ‰. Alternatively, the fractionation factor may be expressed as an enrichment factor, which is the notation used to describe isotope fractionation effects occurring in C, N and S during cycling in lakes in chapter 2.3. It is approximately equivalent to the difference between the delta values of the product and the substrate (reactant):

$$\varepsilon \cong \delta_p - \delta_s \qquad [3]$$

Where δ_p is the stable isotope value of the product, and δ_s is the isotopic signature of the substrate (reactant). Thus any value of ε which is positive indicates that the heavier isotope is preferentially incorporated into the product, and a negative value of ε indicates that the reaction concentrates the lighter isotope in the product (Fogel and Cifuentes, 1993).

2.3 Cycling and Stable Isotope Fractionation Effects of Elements in the Lacustrine Ecosystem

For this study, the isotopic signatures of lake sediment organic matter is of primary interest, and thus it is important to understand the in-lake processes which influence sedimentation, early alteration and degradation of sedimented OM, as well as the isotope fractionation effects associated with these processes. The majority of these fractionation effects are mass-dependent and kinetic (Fogel and Cifuentes, 1993). The final isotopic composition of a product, OM in lake sediments in the case of this

study, is a function of two factors; the isotopic composition of the substrate (reactant) for any given process, and the isotope fractionation effect associated with this process.

The following sections discuss the major sources of C, N and S in the water column and in lake sediments, and the most common processes by which these elements are carried from their sources to the sink of lake sedimentary organic matter. Additionally typical $\delta^{13}C$, $\delta^{15}N$ and $\delta^{34}S$ values of involved species are given, and fractionation effects associated with processes are provided. It is important to note that these are general, simplified versions of "typical" C, N and S cycles in lakes.

2.3.1 Carbon Cycling and Stable Isotope Fractionation

The carbon required for photosynthesis by submergent macrophytes and phytoplankton is provided by the dissolved inorganic carbon (DIC) pool in the water column of a lake. DIC occurs in the forms $CO_{2(aq)}$, HCO_3^- and CO_3^{2-}, dependent on the pH of lake water (Figure 2.1) (Carroll and Mather, 1992). The majority of DIC in lake water is often derived from the dissolution of atmospheric CO_2. $\delta^{13}C$ values of atmospheric CO_2 are typically between -7 and -8‰ (Fahrquhar et al., 1989), and dissolution occurs without any significant isotope fractionation effect (Leng et al., 2005; Meyers and Teranes, 2001). Other DIC sources may include inflowing groundwater and wash-in of decomposed soil organic matter from the terrestrial ecosystem; these have $\delta^{13}C$ values which may vary by region but are typically between -30 and -5‰ (Meyers and Teranes, 2001).

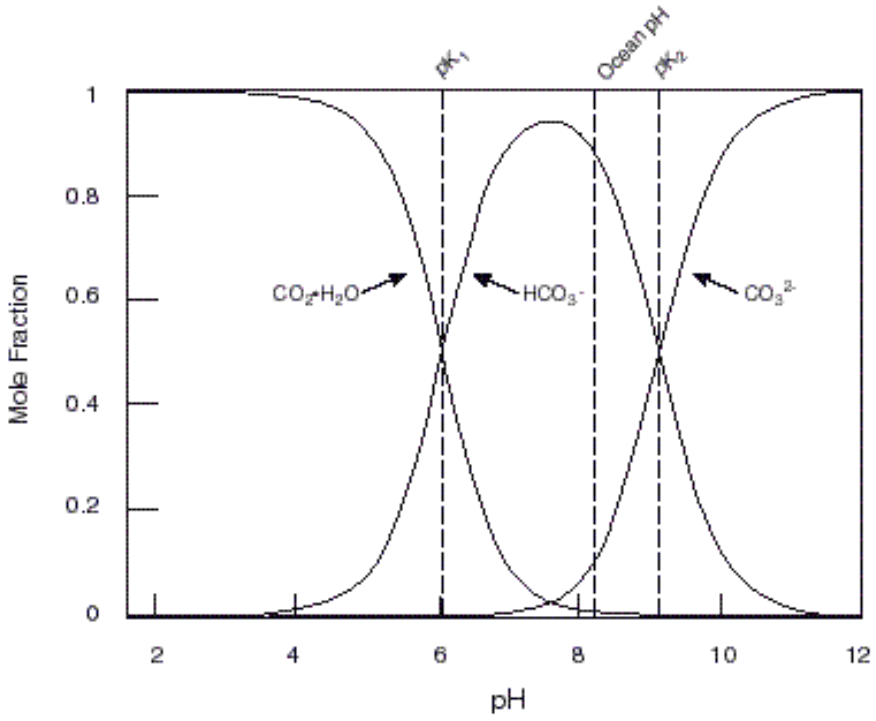

Figure 2.1: Speciation of total dissolved carbon versus water pH in the H_2O-CO_2 system (from Jacob, 1999).

The fractionation effect associated with assimilation of carbon during photosynthesis depends on the photosynthetic pathway used by organisms (Leng et al., 2005; Keeley and Sandquist, 1992; Farquhar et al., 1989; O'Leary, 1988). Typical isotope fractionation effects associated with photosynthesis by the C4 and CAM pathways are -4 to -6‰ (Hoefs, 2009; O'Leary, 1988) and -4 to -20‰ (Farquhar, 1989; Osmond et al., 1973) respectively (Table 2.2), preferentially accumulating the lighter ^{12}C isotope in plant tissues, though the $\delta^{13}C$ values of the plants depend upon the $\delta^{13}C$ value of the assimilated DIC source . The C3 pathway, which is used by most aquatic plants and phytoplankton (Leng et al., 2005; Keeley and Sandquist, 1992), discriminates against the heavier ^{13}C isotope and produces OM which is around 20‰ lower than the source of DIC (O'Leary, 1988).

Table 2.2: Biochemical processes involved in the idealized lacustrine carbon cycle, and associated enrichment factors (compiled from Ghashghaie et al., 2003; Dawson et al., 2002; Meyers and Teranes, 2001; Whiticar, 1999; Lin and Ehleringer, 1997; Fogel and Cifuentes, 1993; Romanek et al., 1992; O'Leary, 1988; Mook et al., 1974).

Biochemical Process	Enrichment Factor (ε)
$CO_{2(aq)}$ -> $HCO_3^-{}_{(aq)}$	**+8 to +12‰**
C3 Photosynthesis/Assimilation $CO_{2(aq)}$ or HCO_3^- -> cell-C	**~-20‰**
C4 Photosynthesis/Assimilation $CO_{2(aq)}$ or HCO_3^- -> cell-C	**-6 to -4‰**
Respiration Cell-C -> $CO_{2(aq)}$	**~0‰**
Authigenic Carbonate Formation $CO_{2(aq)}$ -> calcite/aragonite HCO_3^- -> calcite/aragonite	 **+12 to +14‰*** **+0.8 to +3.3‰**
Methanogenesis Cell-C -> CH_4	**-95 to -49‰**

*temperature-dependent

Assuming that the DIC source is mainly atmospheric CO_2, "typical" $\delta^{13}C$ values of autochthonously-produced OM using the C3 pathway for photosynthesis would be around -28‰. Variations in the $\delta^{13}C$ value of assimilated DIC produces OM with "atypical" $\delta^{13}C$ values. $\delta^{13}C$ values of DIC in lakes between -29.6 and +2.3‰ have been recorded (Bade et al., 2004 and references therein). For example, where availability of CO_2 is limited during periods of high primary productivity or where elevated pH results in a much greater concentration of aqueous HCO_3^- over CO_2, photosynthesizing organisms may take up HCO_3^-, which has a $\delta^{13}C$ value around 9 to 12‰ higher than CO_2 (Mook et al., 1974). This may produce OM with $\delta^{13}C$ values as high as -9‰ (Bernasconi et al., 1997; Hassan et al., 1997; Keeley and Sandquist, 1992).

In lakes where OM is derived mostly from primary in-lake production with insignificant terrestrial input, trends in $\delta^{13}C$ values of sediments may indicate changes in lake conditions related to pH, temperature, nutrient limitation and growth rates of phytoplankton (Laws et al., 1995; Fogel and Cifuentes, 1993; Takahashi et al., 1990). It was concluded by a study of 32 lakes in the Northern Highlands located in Wisconsin and Michigan by Bade et al. (2004) that in this case, geochemical and morphometric variables, eg. lake area, pH, temperature, alkalinity were of greater importance in variations of the $\delta^{13}C$ value of the DIC pool relative to biologic factors such as rate of primary production and respiration.

In addition to OM, lake sediments may also contain authigenic carbonates (Figure 2.2). Formation of carbonates favors incorporation of the heavier ^{13}C isotope (Romanek et al., 1992), resulting in carbonates with higher $\delta^{13}C$ values than the DIC used in their formation (Table 2.2) (Leng and Marshall, 2004; Schwalb et al., 1999). It was noted by Dean (1999) that relative quantities of OM carbon and authigenic carbonate have an inverse relationship; where the rate of primary production is high, the amount of authigenic carbonate preserved is low.

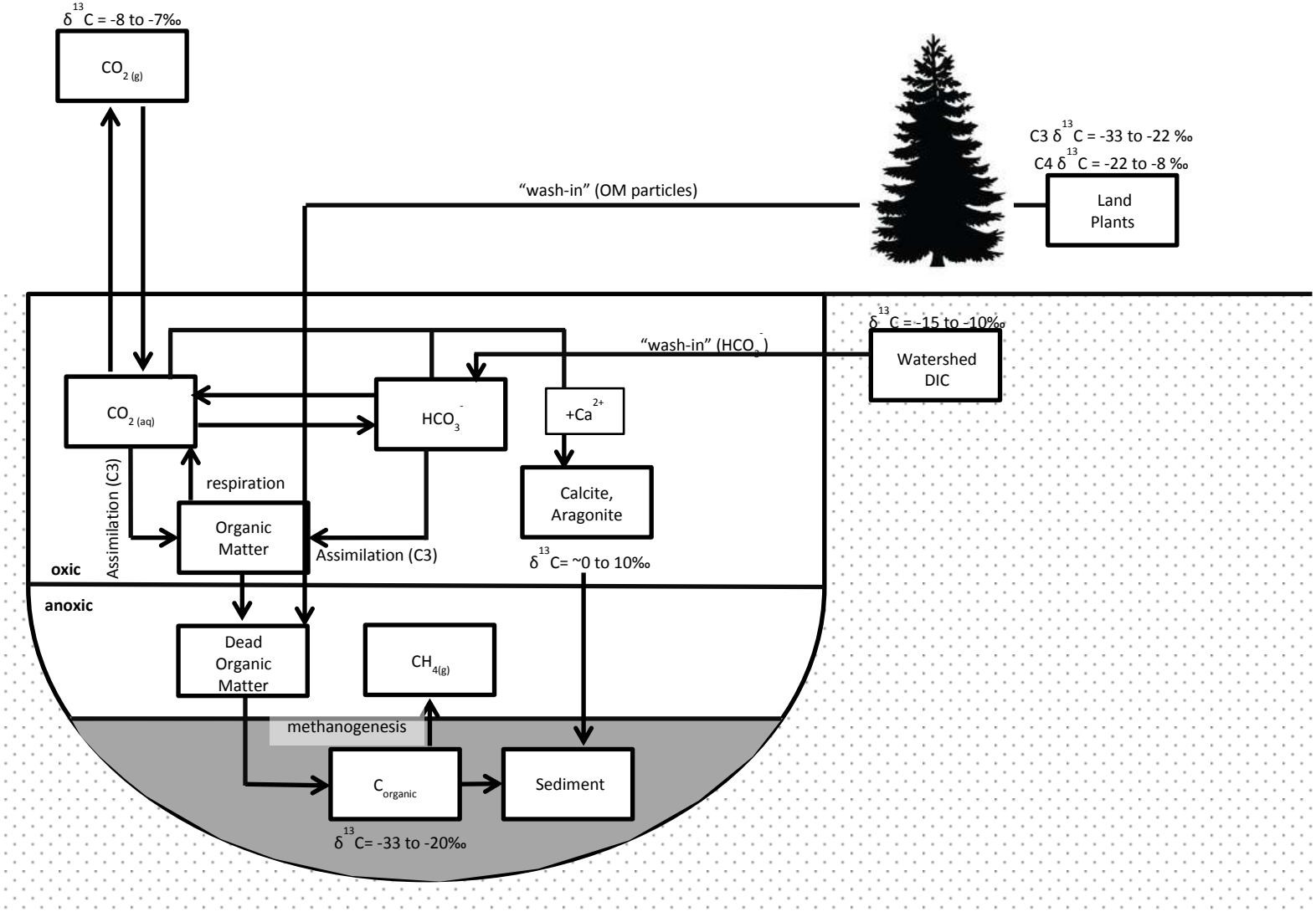
δ13C = -8 to -7‰
CO2 (g)
C3 δ13C = -33 to -22 ‰
C4 δ13C = -22 to -8 ‰
"wash-in" (OM particles)
Land Plants
δ13C = -15 to -10‰
"wash-in" (HCO3-)
Watershed DIC
CO2 (aq)
HCO3-
+Ca2+
Calcite, Aragonite
respiration
Assimilation (C3)
Organic Matter
Assimilation (C3)
δ13C= ~0 to 10‰
oxic
anoxic
Dead Organic Matter
CH4(g)
methanogenesis
Corganic
Sediment
δ13C= -33 to -20‰

Figure 2.2: The idealized lacustrine carbon cycle. $\delta^{13}C$ values are compiled from Dawson et al. (2002), Meyers and Teranes (2001), Fogel and Cifuentes (1993), Romanek et al. (1992), Fahrquhar et al. (1989).

Diagenesis of OM carbon is thought to produce geopolymers, which are later converted to kerogen (Macko et al., 1993). Generally, geopolymers are slightly enriched in ^{13}C relative to the OM from which they formed as a result of preferential utilization of the light ^{12}C isotope by microbes during diagenesis (Macko et al., 1993; Galimov, 1980; Nissenbaum, 1974; Nissenbaum et al., 1972). This produces a "typical" profile of $\delta^{13}C$ values which increase with increasing depth (Macko et al., 1993). Methanogenesis, which occurs under anoxic conditions and is the final "step" in the remineralization of organic C, converts CO_2 or acetic acid produced by bacterial degradation of OM into CH_4, has a significant associated carbon isotope effect, producing CH_4 which is 49 to 95‰ lower in $\delta^{13}C$ than the OM from which it was derived (Whiticar, 1999).

2.3.2 Nitrogen Cycling and Stable Isotope Fractionation

Primary producers such as algae and phytoplankton assimilate nitrogen in the form of NO_3^- and NH_4^+ while "fixation" of atmospheric N_2 is attributed primarily to cyanobacteria (Talbot, 2001). These N species enter the lake water column through wash-in from the surrounding watershed (NO_3^- and NH_4^+), via atmospheric deposition (NO_3^- and NH_4^+) or exchange with the atmosphere (N_2) (Figure 2.3). $\delta^{15}N$ values of ammonium and nitrate in atmospheric deposition typically range between -18 and +4‰ (Heaton, 1987; Owens, 1987) and tend to be subject to seasonal variations (eg. Proemse et al., 2013). Atmospheric N_2 has a constant $\delta^{15}N$ value of 0‰.

Uptake of N either by assimilation of nitrate and ammonium or by fixation of dissolved nitrogen occurs with a fractionation effect which tends to concentrate the lighter ^{14}N isotope in the product, leaving the heavier ^{15}N isotope in the remaining solution species (NO_3^-, NH_4^+, N_2)(Table 2.3). Enrichment factors associated with the assimilation of NO_3^- range between 0 to -24‰ with typical "field observation" values of -4 to -5‰ (Talbot, 2001; Fogel and Cifuentes, 1993 and references therein). Assimilation of NH_4^+ occurs with enrichment factors ranging between +7 and -27‰ with typical field observation values around -10‰ (Talbot, 2001; Fogel and Cifuentes, 1993 and references therein). N_2 fixation is associated with enrichment factors of -3 to +4‰ (Talbot, 2001; Fogel and Cifuentes, 1993 and references therein). The magnitudes of these fractionation effects depend on whether the assimilation/fixation is enzyme-limited, diffusion-limited or nitrogen-limited (Fogel and Cifuentes, 1993).

The $\delta^{15}N$ values of the biomass produced through assimilation of NO_3^- and NH_4^+, primarily algae and phytoplankton, depends upon the isotopic composition of the assimilated aqueous N species, but typically range between -3 and -18‰ (Cifuentes et al., 1988; Owens, 1987; Turner, 1982) while nitrogen-fixing marine algae have $\delta^{15}N$ values between -2 and +4‰ (Fogel and Cifuentes, 1993). During and after sedimentation of dead OM, biologically-mediated processes further alter the $\delta^{15}N$ values of the OM (Figure 2.3). The most significant of these processes include remineralisation, nitrification and denitrification (Table 2.3).

Remineralisation, which converts cell-N to NH_4^+, concentrates ^{14}N in the produced NH_4^+ with an enrichment factor of about +1‰ (Talbot, 2001). Nitrification occurs by biological oxidation of NH_4^+ using O_2 to NO_3^-, with NO_2 as an intermediate product. The enrichment factor associated with this reaction ranges between -40 to -10‰, concentrating ^{14}N in the produced NO_3^- (Talbot, 2001; Peterson and Fry, 1987; Mariotti et al., 1981). Denitrification is the reduction of NO_3^- to N_2 by bacteria in the presence of organic matter, in anoxic environments. This process concentrates ^{14}N in the product (N_2), with variable

enrichment factors which typically range between -10 and -20‰ in natural systems (Talbot, 2001), but may vary as widely as -40 to -5‰ (Lehmann et al., 2003).

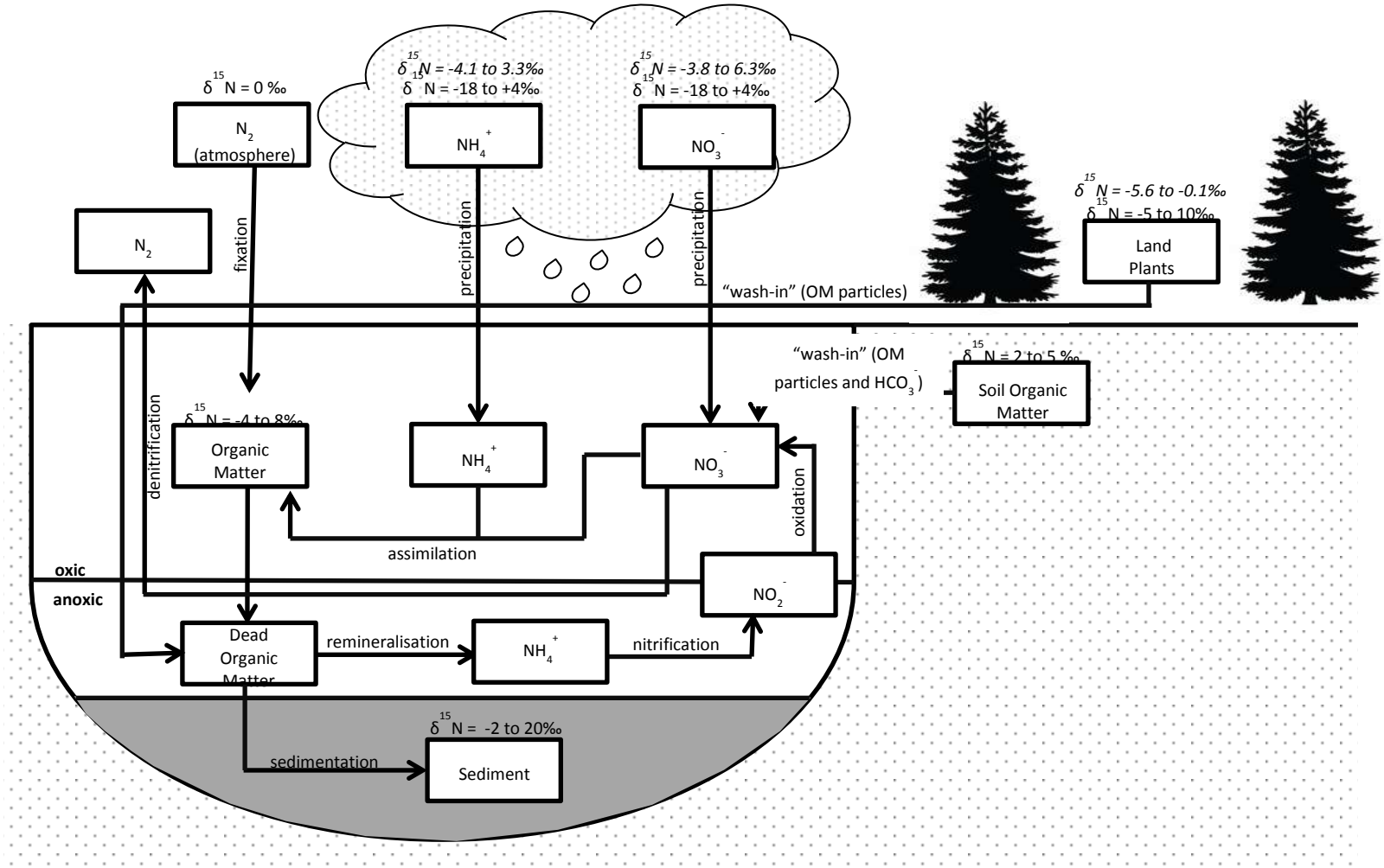
δ 15N = 0 ‰
N2 (atmosphere)
δ 15N = -4.1 to 3.3‰
δ 15N = -18 to +4‰
NH4+
δ 15N = -3.8 to 6.3‰
δ 15N = -18 to +4‰
NO3-
δ 15N = -5.6 to -0.1‰
δ 15N = -5 to 10‰
Land Plants
N2
fixation
precipitation
precipitation
"wash-in" (OM particles)
"wash-in" (OM particles and HCO3-)
δ 15N = 2 to 5 ‰
Soil Organic Matter
δ 15N = -4 to 8‰
Organic Matter
denitrification
NH4+
NO3-
oxidation
assimilation
oxic
anoxic
NO2-
Dead Organic Matter
remineralisation
NH4+
nitrification
δ 15N = -2 to 20‰
sedimentation
Sediment

Figure 2.3: **The idealized lacustrine nitrogen cycle. Italicized $\delta^{15}N$ values for NO_3^- and NH_4^+ in atmospheric precipitation are from Proemse et al. (2013), and represent local (AOSR) values. Italicized $\delta^{15}N$ values of land plants represent stable isotope analyses of jack pine and spruce needles in the AOSR from Proemse et al. (2013). Non-italicized $\delta^{15}N$ values are compiled from Hoefs (2009), Meyers and Teranes (2001) and Talbot (2001) Kendall (1998),Fogel and Cifuentes (1993).**

Table 2.3: Biochemical processes involved in the idealized lacustrine nitrogen cycle, and associated enrichment factors (compiled from Hoefs, 2009; Lehmann et al. 2003 and references therein; Talbot, 2001, Fogel and Cifuentes, 1993; Peterson and Fry, 1987; Mariotti et al., 1981).

Biochemical Process	Enrichment Factor (ε)
N_2 Fixation: $N_{2(aq)}$ -> cell-N	**-3 to +4‰**
Ammonium Assimilation $NH_4^+{}_{(aq)}$ -> cell-N	**-27 to 0‰**
Nitrate Assimilation $NO_3^-{}_{(aq)}$ -> cell-N	**-27 to 0‰**
Remineralization cell-N -> $NH_4^+{}_{(aq)}$	**-1‰**
Nitrification $NH_4^+{}_{(aq)}$ -> (NO_2^-) -> $NO_3^-{}_{(aq)}$	**-40 to -10‰**
Denitrification $NO_3^-{}_{(aq)}$ -> $N_{2(g)}$	**-20 to -10‰**

Typical $\delta^{15}N$ values in sediments vary between -2 to +20‰ (Meyers and Teranes, 2001; Talbot, 2001), though simple interpretations of these values are not usually possible, given the complexity of cycling and recycling processes which fractionate N isotopes. Further complicating historic studies of lake sediments using $\delta^{15}N$ is the effect of anthropogenic additions of N compounds to the hydrosphere and atmosphere (Vitousek et al., 1997). Anthropogenically-produced fertilizers utilize atmospheric

nitrogen ($\delta^{15}N$=0‰), and have similar $\delta^{15}N$ values, typically between -4 to +4‰ (Kendall, 1998), while organic fertilizers have a greater range of $\delta^{15}N$ values relative to anthropogenically-produced ones, owing to more diverse origins (+2 to +30‰)(Kendall, 1998). Animal waste associated with widespread agricultural activities adds NO_3^- with $\delta^{15}N$ values ranging from +10 to +20‰ (Kendall, 1998; Fogel and Cifuentes, 1993; Kreitler, 1979; Kreitler, 1975). When added to groundwater and surface water which may transport NO_3^- to lakes, these may further alter the $\delta^{15}N$ values of lacustrine OM. A study of sediment cores from oligotrophic lakes by Holtgrieve et al. (2011) showed a widespread up-core decrease in lake sediment $\delta^{15}N$ values (1 to 3‰ in boreal lakes) in remote lakes since 1900. This is postulated to have been a result of enhanced fractionation effects owing to the addition of reactive N to the atmosphere by anthropogenic activities associated with industrialization.

2.3.3 Sulfur cycling and stable isotope fractionation

Most sulfur which is assimilated by primary producers in lake ecosystems is derived from SO_4^{2-}. Typically, the concentration of SO_4^{2-} in fresh water is low (0.1 to 0.2 mmol/L) relative to concentrations observed in ocean water (Ingvorsen et al., 1981). Sulfur dissolved in lake water is partly derived from sulfate contained in atmospheric deposition. Additional sources are sulfates formed in the terrestrial watershed surrounding the lake or organic sulfur compounds that enter the lakes with shallow groundwater or as surface water runoff (Mitchell et al., 1992; David and Mitchell, 1985).

Contributions to atmospheric sulfur have both natural and anthropogenic origins including volcanic emissions, sea spray, fossil fuel burning and the smelting of ores (Nielsen, 1974; Nakai and Jensen, 1964). The relative contributions from each of these sources and the wide ranges of $\delta^{34}S$ observed in each source makes it impossible to give a global “typical” value for atmospheric sulfur and the sulfate in precipitation it produces; rather, these vary by study area and must be measured (Nielsen,

1974). In the AOSR, "background" average $\delta^{34}S$ values of SO_4^{2-} in precipitation vary seasonally, from 4.1‰ in summer and 5.2‰ in winter (Figure 2.4) (Proemse et al., 2012). Total sulfur in jack pine and spruce needles in the AOSR had $\delta^{34}S$ values ranging between -3.5 to 11.8‰ (Figure 2.4) (Proemse and Mayer, 2013), though this does not constitute a comprehensive analysis of all terrestrially-derived sulfur which may have washed into the lakes covered in this study.

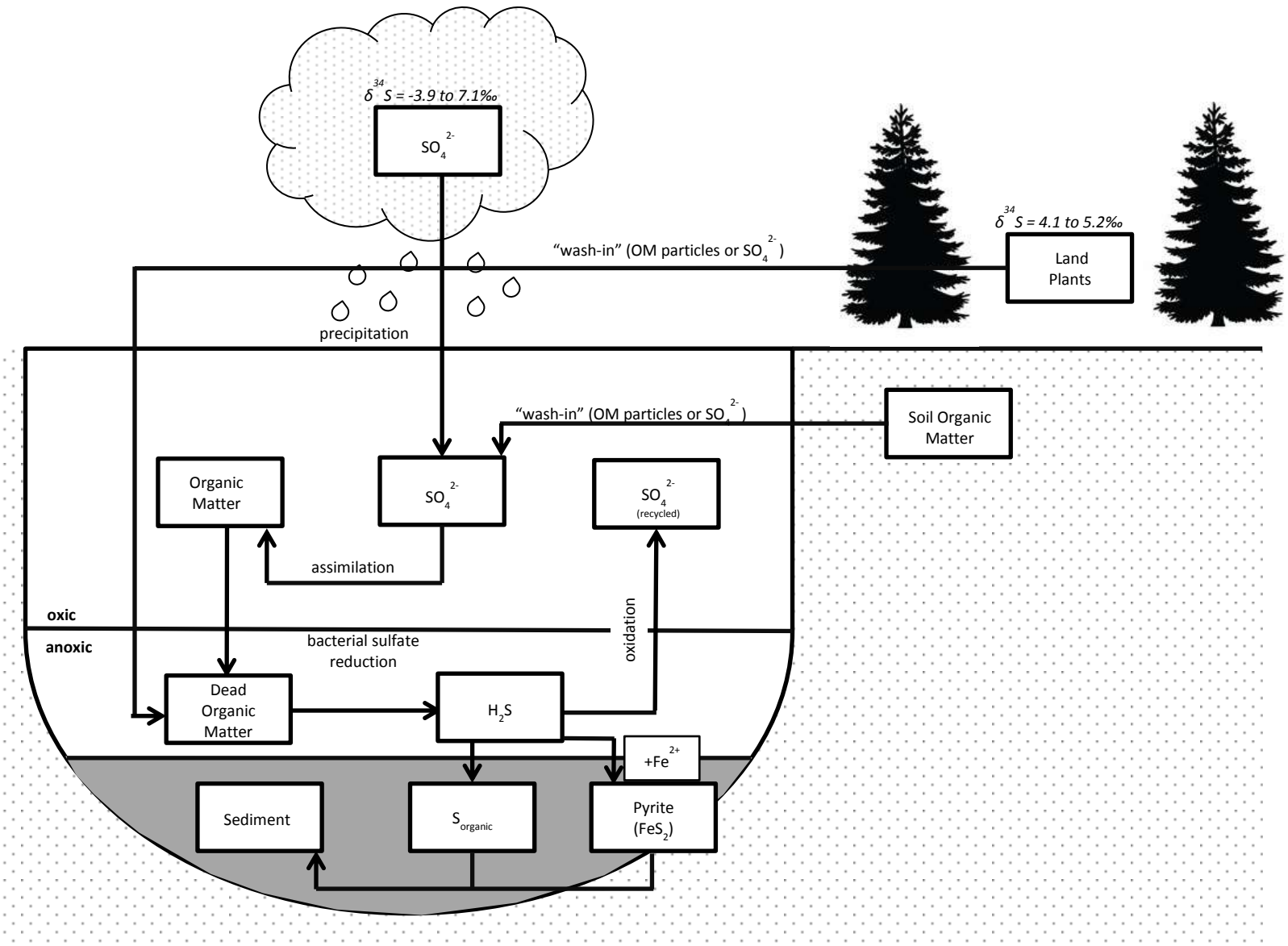
δ 34 S = -3.9 to 7.1‰
SO4 2-
δ 34 S = 4.1 to 5.2‰
Land Plants
"wash-in" (OM particles or SO4 2-)
precipitation
"wash-in" (OM particles or SO4 2-)
Soil Organic Matter
Organic Matter
SO4 2-
SO4 2- (recycled)
assimilation
oxic
anoxic
bacterial sulfate reduction
oxidation
Dead Organic Matter
H2S
+Fe 2+
Sediment
Sorganic
Pyrite (FeS2)

Figure 2.4: The idealized lacustrine sulfur cycle. Italicized $\delta^{34}S$ values for SO_4^{2-} in atmospheric precipitation are from Proemse et al. (2012), and represent local (AOSR) values. Italicized $\delta^{34}S$ values of land plants represent stable isotope analyses of jack pine and spruce needles in the AOSR from Proemse et al. (2012).

SO_4^{2-} is assimilated by phytoplankton and macrophytes in the water column and is converted to organic sulfur which is ultimately incorporated into sediments as dead organic matter (Cook and Kelly, 1992). Depending on lake conditions, the dead OM accumulates and may be preserved or recycled back into the water column through remineralization (Cook and Kelly, 1992). The process of assimilation of sulfate by phytoplankton favors the lighter ^{32}S isotope slightly, producing organic sulfur which is 1 to 2‰ lower than the sulfate which was assimilated (Table 2.4)(Kaplan and Rittenberg, 1964).

Table 2.4: Biochemical processes involved in the idealized lacustrine sulfur cycle, and associated enrichment factors. Compiled from Habicht and Canfield (1997), Chambers et al. (1975), Kemp and Thode (1968), Kaplan and Rittenberg (1964), Harrison and Thode (1958).

Biochemical Process	Enrichment Factor (ε)
Sulfate Assimilation SO_4^{2-} -> cell-S	**-1 to -2‰**
Bacterial Sulfate Reduction (BSR) SO_4^{2-} -> H_2S	**-43 to -5‰*** **-42 to -16‰****

*studies of pure cultures

**studies of actual lakes

Within the anoxic zone of the sediment SO_4^{2-} may be reduced by sulfate reducing bacteria (SRB) to H_2S gas which can be further incorporated into organic sulfur compounds (Einsiedl et al., 2008; Rudd et al., 1986) or pyrite (FeS). Alternately, H_2S may be re-oxidized to SO_4^{2-} in the oxic part of the water

column, or may escape into the atmosphere (Holmer and Storkholm, 2001; Cook and Kelly, 1992). Because of the low concentrations of SO_4^{2-} in typical lakes, BSR generally occurs in the top 10cm of sediment only, before SO_4^{2-} becomes completely consumed and methanogenesis becomes the dominant process by which bacteria break down deposited OM (Holmer and Storkholm, 2001). BSR discriminates against the heavier ^{34}S isotope and produces sulfide with a $\delta^{34}S$ value that is depleted in ^{34}S relative to dissolved SO_4^{2-}. The enrichment factor has been measured to vary between -43 to -5‰ in studies of pure cultures (Table 2.4) (Chambers et al., 1975; Kemp and Thode, 1968; Kaplan and Rittenberg, 1964; Harrison and Thode, 1958) and -42 to -16‰ in actual lake sediments (Table 2.4) (Habicht and Canfield, 1996). The rate of bacterial sulfate reduction (BSR) appears to play some role in the magnitude of the fractionation effect, with larger fractionation effects associated with lower rates of BSR and vice-versa, though the factors which determine the rate of BSR are not well understood (Holmer and Storkholm, 2001; Habicht and Canfield, 1996; Cook and Kelly, 1992).

CHAPTER THREE: STUDY AREA

3.1 Geologic Setting

The area encompassing operations in the AOSR and the study sites lies in NE Alberta and NW Saskatchewan and is located in the Western Canadian Sedimentary Basin (WCSB). Accretion of the terranes which now make up the Canadian Cordillera during Middle Jurassic to Middle Eocene time caused isostatic flexure of the adjacent crust, creating the northwest-trending, wedge-shaped Alberta Basin (Price, 1994). The shallow Western Interior Seaway covered much of Alberta and Saskatchewan throughout the Cretaceous, accommodating the deposition of sediments mainly derived from erosion of the newly-formed Rocky Mountains to the west. As high levels of sedimentation filled the basin and pushed the interior seaway's shoreline northward and eastward, quartzose sediments derived from the Precambrian Shield created the McMurray deltaic complex on the seaway's eastern shoreline, which is the reservoir from which bitumen in the AOSR is produced (Hayes et al., 1994).

Throughout most of the AOSR in northern Alberta and Saskatchewan, Tertiary strata have been eroded (Mossop and Shetsen, 1994) and bedrock consists of either the Cretaceous-aged non-marine sandstones of the Mannville Group, marine shales of the Clearwater Formation (Hayes et al., 1994), or the Archean-aged rocks which comprise the Rae-Hearne craton section of the Canadian Shield (Macdonald, 2006; Böhm et al., 2004). These are granitic and granitoid rocks which have been metamorphosed to granulite grade (Böhm et al., 2004).

During the Quaternary, advances and retreats of ice sheets deposited a succession of unconsolidated till, lacustrine and fluvial sediments (Fenton et al., 1994), which now cover the bedrock throughout much of Alberta and Saskatchewan. The thickness of the drift is variable, ranging from 0m where bedrock is exposed to 150m. Areas where drift is thicker than 90m occur almost exclusively north of 54°N latitude (Pawlowicz and Fenton, 1995). The retreat of the Laurentide ice sheet shaped much of

the topography in Northern Saskatchewan (Dale, 2006a) and created numerous proglacial lakes, some of which still exist presently (Dale, 2006b). It is likely that the lakes described in this thesis ultimately originated from these proglacial lakes.

3.2 Study Sites

Sites for lake sediment sampling were selected by members of the Coal & Oil Resources Environmental Sustainability (CORES) project, of the Geological Survey of Canada (GSC). Headwater lakes which were accessible by helicopter, and which were of an appropriate depth for sampling by freeze-coring (5-10m) were targeted for this study. Three targeted lakes were assigned the identifiers Alberta Lake E (ALE), Saskatchewan Lake 10W (SL10W) and Saskatchewan Lake 10M (SL10M). Table 3.1 gives the locations of the studied lakes, ALE located in Alberta, northeast of Fort McMurray and two more, SL10W and SL10M, located roughly east of ALE in Saskatchewan (Figure 3.1). Approximate distances and bearings relative to the Syncrude upgrader in the AOSR are included; the upgrader is taken to be the "center" of industrial emissions in the AOSR. ALE lies approximately 97km east-southeast of the upgrader, SL10W is located ~132km east, and SL10M is located ~143km east-southeast of the upgrader. These distances are important for interpretations of data, as a study by Proemse and Mayer (2013) notes some spatial trends in rates of N and S atmospheric deposition, with respect to the distance between sampling sites and the Syncrude upgrader.

Prevailing winds in the region are from the west in the summer and winter months (June, July, August and December, January, February), and from the east in the spring and the fall (March, April, May and September, October, November) (Government of Alberta, 2010). Thus it is likely that most of the N or S from the industrial operations occurring in the AOSR was deposited during the summer or winter months, when winds carry emissions eastward.

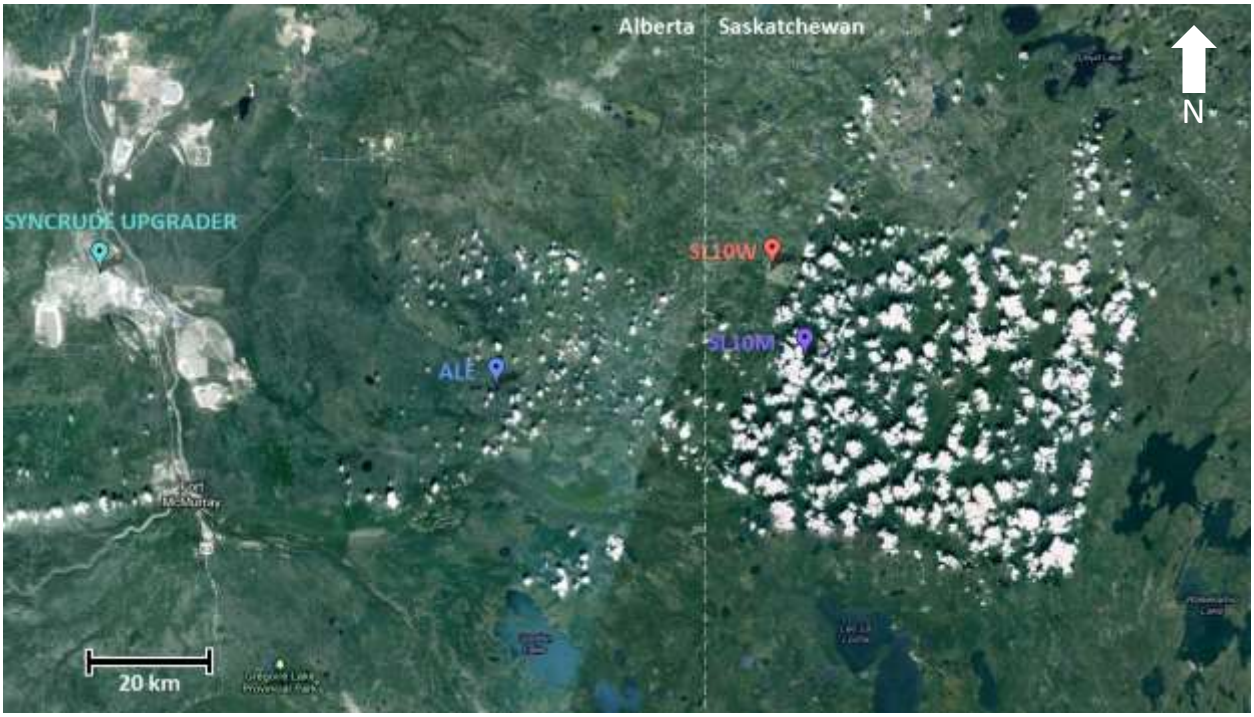

Figure 3.1: Locations of sampled lake sites from Google satellite images, accessed May 2013. Locations of the Syncrude upgrader taken to represent the location of the AOSR, as well as locations of ALE, SL10W and SL10M are indicated.

Table 3.1: Locations of study site lakes and distance from Syncrude upgrader taken to be the location of AOSR activities. Location of upgrader is taken from Proemse et al. (2012).

Site	Latitude	Longitude	Approximate distance and bearing relative to Syncrude upgrader (km)
ALE	56°52'47.13"N	110°33'44.45"W	97 ESE
SL10W	57° 3'19.28"N	109°49'16.46"W	132 E
SL10M	56°55'24.18"N	109°44'4.91"W	143 ESE

Sampling was performed in October 2009 by CORES researchers. Basic water chemistry parameters (pH, temperature) were measured by probe and recorded on-site, or were analyzed in GSC laboratories (alkalinity). Lake sediments collected by freeze-coring were returned to the laboratory for further analysis. One core was collected from ALE, one from SL10M, and two cores were taken from SL10W resulting in a total of four cores.

All three lakes are headwater lakes, and therefore received negligible stream input. Instead, lakes are dominantly fed by shallow groundwater and precipitation (J. Ahad, pers. communication). Average measured depths of lakes ALE1, SL10W and SL10M were between 6 and 7m. Because these lakes are shallow relative to the thickness of till units, it is unlikely that there is any significant interaction of the lake water with bedrock, and thus any contributions to total dissolved solids (TDS) from mineral dissolution are due to shallow groundwater input during infiltration through the Quaternary tills.

The AOSR and three studied lakes are all located in the Canadian Boreal Forest (Figure 3.2) which covers most of northern Alberta and Saskatchewan. This region is associated with subarctic climates, within which long, harsh winters and short warm summers are typical (Runesson, 2011). No extensive prior studies have been conducted on these lakes, and therefore the details of seasonal cycles within the lakes are unknown, though the time scale used in this study does not have adequate resolution to comment on the impact of seasonal changes within the sedimentary record. Average temperatures recorded at the Fort McMurray Airport in northern Alberta indicate that monthly average wintertime temperatures are as low as -19^{o}C in January, and monthly average summertime temperatures climb as high as 17^{o}C in July (Environment Canada, 2013). Hence the lakes' surfaces are frozen and thus cut off from open exchange with the atmosphere, for at least part of the winter and are unfrozen during the summer. Spruce and fir are the most common tree species in the region, growing

on soils which tend to be acidic resulting from decomposition of fallen needles, and wet owing to the heavy cover of the forest canopy (Runesson, 2011). Frequent forest fires are typical of the boreal forest ecosystem (Government of Saskatchewan, 2012; Runesson, 2011); field notes recorded by CORES researchers during the sampling trip remarked that there was some evidence for recent forest fires along the shoreline of SL10M. Fires may also have resulted in the patch of deforested land surrounding SL10W (Figure 3.2). Alternately, it is possible that these were once lake-bottom sediments which have been exposed subaerially by evaporation (J. Carrie, pers. communication).

Figure 3. 2: Images of 3 lakes included in this study, from Google satellite images accessed May 2013. A) ALE, surrounded by boreal forest. B) SL10M, surrounded by boreal forest. White masses on the left side of the image are clouds captured by Google satellite imaging. C) SL10W, surrounded by a "halo" of deforested land. In the upper left corner of the image, a sharp boundary occurs between forested and non-forested areas, while linear gaps in the forested area closely resemble relict paths of streams which may have been connected to the lake.

CHAPTER FOUR: METHODS

Lake sediments were analyzed by radiometric dating techniques (^{210}Pb), Rock-Eval pyrolysis, organic petrology and stable isotope techniques. Parameters from Rock-Eval, along with the qualitative analysis of organic petrology, C/N ratios, and δ^{13}C were used to characterize the sediments geochemically, with particular focus on the organic fraction (quantity, source, quality) contained therein. Stable isotope analyses of S and N were hypothesized to be the most likely parameters to show impact from industrial emissions given elevated levels of deposition of SO_4^{2-}, NH_4^+ and NO_3^- in the vicinity of the major emission sources (<30km) in the AOSR (Proemse and Mayer, 2013; Proemse et al., 2013; Proemse et al., 2012). These parameters were used in conjunction with ^{210}Pb data in order to contrast sediments deposited prior to the onset of anthropogenic activity in the AOSR with those deposited after, with the objective of assessing whether or not industrial emissions from the AOSR had impacted lake sediments.

4.1 Field Sampling Techniques

Basic water chemistry parameters (pH, temperature) were measured at 1m depth intervals by probe and recorded on-site. Lake sediment samples were collected by freeze-coring and returned to the laboratory for further analysis.

The freeze-coring technique was utilized for collection of sediment cores. The centre of a two-sided freeze corer (Figure 4.1) was filled with a mixture of dry ice and ethanol. This was lowered into the sediments from a stationary raft by winch, and held in place in the sediment for 20 minutes, and frozen sediment cores were withdrawn. Cores were kept frozen during transport back to the laboratory, and were sectioned in a walk-in freezer at -20°C (J. Ahad, pers. communication).

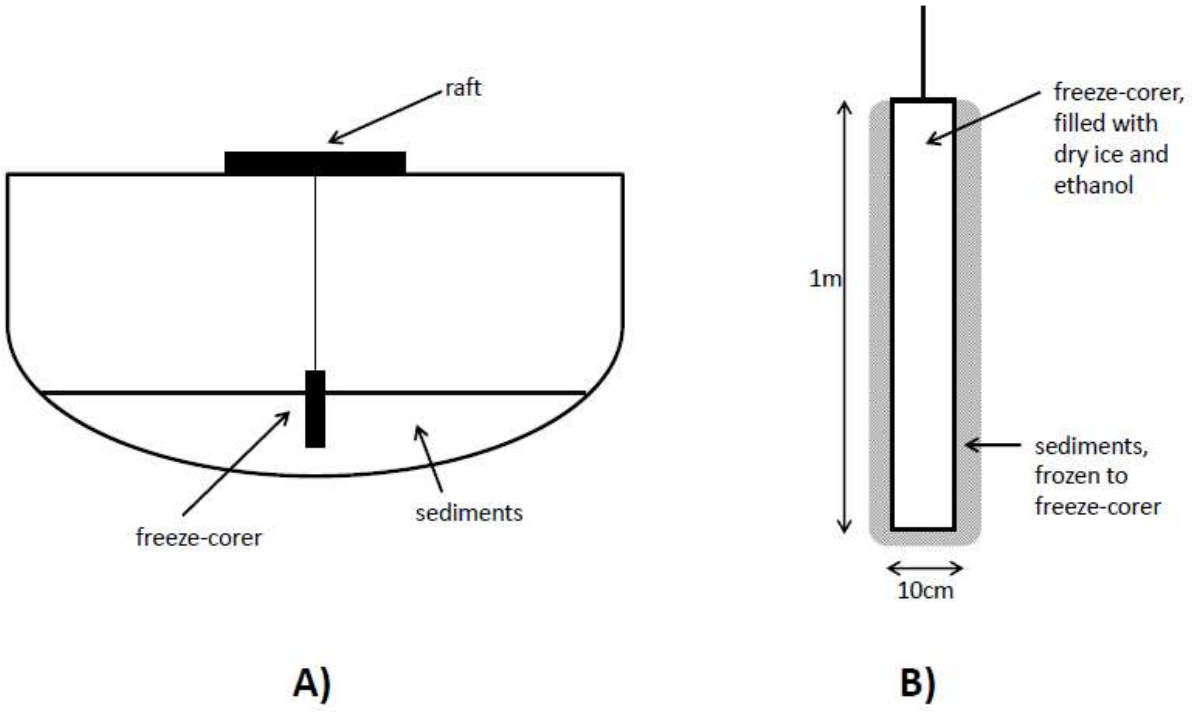

Figure 4.1: Schematic representation of the freeze-coring technique for coring lake sediments. A) Setup with freeze-corer lowered by winch from a raft into lake sediments. B) Close-up of freeze-corer filled with dry ice and ethanol.

4.2 ^{210}Pb Dating

Radiometric dating is a technique used to estimate ages of rock and sediment samples (USGS, 2013). The quantities of parent and daughter products of a radioactive isotope may be measured through detection and counting of decay particles over a known period of time. Using the half-life of the parent isotope, which is a known value, it is possible to calculate the approximate age of a sample by comparing relative quantities of a parent to a daughter isotope. This is done using the age equation (USGS, 2013):

$$t = \frac{1}{\lambda}\ln(1 + \frac{D}{P})$$

Where t is the age of the rock, sediment or mineral specimen, D is the number of atoms of a daughter product today, P is the number of atoms of the parent isotope today, and λ is the decay constant, which is related to the half-life of a parent isotope by the equation (USGS, 2013):

$$t_{1/2} = \frac{ln2}{\lambda}$$

^{238}U is a naturally-occurring radioactive element (Figure 4.2) which is present (at low levels) in essentially all soils and sediments. Because its half-life is extremely long at 4.5 Ga, its concentration is considered to be almost constant over short periods of time. ^{226}Ra, a member of the ^{238}U decay series, exhibits the same level of radioactivity as ^{238}U, which is a result of secular equilibrium, meaning that the concentration of an isotope remains unchanged over time, as the rate of decay producing the isotope equals the rate of decay which converts the parent isotope into its daughter isotope. As such, soils everywhere are assumed to contain a low and approximately constant concentration of ^{226}Ra. The decay of ^{226}Ra produces ^{222}Rn, an inert gas which escapes into the atmosphere and further decays in the atmosphere to ^{210}Pb via few more decays involving isotopes with short half-lives (Figure 4.2), which is deposited as dust and in precipitation into lakes. ^{210}Pb is incorporated into sediment cores as it is fixed to sediment particles (Figure 4.3) (Wetzel, 2001; Flett, 2013). In recent sediments (age < 200 years), ^{210}Pb having a half-life of 22.3 years, can be used to calculate approximate ages of sediment samples (Appleby, 2001). The actual procedure for determining ^{210}Pb activity does not directly count the beta or gamma particles produced by its decay, as these are difficult to detect due to their low energy. Instead, it is common practice to calculate the activity of ^{210}Pb from counts of decays of ^{210}Po, its granddaughter isotope, as the higher energy alpha particle produced by the decay of ^{210}Po is more easily measured by less costly equipment, and ultimately yields more accurate measurements of the activity of ^{210}Pb (Evans and Rigler, 1980). Secular equilibrium between ^{210}Pb and ^{210}Po is established after 2 years, assuming a

closed system which allows no further exchange of ^{210}Pb. This is typically assured by storing sediment samples in sealed containers for a period of 2 years.

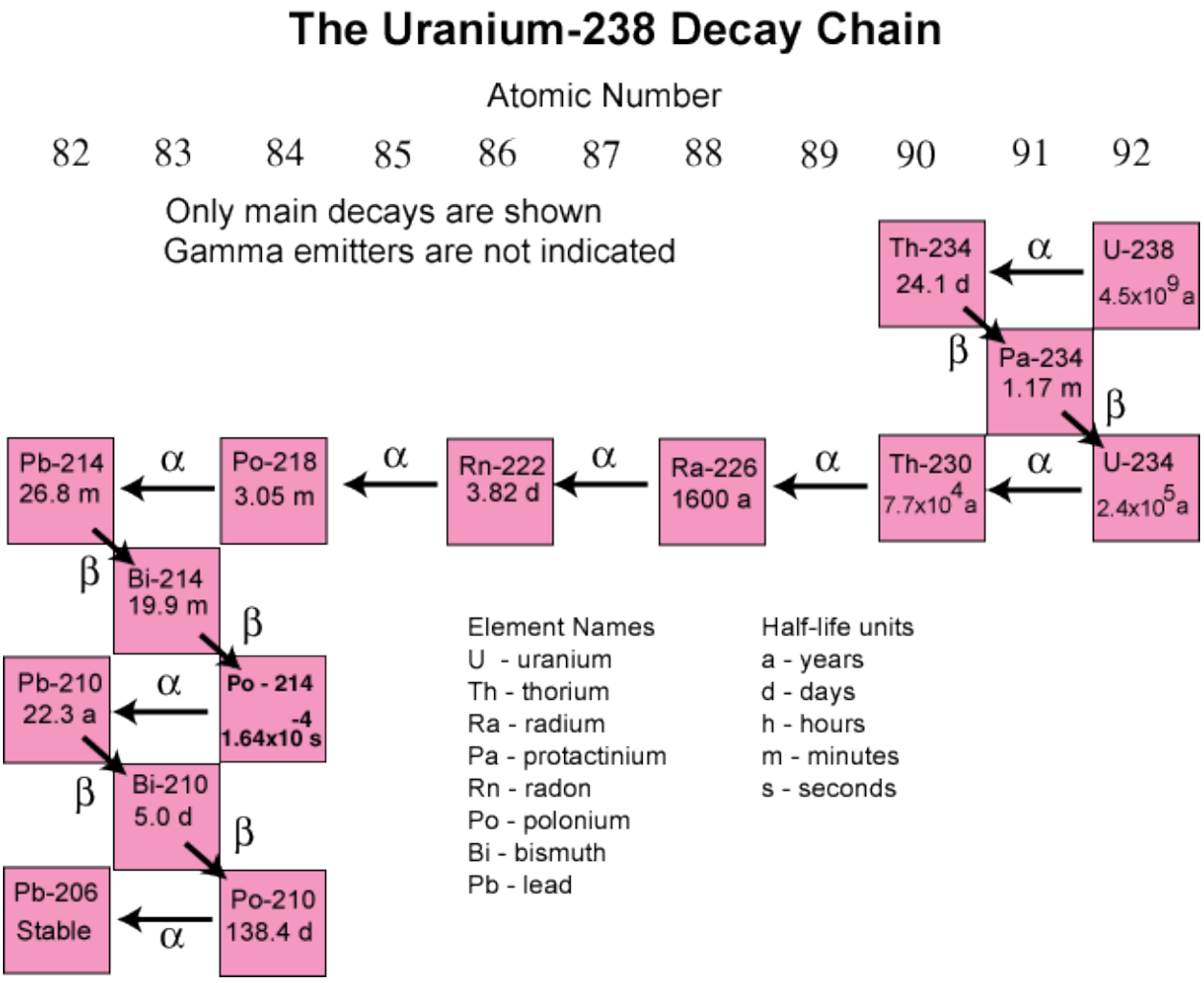

Figure 4.2: The ^{238}U decay series with half-lives of radioactive isotopes (modified from USGS, 2013).

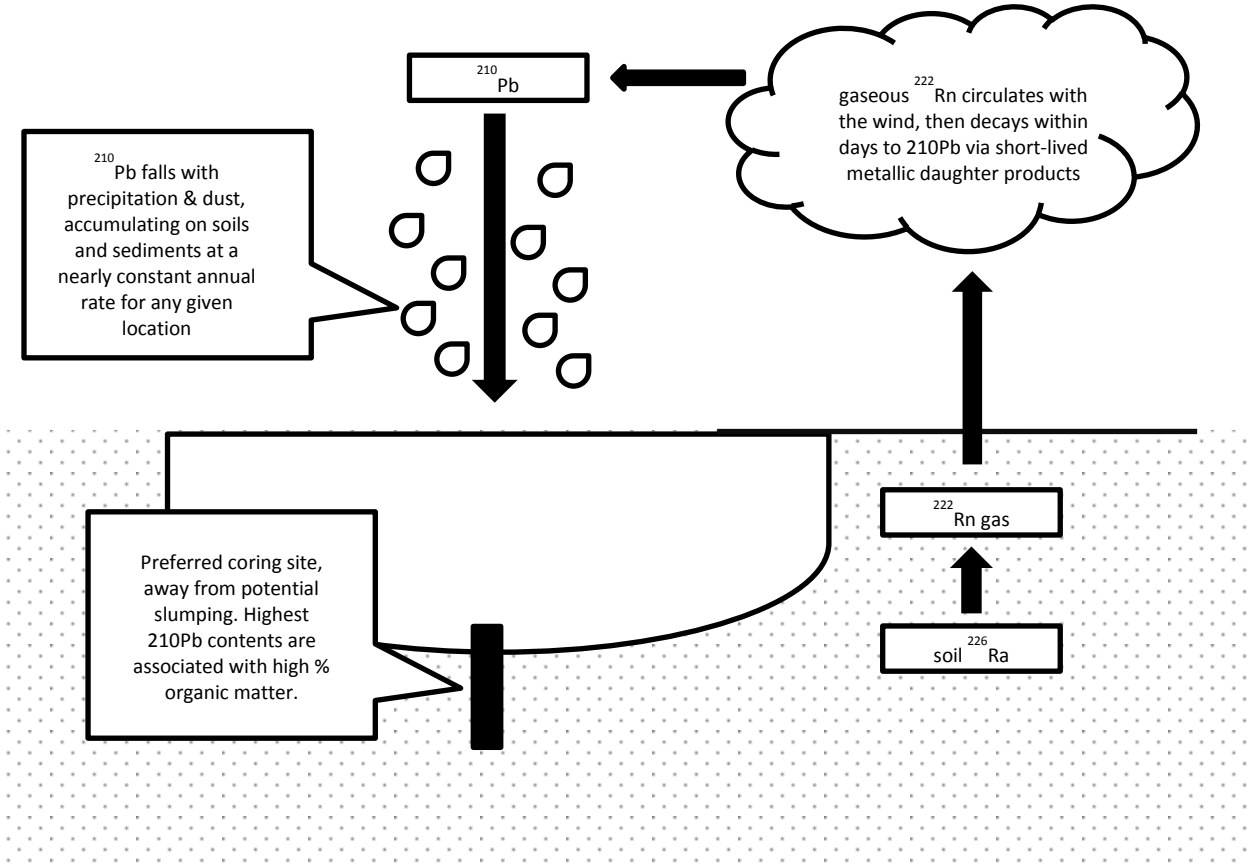

Figure 4.3: Schematic diagram illustrating the process by which ^{210}Pb is incorporated into lake sediments (modified from Flett, 2013).

Measurements of ^{210}Pb and calculations of sediment age using the constant rate of supply (CRS) model were performed by MyCore Scientific Inc. (Deep River, Ontario) in 2011, using samples from ALE1 and SL10M1. Age models for SL10W were compiled using data from an unpublished study by the Saskatchewan Ministry of the Environment. Under the CRS model, it is assumed that the bottom of the core is old enough (>150 years) that background levels of ^{210}Pb are reached. The ^{210}Pb activity of the most recent sediments is assumed to be 100% parent isotope at the time of deposition (t=0) and the bottom of the core contains 100% daughter isotope; the activity of ^{210}Pb at the bottom of the core is considered the "background" quantity. Given these assumptions, it is possible to calculate the approximate age of the sediment at any point in the core by:

i. measuring the activity of ^{210}Pb

ii. subtracting the "background" quantity

iii. establishing what proportion of the initial concentration of ^{210}Pb still remains, and

iv. calculating the time elapsed using the known half-life of ^{210}Pb of 22.3 years.

In order to improve the accuracy of the calculation of the ^{210}Po content, a known quantity of the radioactive isotope ^{209}Po having a half-life of 103 years, was added to each subsample from each core. Given that the counts of decay particles tend to "miss" a proportion of the particles, the difference between the activity calculated by counting of ^{209}Po alpha decay particles and the actual activity of ^{209}Po is expressed as a percentage and called the "carrier yield". It is used to correct the calculated activity of ^{210}Po, for greater accuracy. Around 100mg of the ^{209}Po carrier was added to the sediment samples, and samples were treated with HCl and HNO_3 and subjected to heating to 80°C over a period of 16 hours, in order to separate ^{210}Po from other alpha particle-emitting radioactive isotopes which would adversely affect the accuracy of the counts. Siliceous matter was separated by centrifugation, and samples were evaporated to dryness. Po isotopes were adhered to silver plates coated in adhesive by electroplating, in preparation for counting (Flynn, 1968). Emissions of alpha particles from ^{210}Po (5.3 MeV) and ^{209}Po (5.1 MeV) were counted for 0.5 to 2 days, and used to calculate the activity of ^{210}Po, which was then used to calculate the activity of ^{210}Pb, and finally the age of the sample. The accuracy of analyses was assured through inclusion of laboratory standards and by isotope dilution with ^{209}Po. Standard deviations (in years) of the calculated sediment ages were provided and are included in chapter 4.1.

4.3 Rock-Eval Pyrolysis

Dried sediment samples were geochemically analysed by pyrolysis and oxidation, using the Rock-Eval 6 apparatus (Vinci Technologies, France) in the organic geochemistry and petrology laboratory at the Geological Survey of Canada (GSC), Calgary.

Pyrolysis of samples (approximately 20mg) occurred in an inert atmosphere of N_2 during heating from 100 to 650°C at a rate of increase in temperature of 25°C/minute. Quantities of volatilized hydrocarbons, as CO and CO_2, were measured throughout by flame ionization detection, providing measurements of the volatile, "free" S1 fraction reported in mg HC/g sample, generated at temperatures <300°C, and the S2 fraction reported in mg HC/g sample, generated at temperatures between 300 to 650°C, which was derived from the cracking of larger molecules of organic matter within the samples. Tmax, reported in °C is recorded as the temperature at which the peak in S2 was observed (Outridge and Sanei, 2010; Sanei and Goodarzi, 2006; Sanei et al., 2005; Lafargue et al., 1998). Simultaneously, CO contents up to 570°C and CO_2 contents up to 400°C produced through thermal cracking of oxygen-bearing compounds was measured by online infrared detectors, and represented the S3 fraction, reported in mg $CO+CO_2$/g sample. Temperature limits imposed on the measurement of S3 served to avoid contamination of the signal by decomposition of inorganic carbon at higher temperatures (Sanei et al., 2005). The sum of S1, S2 and S3 is called the pyrolyzable carbon in the sample, abbreviated as PC, reported in % wt..

Following pyrolysis, samples were automatically transferred to an oxidation oven, where all of the remaining carbon was incinerated as samples were heated from 400 to 850°C. The CO and CO_2 produced were measured by online infrared detectors, yielding the residual carbon fraction between 400 and 650°C, abbreviated as RC, reported in % wt., and mineral carbon fraction between 650 and 850°C, abbreviated as MinC, reported in % wt. (Outridge and Sanei, 2010; Sanei and Goodarzi, 2006;

Sanei et al., 2005). The sum of PC and RC yields the total organic carbon in the sample, abbreviated as TOC and reported in %wt..

Hydrogen index, abbreviated as HI, is proportional to H/C and oxygen index abbreviated as OIRE6, is proportional to O/C. These parameters represent the quantities of hydrogen and oxygen-bearing compounds, respectively, normalized to the quantity of organic carbon (TOC) in the samples. They were calculated by:

$$HI = \frac{S2}{TOC} \times 100$$

$$OIRE6 = OI(CO_2) \times \frac{32}{44} + OI(CO) \times \frac{16}{28}$$

Note that OIRE6 distinguishes oxygen index calculated using measurements of CO_2 only using the older Rock-Eval 2 apparatus from those calculated by Rock-Eval 6 which uses measurements of both CO and CO_2 (Outridge and Sanei, 2010; Lafargue et al., 1998).

Inclusion of analyses of laboratory standards (9107 shale) showed accuracy and precision to be better than 5% relative standard deviation (RSD) of the measured values.

4.4 Organic Petrology

Qualitative analysis of OM in lake sediment samples was performed by microscopy in the organic geochemistry and petrology laboratory at the GSC (Calgary). Samples were placed in round plastic molds 3cm in diameter, and were impregnated with cold-setting EPOTECH epoxy-resin mixture. Cured slugs were ground and polished in stages using carborundum grit on Pelon, and then a silk-covered lap with alumina-water slurries of 0.3 and 0.05 μm.

An incident-light Zeiss Axioplan II microscope system with white and fluorescent light sources was used for examination of OM in the lake sediments. Samples were examined (total magnification

from 100x to 2500x) and digital images were captured using Zeiss Axiocam and Axiovision software. Fluorescence of OM as seen in photomicrographs was caused by ultraviolet G 365 nm excitation with a 420 nm barrier filter (Outridge and Sanei, 2010; Sanei and Goodarzi, 2006; Sanei et al., 2005).

4.5 Concentration and Stable Isotope Analysis

4.5.1 Sulfur

Total sulfur was extracted from sediment samples by Parr bomb oxidation (Seigfriedt et al., 1951). Combustion of dried sediment samples released SO_2 gas, which dissolved in a small quantity of deionized water, producing a solution containing SO_4^{2-} inside the Parr vessel over a period of approximately 20 minutes, during which the vessel was left sealed. All surfaces inside the Parr vessel were rinsed with deionized water to collect as much of the dissolved SO_4^{2-} as possible. This solution was filtered under suction to remove any particulate matter which was not combusted, and the solution was then reacted with an excess quantity of $BaCl_2$ in order to precipitate pure $BaSO_4$ for stable isotope analysis. Sediment samples were weighed prior to Parr bomb oxidation (approx. 0.2 mg), and the amount of $BaSO_4$ precipitated was weighed which allowed the quantity of sulfur (% wt.) in the sediments to be calculated.

Because of the considerable number of steps involved in producing $BaSO_4$, and the probability of incomplete combustion and precipitation reactions, the calculations of S content are not very accurate and may have errors around 20% RSD of the measured value depending on the quantity of $BaSO_4$ analyzed (B. Mayer, pers. communication).

Stable sulfur isotope analysis was performed by Continuous-Flow Isotope Ratio Mass Spectrometry (CF-EA-IRMS) using a Carlo Erba NA 1500 elemental analyzer interfaced with a Thermo Delta+XL mass spectrometer. Approximately 0.2 mg of the $BaSO_4$ precipitate was packed into high purity

tin cups and was thermally decomposed by "flash-combustion" initiated by injection of a pulse of O_2 upon sample drop onto a quartz tube combustion reactor maintained at 1050°C. Eluent SO_2 gas was swept by a He stream into the ion source of the mass analyzer (Giesemann et al., 1994).

Values of $\delta^{34}S$ were determined by comparison of sample peak areas (Vs) to those of a reference gas. Raw $\delta^{34}S$ values were corrected for instrument drift and normalized to the Vienna Canyon Diablo Troilite (VCDT) scale (Krouse and Coplen, 1997) reported in units of permil (‰), using reference materials and laboratory standards using the United States Geological Survey's Laboratory Information Management System (USGS LIMS) software. Because particulate matter which did not combust during Parr bomb oxidation was filtered out of the sample prior to stable isotope analysis, the fraction of sulfur contained in these particles eg. biogenic pyrite, is not included in the final reported value of $\delta^{34}S$ of "bulk" sulfur in the sediments. Precision of the $\delta^{34}S$ measurement of total S in sediment samples is generally better than ±0.5‰ (n=10).

4.5.2 Carbon and Nitrogen

Because this study focuses on the organic material contained within lake sediments, it was necessary to remove any carbonate minerals which may bias the measurement of $\delta^{13}C$ of organic carbon, although based on the MinC parameter analyzed by Rock-Eval pyrolysis, each sample contained less than 3% by weight of carbon-bearing inorganic minerals. Ground samples were weighed into silver capsules and placed in an ungreased glass desiccator above 500 mL of 12N hydrochloric acid. Acidification occurred over 18 hours, and calcium carbonate comprising carbonate minerals reacted with HCl to liberate C as CO_2 gas, removing it from the samples (Yamamuro and Kayanne, 1995).

Analysis of $\delta^{13}C$ and $\delta^{15}N$ in solid samples were performed by Continuous Flow-Elemental Analysis-Isotope Ratio Mass Spectrometry (CF-EA-IRMS) technology, using a Finnigan Mat Delta+XL mass

spectrometer interfaced with a Costech 4010 elemental analyzer. Dried samples were finely ground, packed into tin cups, and weighed prior to analysis. The 'Zero Blank' auto sampler dropped each sample onto a quartz tube combustion column (temperature = 1020°C), and a rapid flash combustion of each sample was initiated by the injection of a pulse of oxygen gas into the system. The produced gases, CO_2 and N_2, from NO_x species flushed through a reduction furnace, were separated and $\delta^{13}C$ and $\delta^{15}N$ values of each sample were established through the comparison of recorded sample peaks with peaks of a continuously-flowing reference gas. International (USGS40L) and internal laboratory standard (Sig-Caf, NIST-2711) materials were included at the beginning, and five-sample intervals throughout the analysis in order to normalize results to international standards, and to correct for instrument drift. Data management and drift corrections were performed using the USGS LIMS software.

$\delta^{13}C$ and $\delta^{15}N$ values were reported relative to the Pee Dee Belemnite (PDB) and atmospheric air standards, respectively, in units of parts per thousand (per mil, ‰) and have an accuracy of ±0.2‰. C and N contents were calculated from the data obtained during stable isotope analysis using the mass of the sample and the peak areas (in Vs) generated. C and N contents are reported in percent weight (%) of the sample. C/N ratios were calculated from these values, though for the purpose of this study, the TOC value from Rock-Eval pyrolysis was used rather than the %C values derived from isotopic analysis, in order to eliminate any effect on the quantity of C which may have resulted from the acid fuming treatment applied to the sediments. Given that values of N content produced during isotopic analysis are typically reproducible to ±0.1% and TOC measurements by Rock-Eval have errors of 5% RSD of the measured value, C/N ratios reported have an accuracy of 5% RSD of the measured value.

CHAPTER FIVE: RESULTS AND DISCUSSION

As the objective of this study was to assess whether industrial operations in the AOSR are having an impact on surrounding lake systems as recorded in their sediments, it is essential to be able to separate natural background values of the studied parameters from those which may have potentially been affected by industrial emissions from the AOSR. To this end, it was necessary to determine the approximate ages of the sediments in order to be able to differentiate between those deposited before the onset of anthropogenic activity in the AOSR around 1970, and those deposited after.

5.1 - ^{210}Pb Dating

Dating of the lake sediments was performed by MyCore Scientific Inc. (Deep River, Ontario), where cores were dated at 1 cm intervals, from the tops of the cores to the depth at which background values of ^{210}Pb were reached. Given that ^{210}Pb has a half-life of 22.3 years, the oldest valid dates obtained for cored samples were around 1870, with a margin of error which increased with increasing depth.

^{210}Pb activity data for ALE1, SL10W and SL10M are summarized in Table 5.1. Data for ALE and SL10M are from MyCore Scientific Inc., and SL10W data are from an unpublished scientific study by the Saskatchewan Ministry of the Environment. ^{210}Pb activity data were plotted vs. depth, and a polynomial line of best fit was applied to generate an equation or "age model" which would allow the calculation of an approximate age from any depth, in each sediment core (Figure 5.1). Equations and R^2 values are summarized in Table 5.2.

Table 5.1: ^{210}Pb activity data from counting of decay particles by MyCore Scientific Inc. (ALE and SL10M) and the Saskatchewan Ministry of the Environment (SL10W). Where a date is reported but no ^{210}Pb activity measurement exists, the date is interpolated.

ALE

Top Section Depth (cm)	210Pb (Bq/g)	Age at Top of Section (date)	Standard Deviation (years)
0	0.569	2011	0
1	0.617	2009	0
2	0.586	2006	0
3	0.537	2003	0
4	0.523	2000	1
5	0.471	1995	1
6	0.451	1991	1
7		1986	
8	0.259	1982	2
9		1977	
10	0.223	1972	3
11	0.162	1966	4
12	0.152	1961	4
13		1955	
14	0.110	1948	7
15		1943	
17	0.078	1930	13
18		1923	
19	0.060	1915	19
20	0.050	1906	25
21		1895	
22	0.032	1887	61
23	0.034	1881	60
24		1871	
25	0.026	1862	122

SL10W

Mid Section Depth (cm)	210Pb (Bq/g)	Age at Mid Section (date)
0.25	1.287	2009
1.25	1.089	2007
2.25	1.286	2003
3.25	1.506	1998
4.25	1.168	1991
5.25	1.105	1984
6.25	0.948	1976
7.25	0.782	1967
8.25	0.468	1959
9.25	0.479	1948
10.25	0.463	1935
12.25	0.483	1912
14.25	0.508	1879

SL10M

Top Section Depth (cm)	210Pb (Bq/g)	Age at Top of Section (date)	Standard Deviation (years)
0	0.423	2011	0
1	0.446	2010	0
2	0.560	2009	0
3	0.438	2007	0
4	0.344	2005	0
5	0.404	2004	1
6	0.404	2002	1
7	0.372	2000	1
8		1998	
9	0.314	1996	1
10		1994	
11	0.265	1993	1
12		1991	
13	0.278	1989	2
14		1987	
16	0.256	1983	2
17		1981	
19	0.249	1975	3
20		1972	
22	0.210	1965	5
23		1961	
25	0.149	1951	6
26		1946	
28	0.140	1935	6
29		1929	
31	0.142	1911	9
32		1896	
34	0.041	1852	36
35		1828	

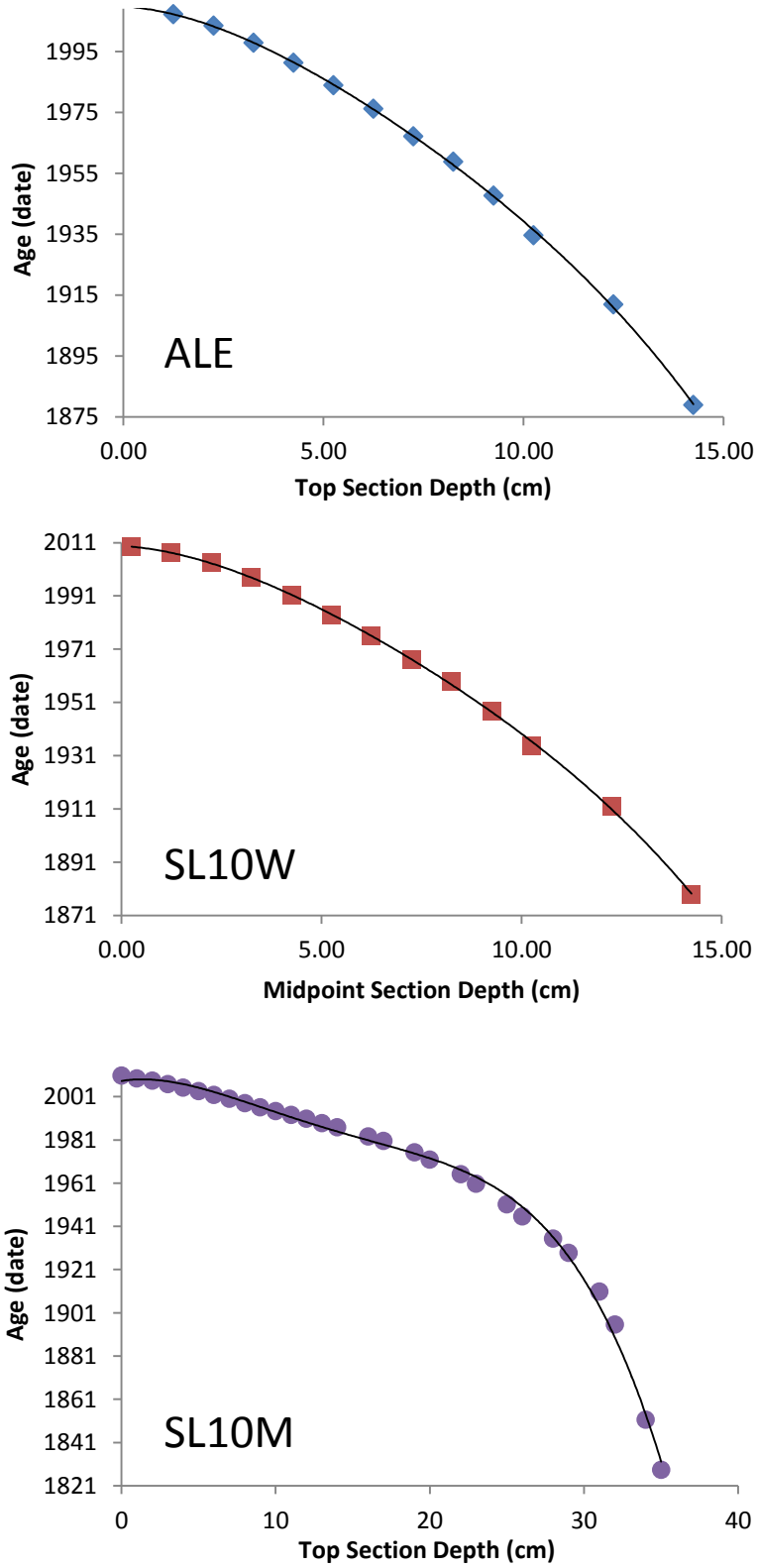

Figure 5.1: Age model graphs for lakes ALE, SL10W, SL10M.

Table 5.2: Age model equations for ALE, SL10W and SL10M with R^2 values.

Lake	Age Model Equation	R^2
ALE1	$y = -2E\text{-}05x^4 + 0.0004x^3 - 0.1279x^2 - 2.695x + 2011.6$	0.9996
SL10W	$y = -0.0026x^4 + 0.0714x^3 - 1.0802x^2 - 0.81x + 2009.8$	0.9997
SL10M	$y = -0.0005x^4 + 0.0269x^3 - 0.4739x^2 + 1.1335x + 2008.3$	0.9969

Because the SL10W core used for ^{210}Pb dating was not the same as the cores analyzed for geochemical parameters (Rock-Eval, stable isotopes, etc.), and because rates of sedimentation vary spatially (albeit only slightly) within the lake, it is expected that the dates obtained for cores SL10W1 and SL10W2 are less accurate than those computed for ALE1 or SL10M1, though it is impossible to be certain how much greater the margin of error may be.

It is important to note that depth scales do not begin at 0 cm for 3 of the 4 cores, as the uppermost sections were not compacted, and contained more water than sediment. Thus, these uppermost intervals of the freeze core were not provided for this study as they did not contain sufficient sediment to be analyzed. The depth labels on subsections of the cores provided by the GSC were used to calculate sediment ages for ALE1, SL10W1 and SL10W2 and SL10M1; assigned ages are reported in Table 5.3.

Table 5.3: Approximate ages of subsections from cores ALE1, SL10W1, SL10W2 and SL10M1 using age models. * indicates sediments which are too old to be dated by ^{210}Pb.

ALE1

Sample	Midpoint Section Depth (cm)	Midpoint Section Age (date)
ALE1-001	1.4	2008
ALE1-002	3.6	2000
ALE1-003	5.6	1993
ALE1-004	7.6	1984
ALE1-005	9.7	1974
ALE1-006	11.8	1963
ALE1-007	14.0	1949
ALE1-008	16.3	1934
ALE1-009	19.2	1913
ALE1-010	21.5	1894
ALE1-011	24.5	1868
ALE1-012	28.2	*
ALE1-013	33.1	*
ALE1-014	44.7	*
ALE1-015	55.0	*
ALE1-016	70.9	*
ALE1-017	84.6	*
ALE1-018	108.0	*

SL10W

Sample	Midpoint Section Depth (cm)	Midpoint Section Age (date)
SL10W1-001	5.3	1993
SL10W1-002	7.6	1977
SL10W1-003	9.2	1963
SL10W1-004	11.7	1937
SL10W1-005	14.3	1901
SL10W1-006	16.3	*
SL10W1-007	18.0	*
SL10W1-008	19.9	*
SL10W1-009	22.0	*
SL10W1-010	23.8	*
SL10W1-011	25.7	*
SL10W1-012	32.3	*
SL10W1-013	38.0	*
SL10W1-014	44.7	*
SL10W1-015	54.4	*
SL10W1-016	65.9	*
SL10W1-017	77.1	*
SL10W2-001	1.8	2008
SL10W2-002	4.6	1997
SL10W2-003	6.3	1986
SL10W2-004	7.7	1975
SL10W2-005	9.1	1964
SL10W2-006	10.5	1951
SL10W2-007	11.7	1938
SL10W2-008	12.9	1922
SL10W2-009	14.4	1900
SL10W2-010	15.6	*
SL10W2-011	16.8	*
SL10W2-012	18.1	*
SL10W2-013	19.6	*
SL10W2-014	21.2	*
SL10W2-015	22.5	*
SL10W2-016	23.8	*
SL10W2-017	25.3	*
SL10W2-018	27.1	*
SL10W2-019	29.2	*

SL10M

Sample	Midpoint Section Depth (cm)	Midpoint Section Age (date)
SL10M1-001	13.8	1986
SL10M1-002	15.8	1983
SL10M1-003	17.5	1980
SL10M1-004	19.3	1978
SL10M1-005	21.2	1975
SL10M1-006	23.0	1971
SL10M1-007	24.5	1967
SL10M1-008	26.0	1962
SL10M1-009	27.4	1955
SL10M1-010	28.8	1946
SL10M1-011	30.4	1934
SL10M1-012	32.1	1915
SL10M1-013	33.9	1890
SL10M1-014	38.9	*
SL10M1-015	44.3	*
SL10M1-016	52.4	*
SL10M1-017	65.2	*
SL10M1-018	77.9	*
SL10M1-019	92.0	*

1970 is taken to be the beginning of major regional anthropogenic activity in the AOSR in this study. In ALE1, only the uppermost 24.5 cm could be dated by ^{210}Pb, and only the uppermost 9.7 cm of sediment were more recent than approximately 1970. In SL10W1 and SL10W2, only the uppermost 14.3

and 14.4 cm, respectively, could be dated by ^{210}Pb and only the uppermost 7.6 and 7.7 cm, respectively, were dated as more recent than 1970. In SL10M1, the uppermost 33.9 cm were dateable by ^{210}Pb, and the uppermost 23.0 cm were dated post-1970. Sediments deposited prior to 1970 at depths greater than 9.7, 7.6, 7.7 and 33.9cm are believed not to have been impacted by any major local anthropogenic activity.

For further geochemical analysis, core subsamples which could potentially show anthropogenic impact from industrial emissions derived from the AOSR after 1970, are ALE1-001 through ALE1-005 (n=5), SL10W1-001 and SL10W-002 (n=2), SL10W2-001 through SL10W2-004 (n=4) and SL10M1-001 through SL10M1-006 (n=6). Deposition under both pre and post-industrialization conditions are represented in each core. However, because of the way the core was subdivided for analysis, there are few data points to establish any potential trend of change occurring in sediments deposited after 1970, particularly in cores from SL10W.

5.2 Characterization of Lake Sediments Using Organic Petrology, Rock-Eval Pyrolysis, C:N Ratios and Carbon Isotope Ratios

5.2.1 Qualitative Analysis by Organic Petrology

Incident reflected light microscopy was used in this study as a qualitative tool to characterize the organic matter (OM) in the sediments, and to support interpretations of the Rock-Eval, C/N ratio and $\delta^{13}C$ data. Three to four slides were created for each core from unaltered (dried, unground, untreated by acid) sediment. Types of OM macerals were analyzed microscopically,using white and fluorescent light microscopy. Labile fractions of OM (lipids, pigments, algal cell walls, etc.) emit blue or red fluorescence (400-700 nm) depending on their degree of chemical reactivity when excited in UV or blue light, and are also the first to be degraded upon OM deposition (Sanei and Goodarzi, 2006; Sanei et al., 2005; Hurley and Armstrong, 1991; Hurley and Armstrong, 1990; Leavitt and Carpenter, 1990; Goossens et al., 1989). Due to a shortage of sediment left-over for creation of the slides, it was necessary to combine some of the depth intervals, thus no comments on changes in quality of OM with depth were possible.

Lake sediments contained some combination of the following organic, organically-derived and inorganic particles:

- organic detritus called liptodetrinite; small lipid-rich detrital particles which are too broken to be identified as a particular liptinite maceral (in all lakes)
- Siliceous diatom frustule with entrapped oil, lipids, and pigments (in all lakes)
- particles of microbial mats (in SL10W and SL10M)
- bisaccate pollen grains typical of conifers having two “chambers” or a “mickey mouse” appearance (EHRC, 2005) (in all lakes)
- “muddy” (clay) matrix composed of inorganic mineral particles too small to be identified by microscopy (in ALE), and

- Char (inertinite), which shows a high degree of reflectance under reflected light and has a distinctive vacuolated “swiss cheese” texture (in ALE1 and SL10W).
- Fragments of bacterial mats (in SL10W and SL10M).

Typical appearances of these components are shown in Figure 5.2.

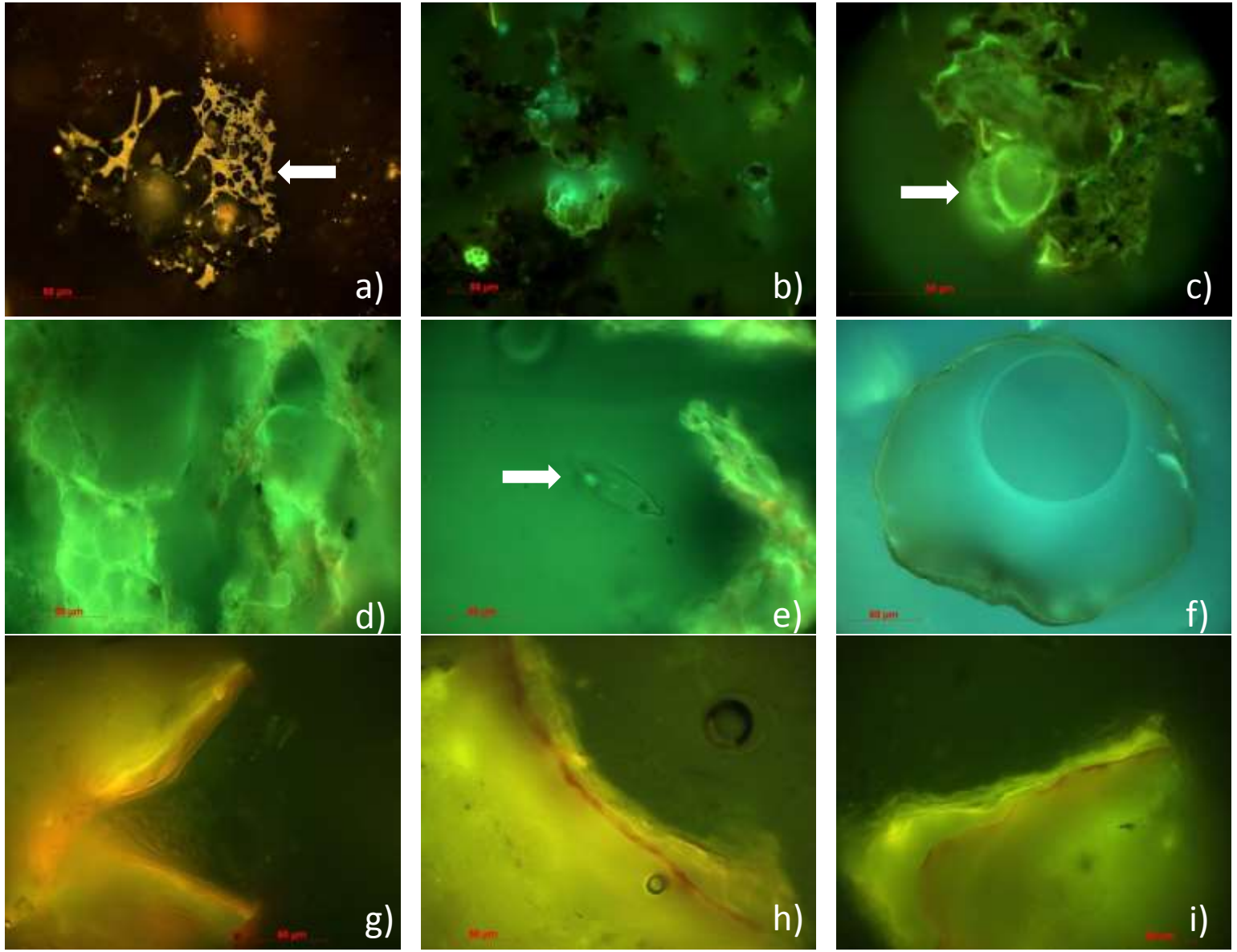
a)
b)
c)
d)
e)
f)
g)
h)
i)

Figure 5. 2: Typical appearances of lake sediment components under the microscope. a) Char exhibiting vacuolated texture. b) "Muddy matrix"; note dark opaque appearance. c) Bisaccate pollen grain with "mickey mouse" shape. Two "chambers" are visible. d) Liptodetrinite, coated with red-fluorescing labile pigments. E) Siliceous diatom frustule. f) "Broken" portion of a microbial mat as it appears after sedimentation/deposition. g), h), i) Microbial mat "standards", illustrating unbroken "original" appearance of mats prior to sedimentation (Sanei and Carrie, unpublished data).

Alberta Lake E (ALE)

"Typical" appearance of ALE sediments is depicted by photomicrographs in Figure 5.3. Muddy matrix is abundant, mixed with particles of liptodetrinite. Blue or red fluorescence indicative of the presence of labile organic fractions such as pigments and geolipids are limited or absent in most sediments of core ALE1, indicating that they have been at least partially degraded.

Some bisaccate pollen grains are also present, typical of the conifers which make up the majority of the trees in the boreal forest region in which this lake is located. Char, exhibiting characteristic vacuolated texture, is also present, indicative of forest fires in the area. No bacterially-derived framboidal pyrites, which would have been a likely indication of bacterial sulfate reduction (BSR) occurring in sediments (Berner, 1984), were observed in ALE sediments. This indicates either an absence of active BSR possibly resulting from a small supply of dissolved sulfate in lake water, or insufficient available Fe, which is required to form pyrite. Given the high level of primary productivity in this lake, it is likely that the lake bottom experiences anoxic conditions which are favorable for BSR, and the lack of framboidal pyrites is more likely a result of a lack of available Fe.

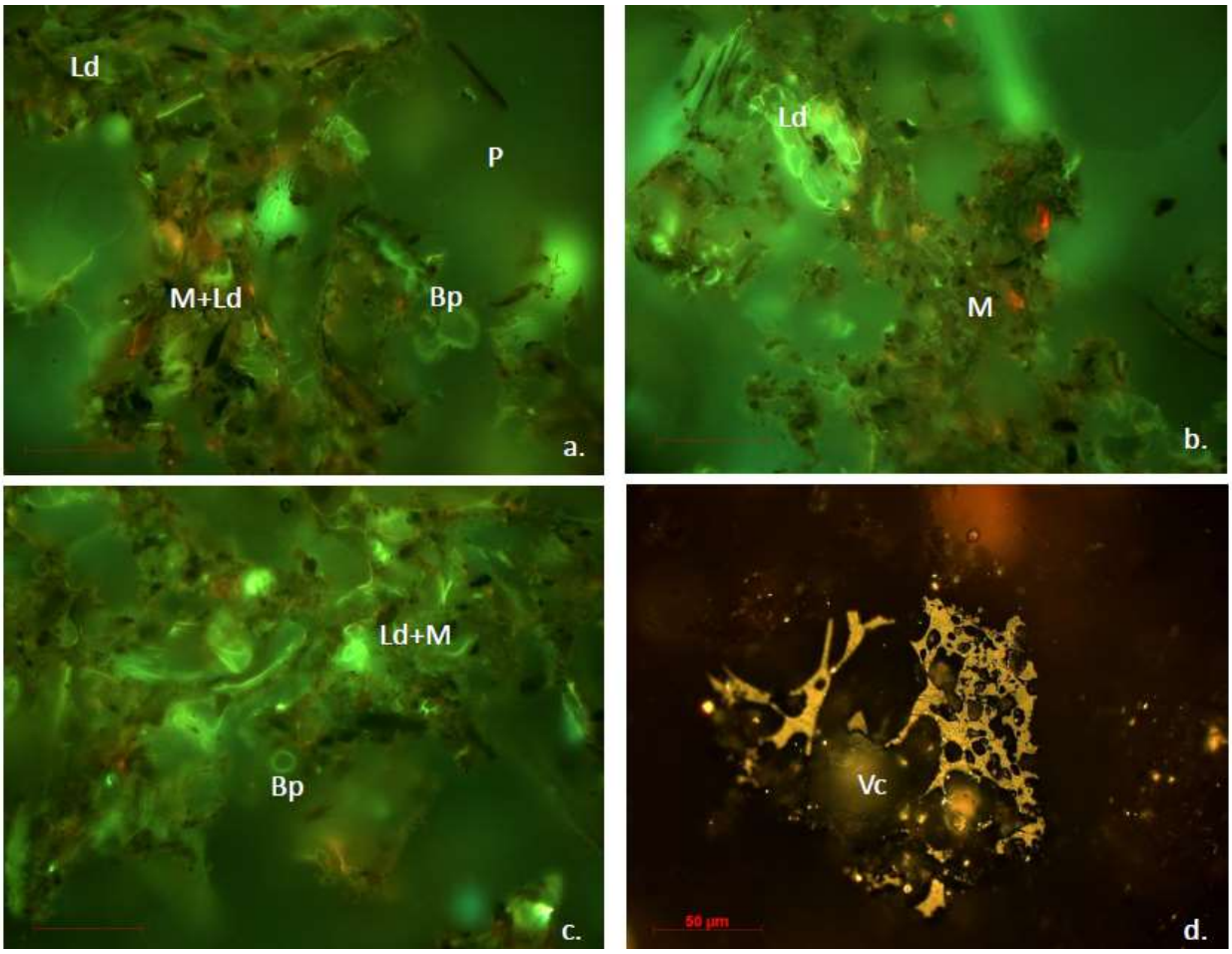

Figure 5.3: Photomicrographs of ALE sediments. a) Sediments in UV light, composed of a mixture of muddy matrix (M) and liptodetrinite (Ld), with a partially-broken bisaccate pollen grain (Bp). Pore space (P) in the sediments is filled with epoxy and appears a dull green color in UV light. Slight red fluorescence indicates the presence of small particles of labile OM. b) Sediments in UV light showing a larger liptodetrinite particle, and muddy matrix. c) UV light photogmicrograph showing a mixture of liptodetrinite particles and muddy matrix and a small bisaccate pollen grain. d) A piece of char in reflected light, exhibiting vacuolated texture.

Saskatchewan Lakes (SL10W, SL10M)

Liptodetrinite particles in SL10W (Figure 5.4) and SL10M (Figure 5.5) were generally larger than those present in ALE. Larger "chunks" of OM containing labile pigments which fluoresced strongly (blue or red) in blue light indicate that OM in SL10W and SL10M is in general more reactive and thus more freshly-deposited or better preserved than that in ALE sediments. Some intact diatoms were visible, as well as better-preserved examples of bisaccate pollen grains. Char particles were present in both SL10W and SL10M. SL10W and SL10M also contained debris from bacterial mats (SL10M to a greater degree than SL10W though exact proportions are difficult to estimate) which had a filamentous or "wavy" appearance similar to standards (Figure 5.2) (Sanei and Carrie, unpublished data). No bacterially-derived framboidal pyrites were observed in these sediments, though like in the case of ALE1, it is more likely that there was a lack of the available Fe required for pyrite formation, rather than a complete absence of BSR in the sediments of SL10W.

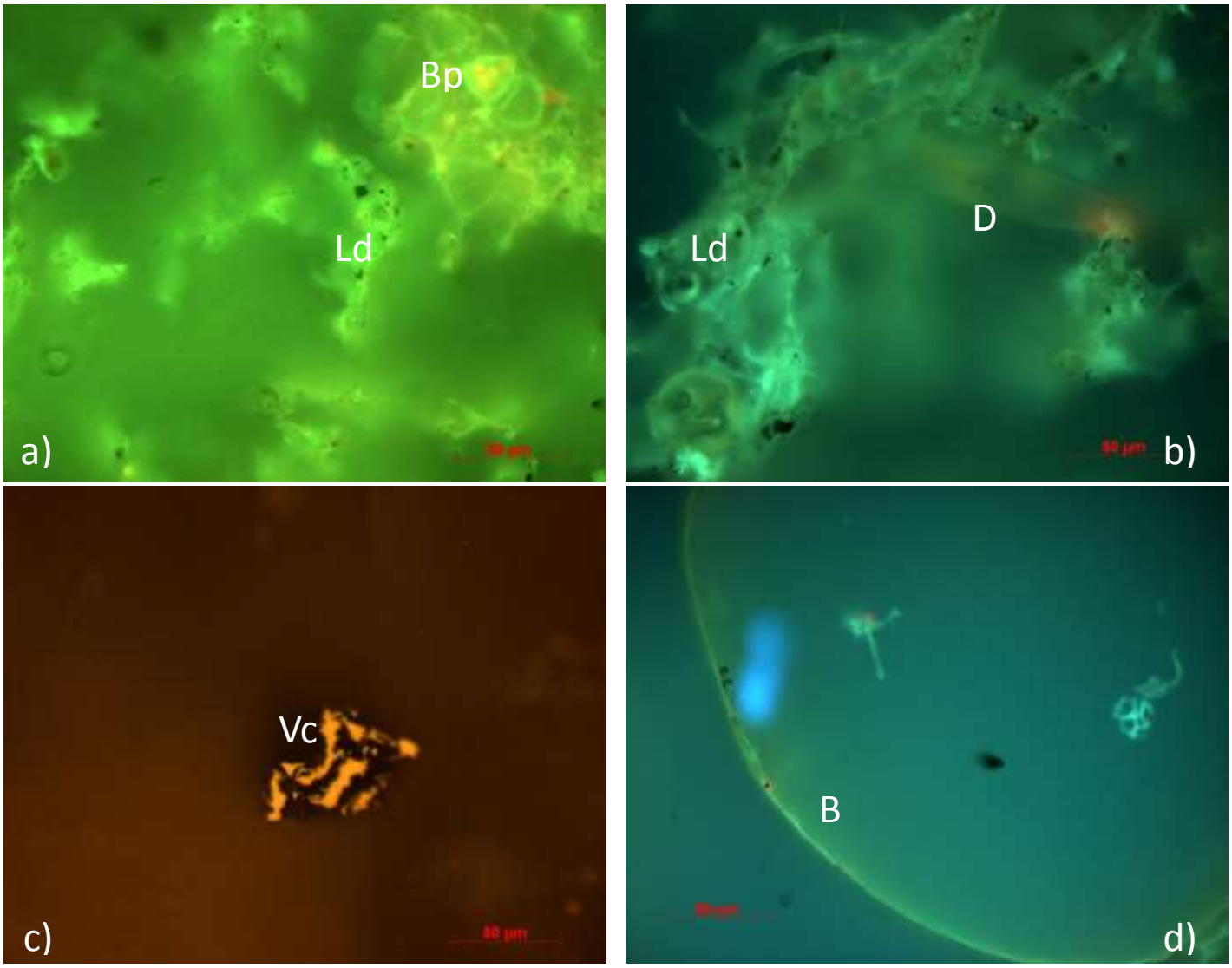

Figure 5.4: Photomicrographs of SL10W sediments. a) Sediments in UV light, composed of a mixture of liptodetrinite (Ld), with a bisaccate pollen grain (Bp). Note reddish fluorescence of labile organic compounds. b) Sediments in blue light showing liptodetrinite particles, and an intact diatom (D). Slight red fluorescence indicates the presence of labile organic compounds. c) Reflected light photomicrograph of a piece of char (Vc) with vacuolated texture. d) A filamentous strand of a bacterial mat (B) in blue light. Blue fluorescence indicates the presence of labile organic compounds in the OM.

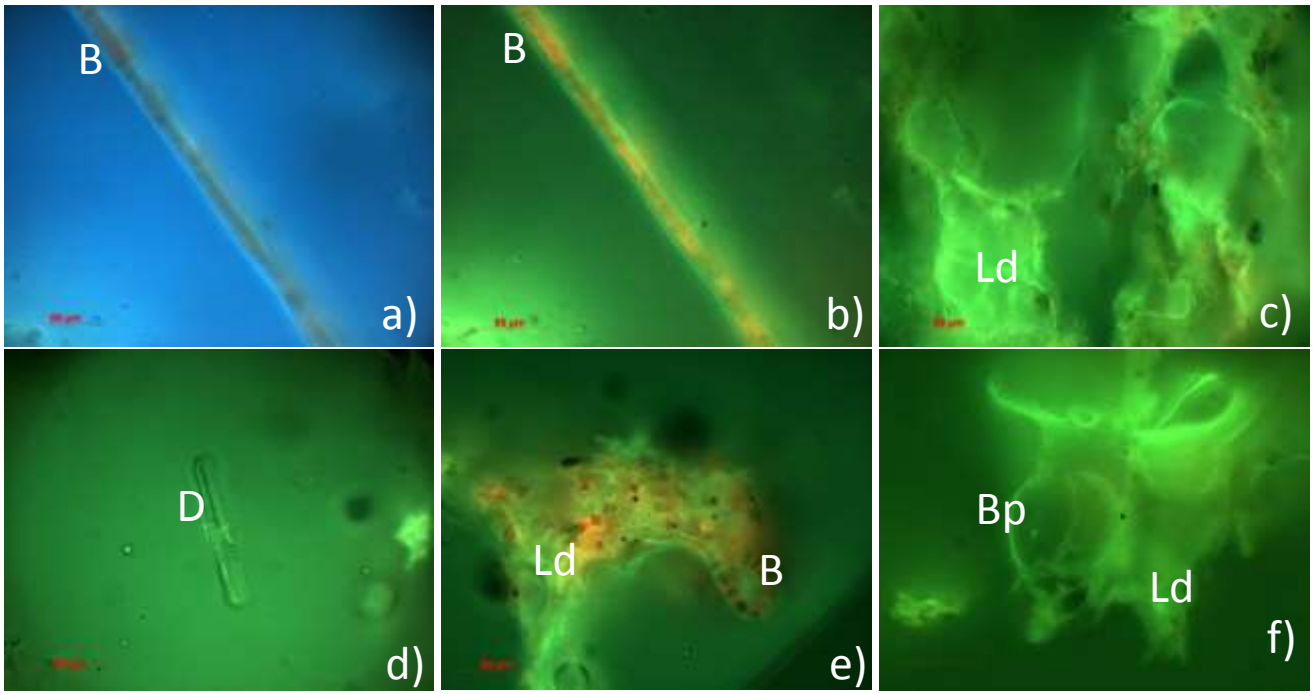

Figure 5.5: Photomicrographs of SL10M sediments. a) Filamentous strand of bacterial mat (B) in UV light. b) Filamentous strand of bacterial mat in blue light. c) Liptodetrinite (Ld) in UV light. Slight red fluorescence indicates the presence of labile organic compounds in the OM. d) A diatom (D) in UV light. e) Red-fluorescing (fresh) liptodetrinite, stuck to a fragment of bacterial mat in UV light. f) Liptodetrinite and a bisaccate pollen grain (Bp) in UV light.

5.2.2 Rock-Eval Pyrolysis

Rock-Eval pyrolysis has traditionally been used for rapid-screening of potential hydrocarbon source rocks (Espitalié et al., 1985). Measured parameters provide information about the quantity (TOC = PC+RC), type and chemical composition (S1, S2, S3, HI, OIRE6) and maturity (Tmax) of OM, as well as the quantity of inorganic C contained in a given sample, composed of carbon-bearing minerals (minC).

More recently, this technique has also been used as a basic analysis tool for OM in recent soils and peats (Outridge and Sanei, 2010; Sebag et al., 2006; Disnar et al., 2003), river and stream sediments (Carrie et al., 2009; Reyes et al., 2006) and lake sediments (Sanei and Goodarzi, 2006; Sanei et al., 2005). The first study intended to standardize Rock-Eval pyrolysis approaches for use in the analysis of OM in recent aquatic sediments was only published very recently (Carrie et al., 2012).

Each subsample of each core from ALE, SL10W and SL10M was analyzed by Rock-Eval pyrolysis, for TOC, S1, S2, S3, HI, OIRE6, PC, RC, Tmax, and MinC.

TOC, representing the sum of pyrolysable (PC) and refractory (RC) organic carbon in a sample, is a proxy for a combination of the rate of primary productivity and degree of preservation of OM in lake sediments (Carrie et al., in press; Meyers and Teranes, 2001). Average TOC contents in cores ALE1, SL10W1, SL10W2 and SL10M1 range between 21.0 and 26.2% (Table 5.4), indicating that the sediments in this study are very rich in organic matter, comparable to an average TOC content of 24.8% reported for lake sediments from the Boreal-Oilsands area in Carrie et al. (in press). TOC contents are fairly constant up through the length of core ALE1 (RSD=3%), while TOC in SL10W1, SL10W2 and SL10M1 were more vertically variable (RSD = 16, 9, 25% respectively) and had a weak upward trend of increasing TOC contents (Figure 5.6), likely related to a greater degree of degradation of OM in older sediments down-depth.

Table 5.4: Measured Rock-Eval pyrolysis parameters and calculated ratios for samples from ALE1, SL10W1, SL10W2 and SL10M1.

Midpoint Section Depth (cm)	TOC (wt. %)	PC (wt. %)	RC (wt. %)	PC/TOC	RC/TOC	MinC (wt. %)
			ALE1			
1.4	27.2	11.4	15.8	0.4	0.6	1.3
3.6	25.8	11.0	14.8	0.4	0.6	1.2
5.6	26.2	11.0	15.2	0.4	0.6	1.2
7.6	25.9	10.7	15.2	0.4	0.6	1.2
9.7	26.5	10.8	15.7	0.4	0.6	1.2
11.8	25.9	10.7	15.1	0.4	0.6	1.1
14.0	26.2	11.1	15.1	0.4	0.6	1.2
16.3	26.4	11.0	15.4	0.4	0.6	1.2
19.2	26.5	11.2	15.3	0.4	0.6	1.1
21.5	26.4	11.2	15.2	0.4	0.6	1.1
24.5	25.6	10.7	14.9	0.4	0.6	1.1
28.2	27.2	12.1	15.2	0.4	0.6	1.1
33.1	26.0	10.7	15.3	0.4	0.6	1.1
44.7	26.0	10.5	15.5	0.4	0.6	1.2
55.0	24.4	9.5	14.8	0.4	0.6	1.1
70.9	27.6	10.8	16.8	0.4	0.6	1.4
84.6	26.0	9.9	16.1	0.4	0.6	1.3
108.0	24.5	9.2	15.3	0.4	0.6	1.3
AVERAGE	**26.1**	**10.8**	**15.4**	**0.4**	**0.6**	**1.2**
S.D.	**0.8**	**0.7**	**0.5**	**0.0**	**0.0**	**0.1**
			SL10W1			
5.3	25.2	13.4	11.8	0.5	0.5	2.9
7.6	28.2	16.0	12.2	0.6	0.4	1.6
9.2	29.2	16.3	12.9	0.6	0.4	1.5
11.7	29.2	16.5	12.8	0.6	0.4	1.5
14.3	30.0	17.2	12.8	0.6	0.4	1.2
16.3	31.1	17.8	13.3	0.6	0.4	0.9
18.0	29.6	16.7	12.9	0.6	0.4	1.1
19.9	28.2	16.0	12.2	0.6	0.4	1.0
22.0	26.8	15.1	11.8	0.6	0.4	0.9
23.8	26.1	14.6	11.5	0.6	0.4	0.9
25.7	26.1	14.8	11.3	0.6	0.4	0.8
32.3	26.2	14.9	11.4	0.6	0.4	0.9
38.0	23.1	13.0	10.1	0.6	0.4	0.8
44.7	20.1	11.0	9.1	0.5	0.5	0.8
54.4	19.3	10.8	8.5	0.6	0.4	0.7
65.9	25.4	14.9	10.6	0.6	0.4	0.8
77.1	15.6	9.1	6.5	0.6	0.4	0.6
AVERAGE	**25.8**	**14.6**	**11.3**	**0.6**	**0.4**	**1.1**
S.D.	**4.2**	**2.4**	**1.8**	**0.0**	**0.0**	**0.5**
			SL10W2			
4.6	19.2	11.3	7.9	0.6	0.4	0.6
6.3	25.9	15.0	10.9	0.6	0.4	0.9

7.7	28.3	16.0	12.3	0.6	0.4	0.8
9.1	28.5	16.4	12.2	0.6	0.4	0.8
10.5	28.5	16.3	12.2	0.6	0.4	0.7
11.7	28.2	16.4	11.8	0.6	0.4	0.7
12.9	28.1	16.0	12.0	0.6	0.4	0.8
14.4	27.8	15.6	12.2	0.6	0.4	0.8
16.8	28.2	16.5	11.7	0.6	0.4	0.7
18.1	24.7	14.7	10.0	0.6	0.4	0.6
19.6	23.9	14.3	9.6	0.6	0.4	0.6
21.2	23.5	14.1	9.5	0.6	0.4	0.5
22.5	26.5	15.7	10.9	0.6	0.4	0.6
23.8	27.1	16.0	11.1	0.6	0.4	0.6
25.3	28.3	16.2	12.0	0.6	0.4	0.6
27.1	27.3	16.1	11.2	0.6	0.4	0.7
29.2	28.6	16.8	11.8	0.6	0.4	0.6
AVERAGE	**26.6**	**15.5**	**11.1**	**0.6**	**0.4**	**0.7**
S.D.	**2.5**	**1.3**	**1.2**	**0.0**	**0.0**	**0.1**

SL10M1

13.8	21.7	11.9	9.8	0.5	0.5	0.7
15.8	25.7	14.2	11.5	0.6	0.4	0.8
17.5	27.0	15.7	11.3	0.6	0.4	0.7
19.3	25.3	14.2	11.1	0.6	0.4	0.7
21.2	26.4	15.2	11.2	0.6	0.4	0.7
23.0	26.0	14.5	11.5	0.6	0.4	0.6
24.5	26.3	14.8	11.5	0.6	0.4	0.7
26.0	21.5	11.8	9.7	0.5	0.5	0.5
27.4	23.4	13.1	10.3	0.6	0.4	0.5
28.8	18.2	10.0	8.2	0.5	0.5	0.6
30.4	14.9	8.1	6.7	0.5	0.5	0.4
32.1	16.6	9.3	7.3	0.6	0.4	0.4
33.9	15.8	8.9	6.8	0.6	0.4	0.4
38.9	22.7	12.7	10.0	0.6	0.4	0.5
44.3	17.7	10.1	7.7	0.6	0.4	0.4
52.4	24.5	13.7	10.8	0.6	0.4	0.5
65.2	20.0	11.3	8.7	0.6	0.4	0.4
77.9	19.0	10.8	8.2	0.6	0.4	0.4
92.0	7.0	4.0	3.0	0.6	0.4	0.2
AVERAGE	**21.0**	**11.8**	**9.2**	**0.6**	**0.4**	**0.5**
S.D.	**5.2**	**2.9**	**2.3**	**0.0**	**0.0**	**0.2**

MinC is the measurement of the quantity (wt. %) of carbon contained in inorganic minerals. The average mineral carbon contents of ALE1 (1.2±0.1%) is somewhat higher than MinC contents of SL10W2 (0.7±0.1%) and SL10M1 (0.5±0.2%), which is expected given the greater quantity of "muddy" mineral matrix observed in photomicrographs of ALE1 sediments relative to those from either Saskatchewan lake. The MinC content of SL10W is consistently around 0.9% from the bottom of the core to a depth of 16.3cm, and increased sharply thereafter, from 0.9 to 2.9%, giving it an overall average of 1.1% with a

standard deviation of 0.5%. Were SL10W1 taken closer to the lake's edge relative to SL10W2, evaporation could provide one possible explanation for the increase in MinC. Presumably, sources of mineral carbon in lake sediments are more likely washed into the lake from the surrounding terrestrial ecosystem, rather than produced in the water column. Were SL10W shrinking over time as a result of evaporation, the point from which SL10W1 was taken would get "closer" to the lake's shoreline. Because lakes tend to be low-energy systems, it is not expected that sediments which have been washed in would be transported far from the lake's shore before being deposited into the sediment record, thus sediments more proximal to the shore would likely be richer in mineral carbon. The observed up-core increase in MinC could be explained by this phenomenon.

RC, which refers to the proportion of highly-resistant refractory or "dead" carbon referred-to as inertinite (Carrie et al., 2012), is notably higher in ALE1 than in either Saskatchewan lake, with an average value of 15.4% versus ~11% or less in SL10W and SL10M. All components of OM contribute to RC to some degree (Carrie et al., 2012), and the boreal forest ecosystem in which these lakes are located likely also contribute to this fraction through particles of char produced during forest fires. PC content is the labile fraction of the OM, and is calculated as the sum of the S1, S2 and S3 fractions (Table 5.5). Depth trends may be qualitatively related to degree of degradation, but the PC, RC, S1, S2 and S3 fractions are more typically used in conjunction with other parameters in order to infer overall type of OM or freshness of OM. S1 and S2, which is the sum of S2a and S2b, are measured in mg HC/g sample. S1 comprises the smallest, most labile compounds (molecular weights <500g/mol) that are typically first to be degraded by microbial action on sedimented OM (Carrie et al., in press; Carrie et al., 2012; Meyers and Teranes, 2001). S2 is composed of slightly more resistant compounds including larger lipid molecules and humified material (S2a and S2b, respectively) (Carrie et al., 2012; Disnar et al., 2003). S3CO and $S3CO_2$ represent more oxygen-rich molecules, such as carbohydrates, and are reported in mg CO/g sample and mg CO_2/g sample, respectively (Carrie et al., 2012).

Table 5.5: Measurements of PC components of OM in samples from ALE1, SL10W1, SL10W2 and SL10M1.

Midpoint Section Depth (cm)	S1 (mg HC/g)	S2a (mg HC/g)	S2b (mg HC/g)	S2a+S2b= S2 (mg HC/g)	S3 CO (mg CO/g)	S3 CO_2 (mg CO_2/g)
			ALE1			
1.4	24.0	39.7	56.3	96.0	10.2	37.8
3.6	23.3	36.9	55.3	92.2	9.9	35.7
5.6	23.8	36.5	55.2	91.7	10.1	36.1
7.6	22.2	35.6	53.8	89.5	9.9	35.8
9.7	22.6	36.0	54.5	90.5	10.0	36.5
11.8	22.8	35.4	54.3	89.7	9.8	35.7
14.0	22.6	36.9	57.0	93.9	10.3	36.5
16.3	22.5	36.1	56.4	92.5	10.3	35.7
19.2	22.4	36.8	58.7	95.4	10.5	36.1
21.5	22.5	36.6	59.1	95.7	10.5	35.8
24.5	20.5	35.1	56.9	92.1	10.3	34.8
28.2	20.7	38.3	69.5	107.8	10.6	34.7
33.1	19.5	34.8	57.8	92.6	10.4	34.6
44.7	18.9	34.2	56.7	90.9	9.9	33.7
55.0	16.6	31.3	51.8	83.1	9.3	31.7
70.9	17.4	34.9	61.3	96.1	10.4	35.0
84.6	16.0	32.0	55.5	87.5	9.7	33.1
108.0	14.9	30.1	50.8	80.9	9.2	31.3
AVERAGE	**20.7**	**35.4**	**56.7**	**92.1**	**10.1**	**35.0**
S.D.	**2.9**	**2.4**	**4.0**	**5.7**	**0.4**	**1.7**
			SL10W1			
5.3	52.7	44.9	42.3	87.2	11.9	47.7
7.6	67.7	53.8	48.4	102.2	12.3	48.9
9.2	71.0	53.7	50.6	104.3	10.8	48.1
11.7	73.9	51.1	52.2	103.3	10.1	48.2
14.3	75.2	55.2	54.5	109.7	10.9	49.6
16.3	79.4	57.5	55.4	113.0	11.4	50.5
18.0	71.7	56.4	52.4	108.8	10.2	46.9
19.9	65.6	54.4	54.1	108.5	9.7	43.1
22.0	57.4	49.7	56.8	106.5	10.0	37.2
23.8	54.9	50.0	54.0	104.0	8.8	37.2
25.7	57.4	48.8	55.4	104.2	9.3	35.1
32.3	56.9	48.6	56.8	105.4	9.5	35.3
38.0	50.1	43.1	49.1	92.1	8.5	31.5
44.7	40.3	36.2	43.5	79.7	7.7	27.2
54.4	36.5	35.1	46.9	82.0	7.0	24.0
65.9	51.6	47.7	65.8	113.5	8.7	29.8
77.1	33.4	30.9	35.1	66.0	5.8	20.7
AVERAGE	**58.6**	**48.1**	**51.4**	**99.4**	**9.6**	**38.9**
S.D.	**13.8**	**7.8**	**6.9**	**13.3**	**1.7**	**9.8**

			SL10W2			
1.8	37.4	30.3	36.4	66.8	6.4	21.1
4.6	38.4	35.1	51.2	86.3	6.4	23.8
6.3	64.8	45.3	53.5	98.8	11.0	35.3
7.7	67.1	47.0	60.4	107.4	12.1	36.6
9.1	70.2	47.8	61.6	109.4	10.6	36.8
10.5	68.1	47.5	63.3	110.7	11.5	36.6
11.7	68.3	47.8	63.4	111.2	11.1	35.9
12.9	67.3	46.2	62.0	108.2	11.0	36.1
14.4	62.2	45.2	62.5	107.7	11.0	36.1
15.6	67.7	47.8	68.1	115.9	11.1	36.3
16.8	69.1	46.3	67.0	113.3	10.9	34.5
18.1	59.1	42.5	60.4	102.9	9.1	30.2
19.6	56.0	40.0	62.5	102.4	9.5	28.2
21.2	53.7	39.4	62.8	102.2	9.3	26.8
22.5	58.6	43.3	71.6	114.9	10.3	30.2
23.8	59.2	44.8	73.2	118.0	10.6	30.8
25.3	57.9	45.3	76.6	121.9	10.5	31.7
27.1	49.0	42.6	88.4	131.0	9.2	28.8
29.2	49.0	46.4	91.7	138.1	10.0	30.2
AVERAGE	**59.1**	**43.7**	**65.1**	**108.8**	**10.1**	**31.9**
S.D.	**9.9**	**4.7**	**12.3**	**15.3**	**1.5**	**4.7**
			SL10M1			
13.8	49.6	33.5	46.7	80.2	8.3	27.8
15.8	58.2	40.8	55.4	96.2	9.8	34.0
17.5	63.2	44.3	64.6	108.9	11.6	34.6
19.3	59.0	40.0	56.3	96.3	9.5	31.9
21.2	61.8	43.3	61.2	104.5	10.6	34.4
23.0	57.1	39.2	62.5	101.7	11.1	31.5
24.5	57.4	41.8	63.6	105.4	9.5	32.5
26.0	45.4	33.1	50.5	83.7	8.4	25.9
27.4	49.4	35.6	59.9	95.5	8.3	27.0
28.8	35.7	27.1	46.5	73.5	7.3	22.1
30.4	29.4	21.9	37.8	59.7	5.9	17.7
32.1	33.4	25.4	44.2	69.6	6.0	19.3
33.9	31.8	24.3	42.6	66.9	5.7	17.9
38.9	43.3	34.1	63.2	97.3	8.0	24.7
44.3	34.0	27.3	50.3	77.6	6.8	19.2
52.4	44.6	36.0	70.8	106.8	9.5	25.7
65.2	36.2	29.6	58.9	88.4	7.7	21.1
77.9	34.6	27.8	57.6	85.4	7.3	19.4
92.0	13.5	10.4	20.8	31.2	2.6	7.7
AVERAGE	44.1	32.4	53.3	85.7	8.1	25.0
S.D.	13.4	8.6	11.8	19.6	2.2	7.2

Residual carbon (RC) and pyrolyzable carbon (PC) contents are typically interpreted in terms of depth trends or in conjunction with other parameters, rather than by individual values. In all three lakes, the relative contributions of RC and PC to the TOC content (PC/TOC, RC/TOC; Table 5.4) are constant

with depth, indicating that any increase or decrease in TOC content is a result of proportional increases or decreases, respectively, in both PC and RC. Figure 5.6 shows variations in TOC and S1 by depth for each of the four cores. ALE1 shows very little variation with depth, while TOC contents of SL10W1 decrease with increasing depth (from ~30 to 15%), likely indicating degradation of the more labile portions of OM, which is also reflected in the plot of S1 data with depth. SL10W2 does not exhibit any strong trend of decreasing TOC with depth, perhaps as a result of its shorter length relative to any of the other 3 cores. TOC contents of SL10M1 sediments also appear to decrease with increasing depth, averaging 25% in the top 27 cm of the core and 18% in the bottom 65 cm, although data from SL10M are considerably more variable (RSD = ~20%) than in ALE or SL10W, making the trend somewhat less apparent.

ALE1 has a lower average S1 content of 20.7±2.9 mg HC/g, relative to SL10W1, SL10W2 and SL10M1 (58.6±13.8, 59.1±9.9 and 44.1±13.4 mg HC/g, respectively) which indicates that there are fewer labile molecules composing the sedimented OM in ALE1, likely a result of a lesser "freshness" of OM in ALE1 versus either of the Saskatchewan lake sediments.

HI and OIRE6 are calculated from S2, S3CO, $S3CO_2$ and TOC (Table 5.6). These are roughly equivalent to H:C and O:C ratios of OM. The original van Krevelen crossplot used H:C and O:C ratios of kerogen in source rocks to assign a "type" to OM, typical of particular provenances and compositions. The pseudo van Krevelen plot uses HI and OIRE6 to the same end (Carrie et al., in press; Meyers and Teranes, 2001). HI and OIRE6 of all samples from ALE1, SL10W1, SL10W2 and SL10M1 plot within the "type II" field, indicative of primary aquatic production, dominantly from protein-rich phytoplankton (Carrie et al., 2012; Meyers and Teranes, 2001). It is also notable that these recent lake sediments plot beyond the extent of the "boundaries" which separate fields representing types of kerogen on the pseudo van Krevelen diagram (Figure 5.7), which was originally created for the analysis of petroleum

source rocks. This is typical of recent sediments, which have a higher proportion of labile, oxygen-containing organic compounds (S3) relative to petroleum source rocks (Carrie et al., in press). It is apparent that SL10W1 plots somewhat apart from the other lakes, and exhibits a roughly linear trend, indicating high values of OIRE6 relative to the other cores. These high values of OIRE6 correspond to the shallowest/most recent subsamples of the SL10W1 core, which provides further evidence in favor of the idea that SL10W1 is closer to the edge of the lake than SL10W2, and is being affected by a decrease in the water depth occurring as SL10W loses water volume to evaporation. As the water becomes shallower, oxygen would likely permeate deeper into the water column, thus it makes sense that the most recent sediments of SL10W1 have been exposed to more oxygen than the deeper ones, which plot similarly to the other lakes in the pseudo van Krevelen diagram.

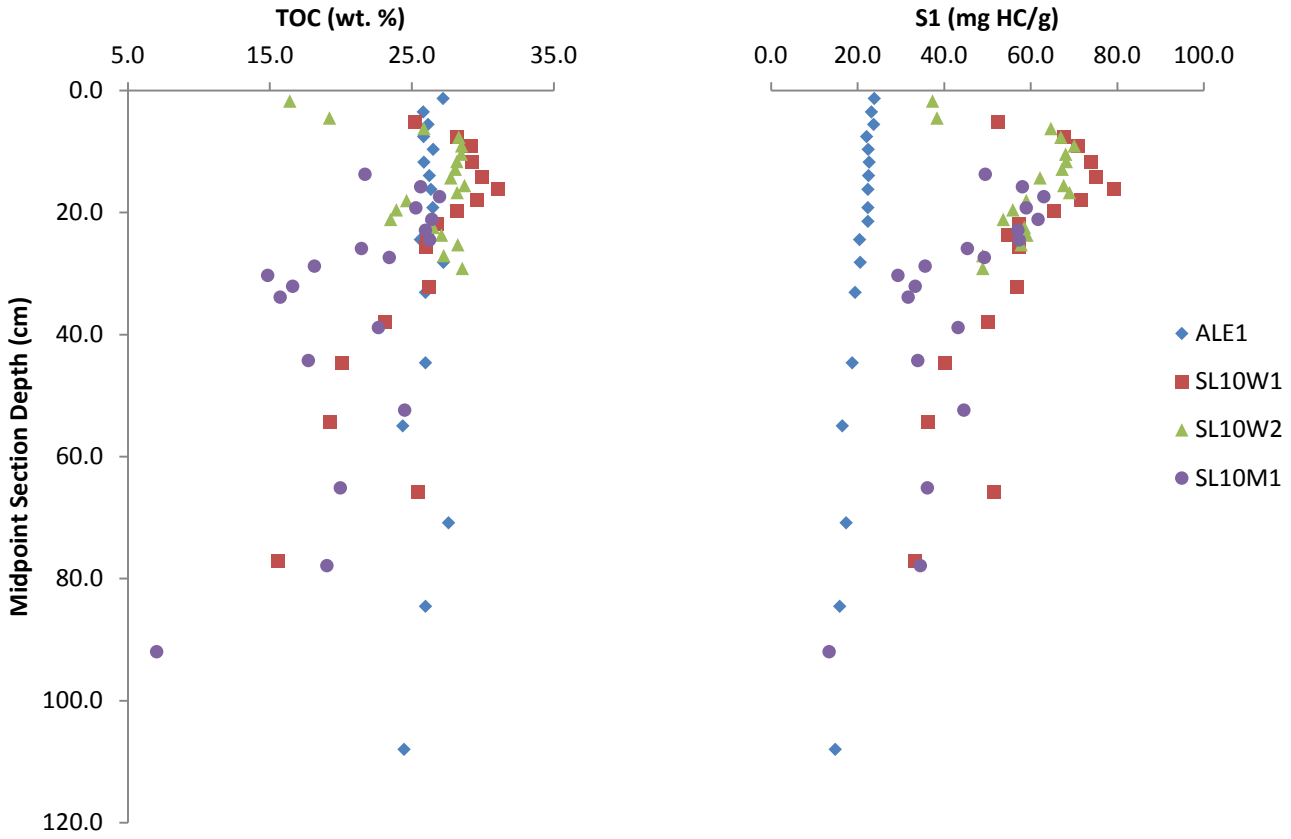

Figure 5.6: Rock-Eval parameters TOC and S1 by depth for ALE1, SL10W1, SL10W2 and SL10M1.

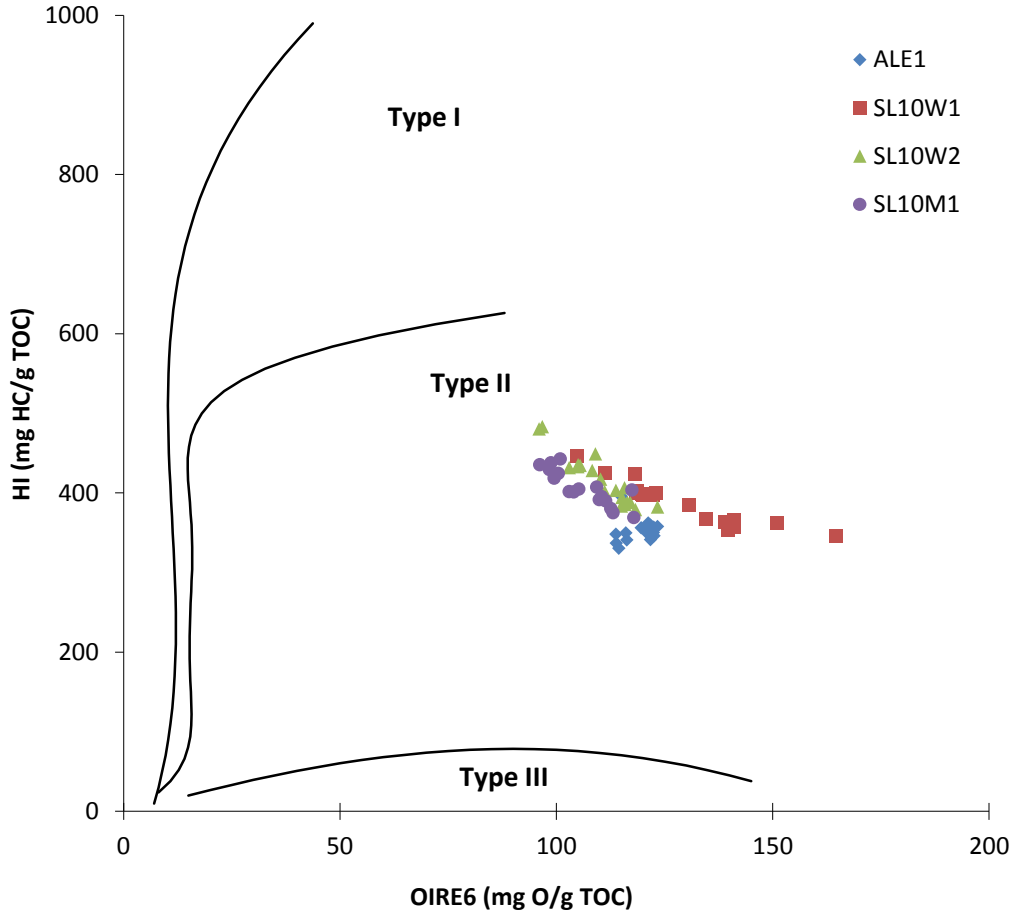

Figure 5.7: Pseudo van Krevelen plot, comparing HI to OI for ALE1, SL10W1, SL10W2 and SL10M1. Fields corresponding to type I, type II and type 3 OM are marked.

Table 5.6: Calculated OIRE6 and HI ratios from S1, S2a, S2b and S3CO and $S3CO_2$ measurements for samples from ALE1, SL10W1, SL10W2 and SL10M1.

ALE1		
Midpoint Section Depth (cm)	OIRE6	HI
1.4	122.2	352.0
3.6	122.5	357.0
5.6	122.5	350.0
7.6	122.6	347.0
9.7	121.8	342.0
11.8	121.8	347.0
14.0	123.4	358.0
16.3	120.7	351.0
19.2	121.5	360.0
21.5	121.3	362.0
24.5	121.8	360.0
28.2	115.1	396.0
33.1	119.7	355.0
44.7	116.1	349.0
55.0	116.3	340.0
70.9	113.8	347.0
84.6	113.8	336.0
108.0	114.5	330.0
AVERAGE	**119.5**	**352.2**
S.D.	**3.5**	**13.9**

SL10W1		
Midpoint Section Depth (cm)	OIRE6	HI
5.3	164.6	386.0
7.6	151.1	383.0
9.2	141.0	386.0
11.7	139.6	392.0
14.3	141.0	398.0
16.3	139.0	388.0
18.0	134.8	391.0
19.9	130.6	406.0
22.0	122.3	405.0
23.8	123.0	420.0
25.7	118.5	431.0
32.3	118.7	437.0
38.0	119.9	436.0
44.7	120.2	439.0
54.4	111.2	434.0
65.9	104.8	480.0
77.1	118.1	484.0
AVERAGE	**129.3**	**417.4**
S.D.	**15.3**	**31.7**

SL10W2		
Midpoint Section Depth (cm)	OIRE6	HI
1.8	115.8	372.0
4.6	109.1	378.0
6.3	123.4	409.0
7.7	118.3	386.0
9.1	115.1	402.0
10.5	116.4	395.0
11.7	115.2	405.0
12.9	115.8	395.0
14.4	117.1	410.0
15.6	113.8	408.0
16.8	111.2	405.0
18.1	110.2	421.0
19.6	108.3	426.0
21.2	105.5	431.0
22.5	105.0	441.0
23.8	105.0	437.0
25.3	103.0	446.0
27.1	96.0	451.0
29.2	96.8	444.0
AVERAGE	**110.6**	**413.8**
S.D.	**7.3**	**23.5**

SL10M1		
Midpoint Section Depth (cm)	OIRE6	HI
13.8	115.0	372.0
15.8	118.2	378.0
17.5	117.9	409.0
19.3	113.1	386.0
21.2	117.5	402.0
23.0	112.6	395.0
24.5	110.6	405.0
26.0	110.0	395.0
27.4	104.0	410.0
28.8	111.4	408.0
30.4	109.3	405.0
32.1	105.2	421.0
33.9	103.0	426.0
38.9	99.5	431.0
44.3	100.5	441.0
52.4	98.4	437.0
65.2	98.8	446.0
77.9	96.2	451.0
92.0	100.9	444.0
AVERAGE	**107.5**	**413.8**
S.D.	**7.3**	**23.5**

HI and OIRE6 can also provide some information about relative freshness of the OM; as OM is degraded by bacterial activity or oxidation, more labile (S1, S2a) compounds (lipids, protein) will first be subject to microbial attack, leaving the more resistant fractions which contribute to the S3 signal (carbohydrates, lignins) intact (Carrie et al., in press; Carrie et al., 2012). Thus, it is typical that HI decreases in sediments which are deeper/older, and OIRE6 increases in deeper, older sediments; these parameters vary inversely with one another. Figure 5.8 shows HI and OIRE6 values by depth for all subsamples of ALE1, SL10W1, SL10W2 and SL10M1, which all appear to have an upward decreasing, and upward increasing trend, respectively, contrary to what is considered "typical".

According to the findings of Talbot and Livingstone (1989), possible reasons for an anomalous upward decrease in HI are subaerial exposure of sediments, an increase in dissolved oxygen in the water column, or a change in the type of OM being deposited into lake sediments. It is unlikely that the type of OM preserved in sediments has changed, given that the pseudo van Krevelen plot indicates that OM is of type 2 in all subsamples from all four cores, and types of OM macerals observed in the organic petrology were consistently aquatically-derived biomass. No evidence was found for subaerial exposure of sediments comprising the lake bottoms (J. Ahad, personal comm.), thus it is likely that a decrease in the water level of the lake and associated increase of dissolved oxygen around the sediment-water interface is responsible for the anomalous depth trends in HI and OI. The Mackenzie River Basin, within which ALE, SL10W and SL10M are located is currently experiencing a warming trend in its climate (Stewart et al., 1998). A warmer climate can increase the rate of evaporation of a lake significantly, particularly in small and shallow lakes where the volume to surface area ratio is low (Schertzer et al., 2004). Rates of evaporation and quantity of dissolved oxygen may also be influenced by the duration of the ice-free period, which increases with warming in the climate (Stewart et al., 1998). Warming of the climate provides one plausible explanation as to why the depth trends of HI and OI differ from what is

considered typical. This explanation is further supported in the case of SL10W1 by the up-core increases in MinC and OIRE6.

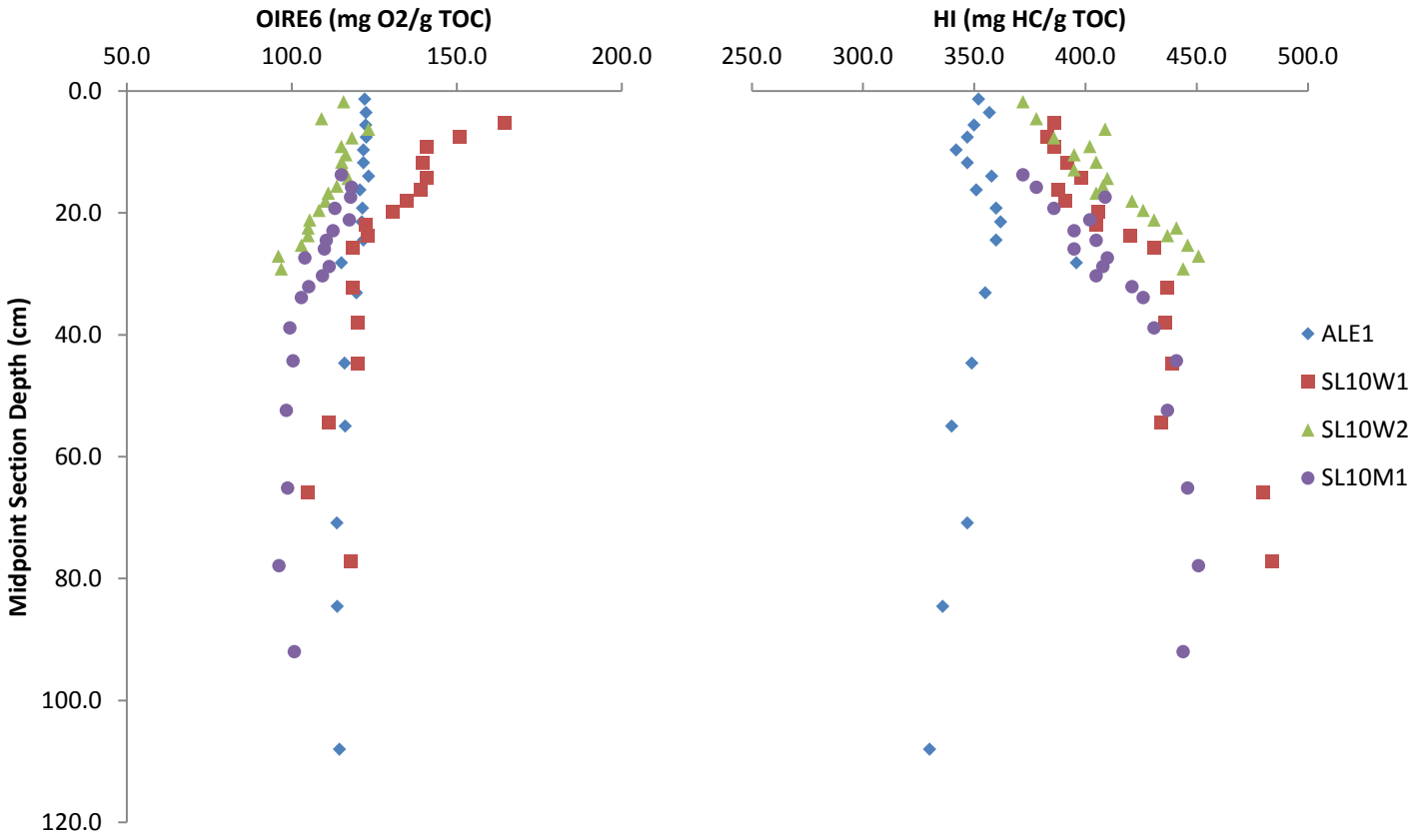

Figure 5.8: Rock-Eval parameters HI and OIRE6 calculated from TOC, S2, S3CO and S3CO2 for ALE1, SL10W1, SL10W2 and SL10M1 by depth.

Carrie et al. (in press) devised a “freshness plot” using ratios of HI:OI versus S1+S2a:S2b in order to characterize the relative freshness of the OM in sediments, where higher values of both ratios (HI:OI and S1+S2a:S2b) indicated a greater degree of freshness. The freshness plot also served to indicate whether recent sediment OM contained a considerable contribution from microbial mats. Sediments rich in microbial mat dominated OM was shown to have a higher S1+S2a:S2b ratio than “typical” sediments (higher than approximately 1.25), and a lower HI:OI ratio (between 0.75 and 3.5). HI:OI and S1+S2a:S2b ratios of subsamples of cores ALE1, SL10W1, SL10W2 and SL10M are plotted in Figure 5.9.

In spite of anomalous values of HI and OI values of SL10W1, SL10W2 and SL10M1, it is clear that OM in all of these cores is fresher relative to the OM in sediments from ALE1. Moreover, some data points derived from subsamples of SL10W1, SL10W2 and SL10M1 plot in the microbial mat-rich field as defined by Carrie et al. (in press). Both the high degree of freshness and the microbial mat content corroborate the observations of the organic petrology.

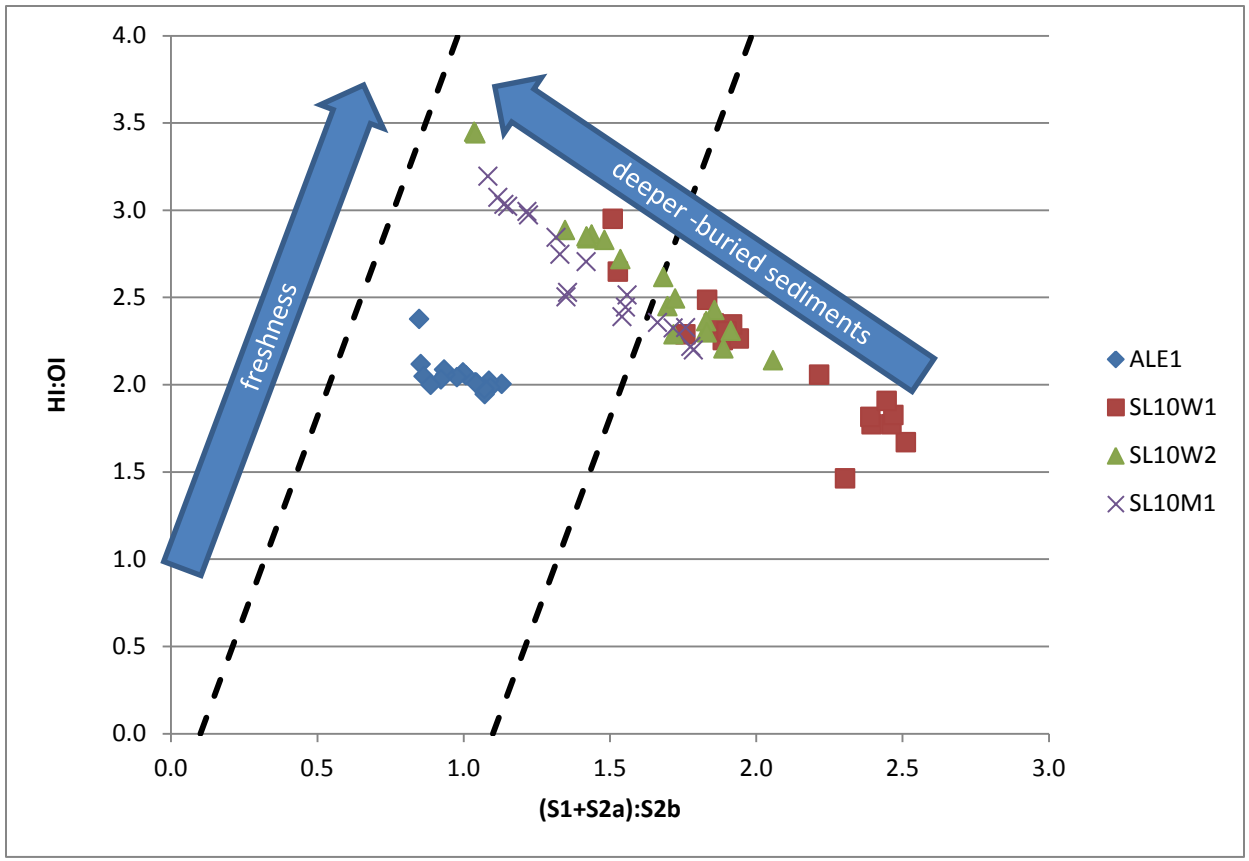

Figure 5.9: Freshness plot after Carrie et al. (in press). Ratios of HI:OI and (S1+S2a):S2b plotted for ALE1, SL10W1, SL10W2 and SL10M1. The direction of increasing freshness for "typical" sediments is shown; because of anomalous HI and OI depth trends, this does not reflect the direction of increasing depth of sediments from this study's cores.

5.2.3 C/N Ratio

The average C/N ratios of sediments from ALE1, SL10W1, SL10W2 and SL10M1 were 9.8±0.5 (n=18), 10.7±3.7 (n=17), 17.5±10.1 (n=19) and 7.4±2.2 (n=19), respectively. Values of TOC and N used for the calculation of C/N ratios, and the C/N ratios by depth are provided in Table 5.7 and shown in Figure 5.10.

The C/N ratio of lake sediments provides additional information about the origin of OM contained in the sediments. Specifically, it serves to differentiate between input of non-vascular "in-lake" algal production versus input from cellulose-containing vascular plants which are derived from surrounding terrestrial ecosystems (Krishnamurthy et al., 1986). A lower C/N ratio between 4 and 10 is typically associated with nonvascular aquatic plants, whereas land plants have a characteristic C/N ratio of 20 or greater and values between 10 and 20 reflect a mixture of authochthonous and allochthonous OM contents (Meyers and Lallier-Verges, 1999; Meyers, 1994; Meyers and Ishiwatari, 1993).

Biochemical alteration of freshly deposited sediments may have a variety of impacts on the C/N ratio. In organic-rich eutrophic lakes, N-rich fractions of algae (eg. proteins) are labile, and preferential degradation of these substances results in an increase in C/N ratio (Meyers and Lallier-Verges, 1999; Sarazin et al., 1992). In oligotrophic lakes, anaerobic consumption of organic carbon may result in a slight decrease in C/N ratios (Meyers and Lallier-Verges, 1999). These early diagenetic changes rarely produce significant effects on the elemental composition of sediments, thus the original C/N signal of organic matter, and by extension whether it is terrestrially or aquatically-derived, is usually preserved (Meyers and Lallier-Verges, 1999; Meyers, 1994; Meyers and Ishiwatari, 1993).

Table 5.7: N contents and calculated C/N ratios (using TOC) for samples from ALE1, SL10W1, SL10W2 and SL10M1

ALE1		
Midpoint Section Depth (cm)	N content (wt. %)	TOC/N
1.4	2.8	9.7
3.6	2.8	9.2
5.6	2.8	9.2
7.6	2.7	9.6
9.7	2.8	9.6
11.8	2.7	9.5
14.0	2.8	9.2
16.3	2.8	9.6
19.2	2.7	9.8
21.5	2.8	9.5
24.5	2.6	9.9
28.2	2.6	10.6
33.1	2.7	9.7
44.7	2.5	10.2
55.0	2.4	10.2
70.9	2.7	10.4
84.6	2.5	10.4
108.0	2.3	10.9
AVERAGE	2.7	9.8
S.D	0.2	0.5

SL10W1		
Midpoint Section Depth (cm)	N content (wt. %)	TOC/N
5.3	1.7	14.9
7.6	2.8	10.0
9.2	2.9	10.0
11.7	3.0	9.7
14.3	2.9	10.3
16.3	3.0	10.5
18.0	2.8	10.8
19.9	3.1	9.2
22.0	2.8	9.4
23.8	2.1	12.5
25.7	1.1	23.1
32.3	2.2	12.1
38.0	2.5	9.1
44.7	2.5	8.0
54.4	2.8	6.8
65.9	2.6	9.7
77.1	2.7	5.7
AVERAGE	2.6	10.7
S.D.	0.5	3.8

SL10W2		
Midpoint Section Depth (cm)	N content (wt. %)	TOC/N
1.8	2.3	7.1
4.6	2.4	8.1
6.3	2.7	9.6
7.7	2.6	10.9
9.1	2.7	10.7
10.5	2.4	11.7
11.7	2.3	12.0
12.9	1.1	25.1
14.4	1.2	23.5
15.6	1.2	23.2
16.8	0.7	42.7
18.1	1.7	14.6
19.6	1.5	16.5
21.2	2.4	9.8
22.5	1.7	15.8
23.8	2.2	12.1
25.3	1.6	17.5
27.1	1.6	17.4
29.2	0.7	43.3
AVERAGE	1.8	17.5
S.D.	0.7	10.4

SL10M1		
Midpoint Section Depth (cm)	N content (wt. %)	TOC/N
13.8	2.3	9.4
15.8	3.3	7.8
17.5	3.6	7.5
19.3	3.8	6.6
21.2	4.0	6.6
23.0	4.2	6.3
24.5	3.8	6.9
26.0	3.5	6.1
27.4	3.5	6.8
28.8	3.4	5.4
30.4	3.4	4.4
32.1	3.3	5.1
33.9	3.0	5.3
38.9	2.3	10.1
44.3	2.1	8.4
52.4	2.6	9.4
65.2	1.6	12.6
77.9	1.7	11.1
92.0	1.8	4.0
AVERAGE	3.0	7.4
S.D.	0.8	2.3

The average C/N ratios of sediments from ALE1, SL10W1 and SL10M1 were all ~10 or less (Table 5.7), indicating that OM in these sediments is primarily of autochthonous origin; aquatic non-vascular plants and micro-organisms. With depth, the C/N ratios of sediments from ALE1 remain fairly constant (max=10.9, min=9.2) (Figure 5.10), indicating little change in the type and degree of degradation of OM over the interval studied. C/N ratios from SL10W1 and SL10M1 do not show a consistent increase or decrease from bottom to top of the cores. At depths greater than ~40cm, sediments from SL10M1 have a C/N ratio of approximately 10, while from ~40 to 20cm depth, the C/N ratio increases from 4.4 to 9.4 (Figure 5.10). This appears to be primarily a function of changes in TOC content, which increases from ~16 to 27% over the same depth interval, while no significant changes were observed in N content (Figure 5.10). This period of elevated TOC contents likely represents an interval characterized by elevated primary production or by better preservation of OM, though the data collected by this study does not provide insight into which of these factors was more significant during the observed period of elevated TOC.

SL10W2 has an average C/N ratio of 17.5±10.1, suggesting that lake sediments contain a greater proportion of terrestrially-derived OM relative to ALE1, SL10M1, and SL10W1. The C/N ratio increases with increasing depth, from around ~7 at the top of the core to around 17.5 at the bottom of the core. This appears to be a result of changes in N content (max=2.7, min=0.7), as TOC contents remain fairly constant between 25 and 29% with the exception of two outliers at the top of the core. N content is more variable, but in general is lower at depths greater than ~13cm (average 1.5%) and higher in the upper portion of the core (average 2.5%). It is possible that preferential degradation of N-bearing compounds is the cause of the trend of increasing C/N ratio with increasing depth; N contents in older sediments may have been depleted as a result of bacterial degradation of OM, while more recent sediments have not yet been degraded to the same extent (Meyers and Lallier-Verges, 1999; Sarazin et al., 1992).

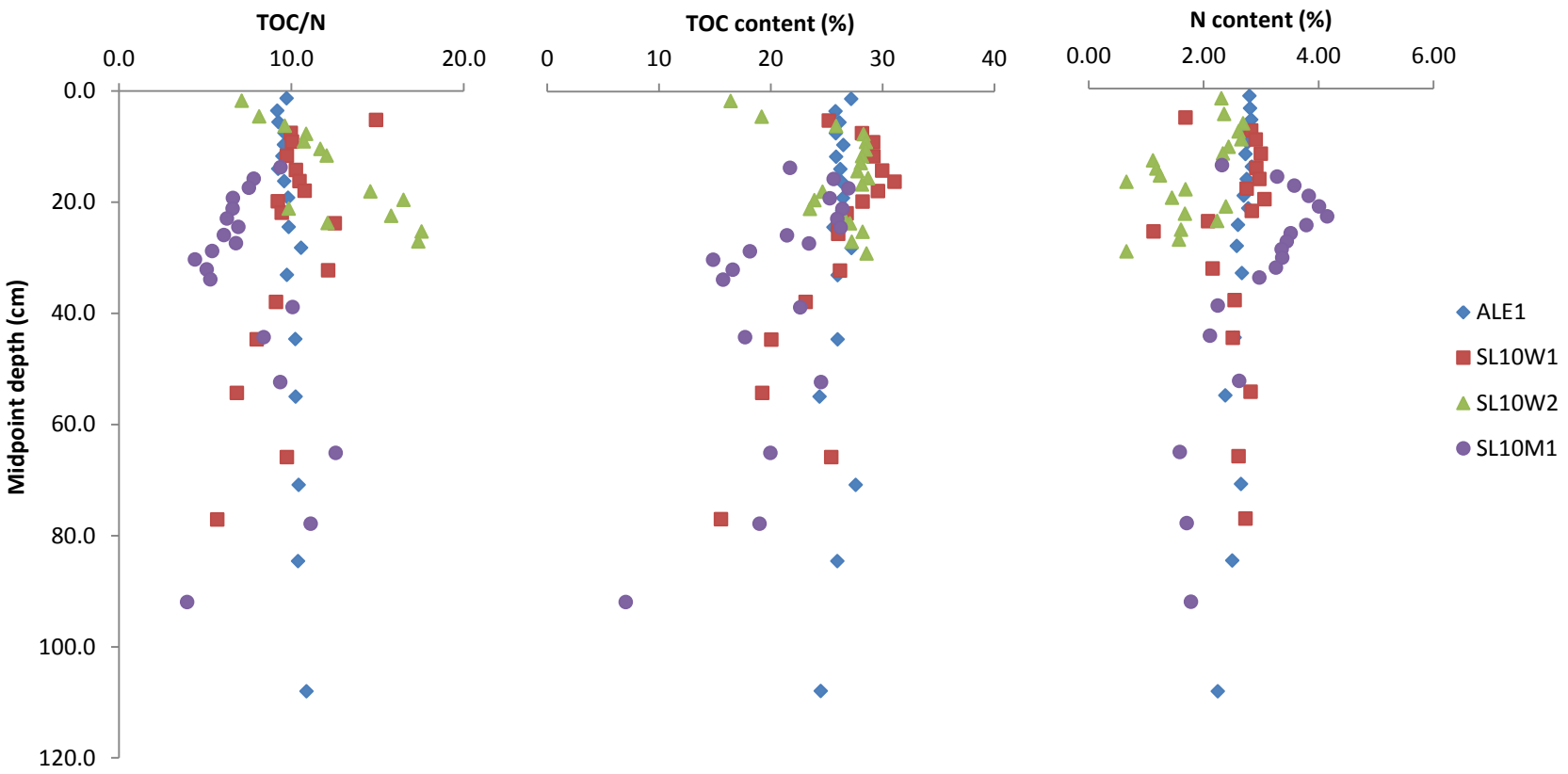

Figure 5.10: C/N ratios by depth, and TOC and N contents from which C/N ratios were calculated, by depth for samples from ALE1, SL10W1, SL10W2 and SL10M1.

5.2.4 Stable Isotope Analysis of Organic Carbon

Stable carbon isotope ratios of lake sediment OM can provide information about the rate of primary productivity in a lake (Brenner et al., 1999; Hodell & Schelske, 1998), and about the source of the OM (C3 vs C4 plants, allochthonous vs authochthonous production) in the sediment record (Meyers and Teranes, 2001; Meyers and Lallier-Vergès, 1999). Variations in $\delta^{13}C$ have been used in conjunction with other geochemical data as evidence of longer-term (10-500 ka) climate change (Lane et al., 2009; Meyers and Lallier-Vergès, 1999), represented as shifts in the source and abundance of OM in lake sediments, and as evidence of changes in rates of in-lake productivity. This study uses $\delta^{13}C$ values of organic carbon in conjunction with Rock-Eval pyrolysis data, C/N ratios, and organic petrology to characterize the recent lake sediments.

$\delta^{13}C$ values in ALE1, SL10W1, SL10W2 and SL10M1 averaged -30.7±0.2‰ (n=18), -20.2±0.8‰ (n=17), -19.9±0.5‰ (n=18) and -13.0±0.9‰ (n=19), respectively (Table 5.8). Very little variation in $\delta^{13}C$ was observed with depth in ALE1, with values remaining essentially constant around -31‰ through the entire length of the core (Figure 5.11). There was an increase in $\delta^{13}C$ values in more recent sediments in both cores from SL10W. $\delta^{13}C$ values increased from -22.2 to -19.9‰ (Figure 5.11) from bottom to the top of the core in SL10W1 and from -21.5 to -19.5‰(Figure 5.11) from bottom to the top of core SL10W2. Variations in $\delta^{13}C$ values were not obviously related to depth in SL10M1, but varied between a maximum value of -12.8 and a minimum of -14.1‰ (Figure 5.11).

Table 5.8: Measured depth intervals and $\delta^{13}C$ values for TOC in core samples from ALE (x1), SL10W (x2) and SL10M (x1).

ALE1	
Midpoint Depth (cm)	**$\delta^{13}C$ (‰)**
1.4	-31.0
3.6	-30.6
5.6	-31.0
7.6	-31.0
9.7	-30.8
11.8	-30.9
14.0	-30.9
16.3	-30.7
19.2	-30.6
21.5	-30.7
24.5	-30.8
28.2	-30.4
33.1	-30.9
44.7	-30.7
55.0	-30.3
70.9	-30.6
84.6	-30.5
108.0	-30.5
AVERAGE	-30.7
S.D.	0.2

SL10W1	
Midpoint Depth (cm)	**$\delta^{13}C$ (‰)**
5.3	-19.9
7.6	-19.8
9.2	-20.1
11.7	-19.7
14.3	-19.7
16.3	-19.7
18.0	-19.7
19.9	-19.7
22.0	-19.8
23.8	-19.8
25.7	-19.7
32.3	-19.8
38.0	-20.2
44.7	-20.4
54.4	-20.6
65.9	-22.1
77.1	-22.2
AVERAGE	-20.2
S.D.	0.8

SL10W2	
Midpoint Depth (cm)	**$\delta^{13}C$ (‰)**
1.8	-19.5
4.6	-19.5
6.3	-19.4
7.7	-19.6
9.1	-19.6
10.5	**
11.7	-19.8
12.9	-19.6
14.4	-19.6
15.6	-19.8
16.8	-19.8
18.1	-19.8
19.6	-20.0
21.2	-20.1
22.5	-19.9
23.8	-20.1
25.3	-20.2
27.1	-20.6
29.2	-21.5
AVERAGE	-19.9
S.D.	0.5

SL10M1	
Midpoint Depth (cm)	**$\delta^{13}C$ (‰)**
13.8	-12.7
15.8	-13.0
17.5	-13.1
19.3	-13.0
21.2	-12.8
23.0	-12.5
24.5	-12.9
26.0	-13.7
27.4	-14.1
28.8	-13.9
30.4	-13.7
32.1	-13.6
33.9	-13.2
38.9	-12.9
44.3	-13.8
52.4	-10.0
65.2	-12.9
77.9	-12.6
92.0	-13.6
AVERAGE	-13.0
S.D.	0.9

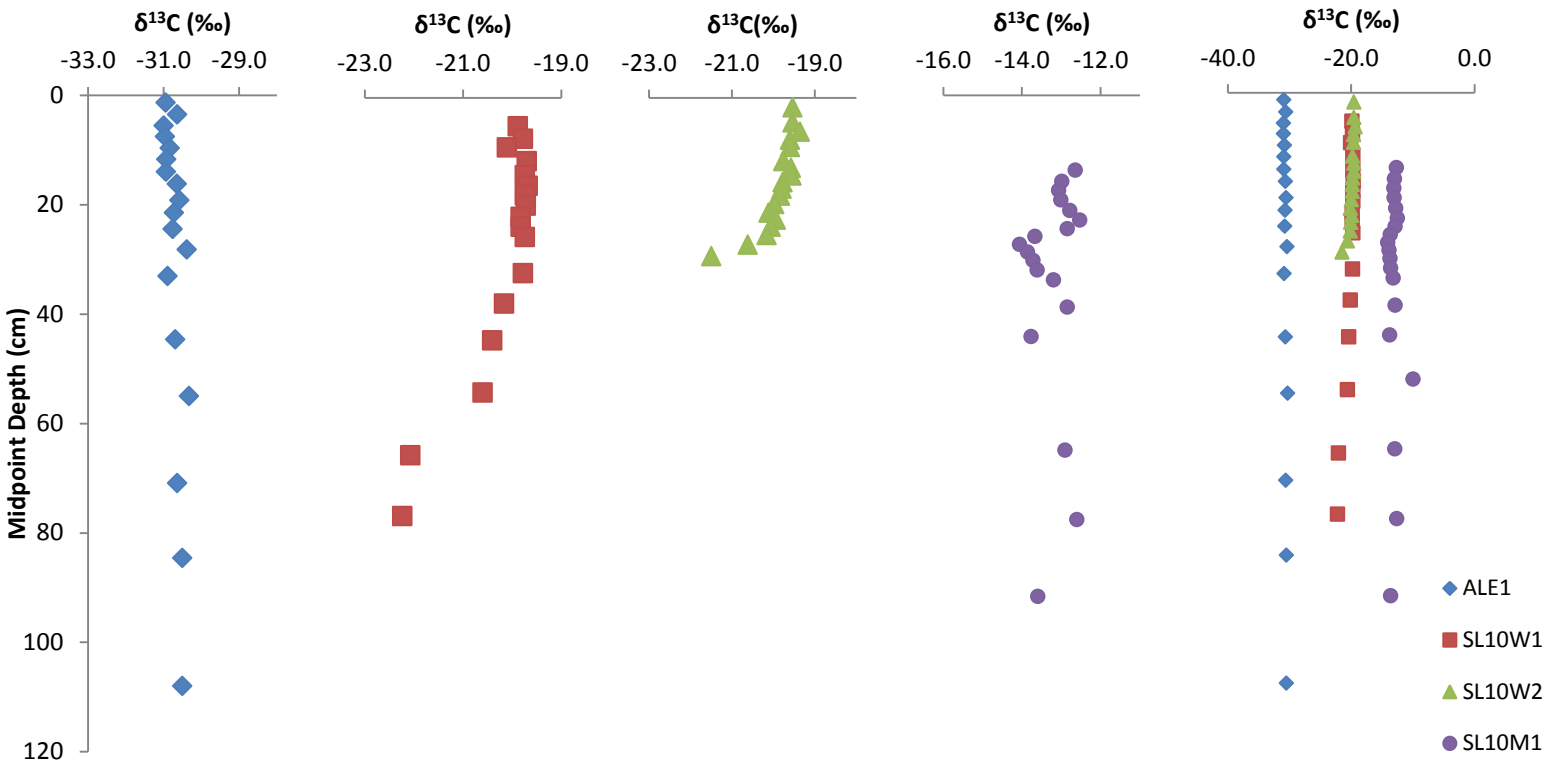

Figure 5.11: Bulk $\delta^{13}C$ values of OM by depth for sediment cores from ALE (x1), SL10W (x2) and SL10M (x1). Lakes are plotted individually in order to remove scaling effects on depth trends.

The average $\delta^{13}C$ value for ALE falls within the "normal" range for C3 plants, which is between approximately -33 to -25‰ (Meyers and Terranes, 2001; Meyers and Lallier-Vergès, 1999). In combination with Rock-Eval and C/N data, $\delta^{13}C$ values in ALE1 further support the characterization of OM as sourced mainly from primary in-lake production.

Although there are some small variations of $\delta^{13}C$ values in SL10W1, SL10W2 and SL10M1, none of these changes is of a sufficient magnitude to conclude that a large-scale shift in climate has occurred over the analyzed period such that the type of organic production in the area has changed considerably. Values of $\delta^{13}C$ in SL10W1 and SL10W2 are slightly more enriched in ^{13}C than is considered typical of phytoplankton-dominated OM, at around -20‰. It is likely that this is a result of incorporation of some proportion of the microbial mats observed in the analysis of organic petrology.

SL10M differs from ALE and SL10W by the very high $\delta^{13}C$ of its organic carbon fraction, with values between -15 and -12‰. A few possibilities exist to explain this anomalously high value of $\delta^{13}C$ in sediments of SL10M1.

$\delta^{13}C$ values of -15 to -10‰ are characteristic of plants which photosynthesize via the C4 pathway. Both the pseudo van Krevelen plot of Rock-Eval data and the C/N data clearly indicate that the organic matter in SL10M has an autochthonous, aquatic source. This precludes the possibility that OM in SL10M has received significant contribution from terrestrial C4 plants. In addition to this, no such plants were observed near SL10M (J. Ahad, pers. communication). It is possible that the microbial mats observed in the photomicrographs of SL10M organic matter are contributing significant amounts of OM to sediment which has a higher $\delta^{13}C$ value than typical phytoplankton. Previous scientific studies (van der Meer et al., 2003; van der Meer et al., 2000; Schidlowski et al., 1984) have reported elevated $\delta^{13}C$ values of bulk OM in bacterial mats around -15 to -13‰, similar to the $\delta^{13}C$ values observed in the sediments of SL10M.

The $\delta^{13}C$ value of the DIC assimilated by algae during photosynthesis influences the final $\delta^{13}C$ value of the OM preserved in the sediment record (Keeley and Sandquist, 1992). In the case where the lake is receiving significant input from groundwater moving through a carbonate-rich aquifer, it is possible that this DIC is enriched in ^{13}C, which would result in an elevated $\delta^{13}C$ value of organic matter. However, given that electrical conductivities (related to the total dissolved solids in water samples) measured in SL10M are low (average of 95.2 μS/cm) relative to those observed in typical shallow groundwater in Alberta (around 1600 μS/cm) (Cheung et al., 2010), it is unlikely that the water in SL10M is dominantly sourced from a carbonate-rich aquifer.

In cases where the availability of CO_2 is limited by elevated levels of productivity/photosynthesis (Bernasconi et al., 1997), or where elevated pH supports a low ratio of CO_2 relative to bicarbonate (HCO_3^-) (Hassan et al., 1997), HCO_3^- may become an important source of DIC for primary production. While atmospheric CO_2 has a $\delta^{13}C$ value between -8 and -7‰ (Meyers and Teranes, 2001), HCO_3^- may have a $\delta^{13}C$ value which is 8 to 12‰ higher (Mook et al., 1974) and previous studies have shown that uptake of HCO_3^- rather than of CO_2 can produce algal OM with $\delta^{13}C$ values of up to -9‰ (Bernasconi et al., 1997; Hassan et al., 1997; Keeley and Sandquist, 1992). The pH values measured throughout the water column in SL10M range from 9.2 to 7.6, indicating that HCO_3^- is the dominant DIC species throughout most of the water column. This provides a plausible explanation for the elevated $\delta^{13}C$ values observed in OM of SL10M1.

5.2.5 Summary of Characterization of Lake Sediments

Analyses of organic petrology, Rock-Eval pyrolysis data, C:N ratios, and $\delta^{13}C$ values all indicate that the bulk of the sediment from ALE, SL10W and SL10M is derived from “in-lake” production of lipid-rich phytoplankton with negligible input from higher (vascular) land plants. According to the freshness plot described by Carrie et al. (in press), OM in SL10M and SL0W is fresher in comparison to what is

considered “typical” for lake sediments, while OM in ALE1 is more degraded than OM from either Saskatchewan lake, and is more representative of “typical” lake sediments. $\delta^{13}C$ values of SL10M sediments are very ^{13}C-enriched which is likely a result of some combination of uptake of HCO_3^- over CO_2 resulting from elevated lake water pH, as well as the presence of significant quantities of OM derived from bacterial mats, as recorded in the section on organic petrology. Somewhat elevated $\delta^{13}C$ values of SL10W OM can be similarly explained through the mixing of a smaller proportion of bacterial mat-derived OM with the phytoplankton OM. The presence of bisaccate pollen grains and particles of char are both typical of the boreal forest ecosystem in which these lakes are located—sourced from abundant conifers and frequent forest fires, respectively.

It is clear that there is significant natural inter-lake variability in the organic petrology and geochemical parameters which were analyzed. This adds an additional dimension of complexity to interpreting whether lake sediments have recorded impact from industrial emissions originating in the AOSR. It is thus necessary to have a clear understanding of a parameter’s natural variability in a particular lake and its sediments in order to establish whether changes to these proxy parameters have occurred as a result of impact from industrial emissions. This study revealed that lake sediments are not analogous among the three lakes studied.

5.3 Sulfur Contents and Stable Isotope Ratios

Rates of atmospheric SO_4^{2-} deposition and $\delta^{34}S$ values of SO_4^{2-} in bulk and throughfall atmospheric deposition were reported for sites around the AOSR by Proemse et al. (2012). While the study recorded elevated rates of bulk and throughfall deposition of SO_4^{2-} at sites closer than 30km to a central emission marker in the AOSR, no strong correlation between $\delta^{34}S$ and distance from the AOSR was observed. It was noted that the sites which were closer to major industrial emitters in the AOSR (<30km) were generally subject to higher levels of SO_4^{2-} deposition, than those taken to reflect "background" at distances greater than 74 km. Sites receiving more than 10kg/ha SO_4^{2-} of throughfall deposition annually had average $\delta^{34}S$ values of +5.0‰ in summer and +6.2‰ in winter whereas "background" sites had average $\delta^{34}S$ values of +4.1 ‰ during summer and +5.2 ‰ during winter. Seasonal variations aside, the $\delta^{34}S$ value of atmospheric deposition of sulfate close to industrial operations was not substantially different (around 1‰) than that observed at more distant sites, taken to represent the background signature of $\delta^{34}S$ in the area (Proemse et al., 2012). It was concluded that $\delta^{34}S$ of SO_4^{2-} in atmospheric deposition does not constitute an effective tracer for industrial emissions in the AOSR.

Total sulfur contents of the lake sediments are low, averaging 0.4±0.1%, 0.2±0.1%, 0.2±0.1% and 0.5±0.2% for ALE1, SL10W1, SL10W2 and SL10M, respectively (Figure 5.11). Although there is an upward increase in S content in SL10W2, it appears to have begun prior to 1970 (Figure 5.12), thus it is unlikely that this is a result of contributions from local or regional industrial emissions, which began with the onset of anthropogenic activity in the AOSR around 1970. There has been no obvious increase in S content in the sediments from the other lakes examined in this study since 1970 (Figure 5.12), although interpretations of S content measurements in this study should be made with caution, given the relatively large errors produced by the techniques used for analysis. It appears that the lake sediments in this study have preserved no evidence of the elevated rates of SO_4^{2-} deposition observed by Proemse

et al. (2012). This is reasonable given that ALE, SL10W and SL10M are all considerably farther from the AOSR than the 30km radius within which the elevated rates of deposition were observed, at 97, 132 and 143 km from the Syncrude upgrader, respectively.

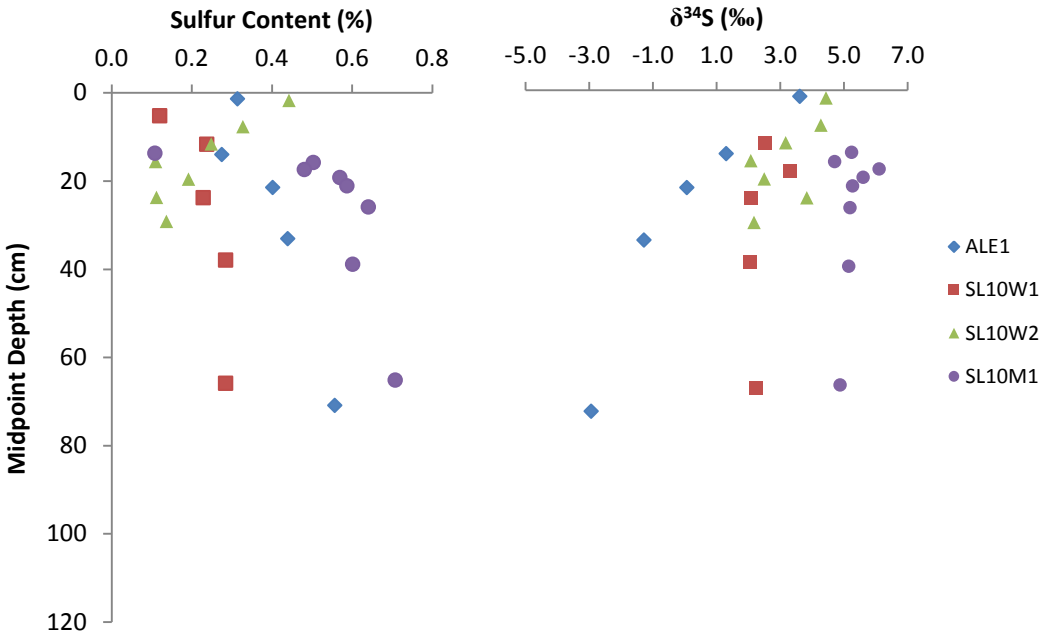

Figure 5.12: Total sulfur contents and $\delta^{34}S$ values of sediments by depth for ALE1, SL10W1, SL10W2 and SL10M.

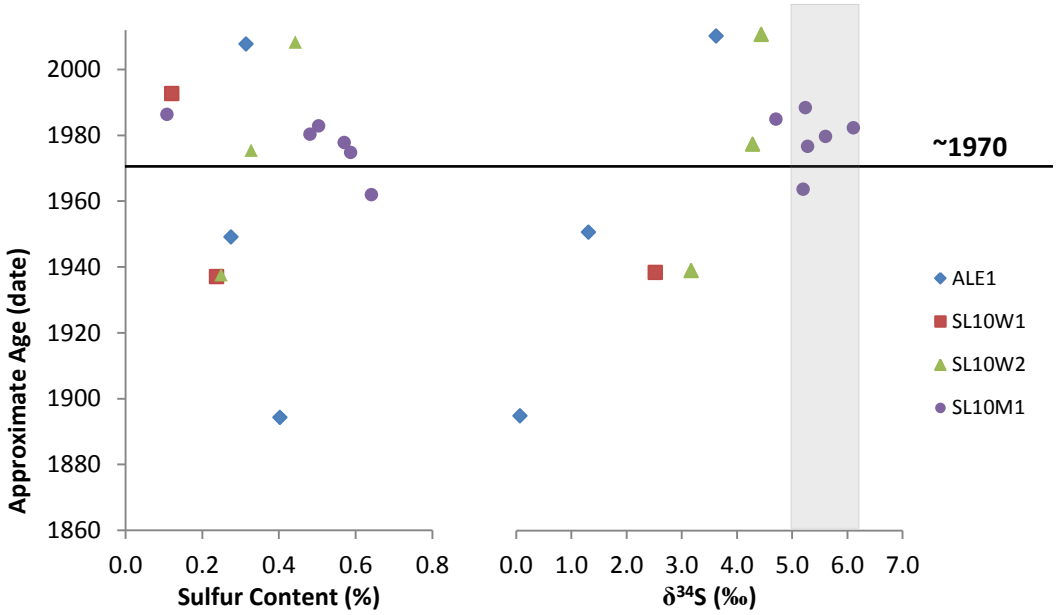

Figure 5.13: Sulfur contents and $\delta^{34}S$ values by age for ALE1, SL10W1, SL10W2 and SL10M. Shaded area indicates $\delta^{34}S$ values (+5.0 to +6.2‰) of sites with high SO_4^{2-} deposition rates (>10kg/ha per year), near (<30km) the source of industrial emissions (Proemse et al., 2012).

The use of sulfur isotope techniques in lake sediments for tracing contamination from anthropogenic sources is well-documented (Mayer et al., 2007; Rudd et al., 1986; Nriagu and Soon, 1985; Holdren et al, 1984; Nriagu and Coker, 1983). It is theoretically possible that isotopically-distinct sulfur emissions from anthropogenic activity could create a shift in $\delta^{34}S$ values of lake sediments from background $\delta^{34}S$ to values closer to the $\delta^{34}S$ of the contaminant S (Peterson and Fry, 1987; Krouse, 1980). However, the observed sulfur isotope shifts in the studied lake sediments appear to be more a function of the increase in the sulfate availability in lakes resulting from industrial emissions rather than the specific $\delta^{34}S$ values of the emissions. In all of the above studies, the onset of anthropogenic activity is marked by an increase in S content of lake sediments, and a decrease in $\delta^{34}S$. This decrease in $\delta^{34}S$ of total S in sediments is thought to be a result of enhanced bacterial sulfate reduction (BSR) as a result of

increased SO_4^{2-} supply, which is associated with a sulfur isotope fractionation effect which preferentially accumulates the lighter ^{32}S isotope in sediments in the forms of pyrite and organic S (Nriagu and Coker, 1983; Mayer et al., 2007). It should also be noted that most of these studies measured $\delta^{34}S$ values for individual sulfur fractions (AVS, CRS, S_{org}, etc.), while the limited quantities of sediment available for this study did not permit for sulfur species-specific analysis, and only the value of $\delta^{34}S$ of total S is reported and discussed.

Averages of $\delta^{34}S$ of total sedimentary S in ALE1, SL10W1, SL10W2 and SL10M1 were 0.2±2.2‰ (n=5), 2.2±0.5‰ (n=5), 3.2±0.9‰ (n=7) and 5.3±0.4‰ (n=8), respectively. Reported average values of $\delta^{34}S$ in atmospheric deposition of SO_4^{2-} at sites close to the AOSR (<30km) were between +5.0 to +6.2‰. In order to conclude that this study's lakes had received input from the industrial emissions originating in the AOSR, a shift from background (pre-1970) $\delta^{34}S$ values, toward the $\delta^{34}S$ values of atmospheric deposition of SO_4^{2-} reported close to the AOSR (+5.0 to +6.2‰) in the sediments deposited since 1970 should be seen. SL10W1 does not provide any data to support this, as there is no data available about the $\delta^{34}S$ values of sediments deposited post-1970 to contrast with those deposited prior to 1970. In SL10M1, though there is arguably an increase in $\delta^{34}S$ values at the top of the core (Figure 5.13), the average $\delta^{34}S$ value of sediments deposited both pre and post 1970 are within the range reported by Proemse et al. (2012) and thus do not suggest that additional input of S from industrial emissions from the AOSR has changed background $\delta^{34}S$ values. $\delta^{34}S$ values in ALE1 and SL10W2 both appear to increase in sediments deposited after 1970, toward the range reported by Proemse et al. (2012). A few possibilities exist to explain this observed trend:

- Background $\delta^{34}S$ values, historically, were lower than what was recorded by Proemse et al. (2012) and the increase observed is a natural shift, or a result of regional emissions of S, but is unrelated to activity in the AOSR.

- Background $\delta^{34}S$ values were lower than what was recorded by Proemse et al. (2012), and have increased as a result of increased atmospheric deposition of S from the AOSR.
- The increase in $\delta^{34}S$ values is unrelated to the $\delta^{34}S$ value of input S compounds—a reduction in the rate of BSR may have resulted in an increase in sediment $\delta^{34}S$ values, just as an increase in the rate BSR typically results in a decrease in sediment $\delta^{34}S$ values.

The upward increase in $\delta^{34}S$ values in ALE1 are unlikely to be a result of contamination by industrial emissions from the AOSR, as any impact from the AOSR would have begun in 1970 at the earliest, while the increasing trend in $\delta^{34}S$ values is occurring in sediments deposited long before this time (Figure 5.13). If we accept, on the basis of this temporal inconsistency, that the increase in $\delta^{34}S$ values in ALE1 is not a result of industrial emissions from the AOSR, then the same conclusion must be drawn for the increase observed in SL10W2, as SL10W is farther from the Syncrude upgrader than ALE by approximately 40km.

It is known that the MacKenzie River Basin is currently experiencing a warm period (Stewart et al., 1998). This in combination with the anomalous depth trend observed in HI values for SL10W could indicate an increase in dissolved oxygen resulting from increased evaporation which has decreased water depth in the lake. If this is the case, conditions would have become less favorable for BSR, which requires anoxic conditions. This reduction in the rate of BSR as a result of greater dissolved oxygen content of water could potentially result in the observed increase in $\delta^{34}S$ values in SL10W2 and ALE1.

It is impossible without further data to either confirm or discount the possibility that regional emissions of S have reached lakes and caused changes to the $\delta^{34}S$ values of sediments. Further information about the historical $\delta^{34}S$ value of sulfate in atmospheric deposition would be required in order to make a plausible conclusion about the impact of regional emissions of S on the $\delta^{34}S$ values of lake sediments.

5.4 Nitrogen Contents and Stable Isotope Ratios

A study which isotopically characterized and measured nitrate and ammonium bulk and throughfall deposition at sites around the AOSR was conducted by Proemse et al. (2013). This study reported that deposition rates of both compounds in throughfall were elevated (approximately 22 times greater for NO_3^- and 14 times greater for NH_4^+) at sites within 30 km of the center of oil sands operations, relative to "background" sites at distances >90km, suggesting that industrial emissions are contributing significantly to atmospheric nitrogen deposition (as both NO_3^- and NH_4^+) at sites in close proximity to the AOSR.

$\delta^{15}N$ values for bulk and throughfall N deposition are summarized in Table 5.9. At "background" sites, $\delta^{15}N$ values ranged between-4.4 to +2.5‰ (average -1.4±2.2‰) for NO_3^- and -4.1 to 3.3‰ (average -1.4±2.3‰) for NH_4^+. Seasonal variations (up to 5‰) were observed in both NH_4^+ and NO_3^-. $\delta^{15}N$ values of NO_3^- and NH_4^+ within 30km of the AOSR, which were influenced by elevated atmospheric N-deposition from industrial emissions were highly variable (-4.9 to +6.3‰ and -6.3 to +11.3‰, respectively) but tended to be higher than those at background sites (averages of +0.3±3.4‰ and -0.2±4.3‰, respectively). $\delta^{15}N$ values of NH_4^+ higher than +4‰ were observed only at sites closer than 18km to the Syncrude upgrader. The study concluded that the variability of measured values of $\delta^{15}N$ limits its usefulness as a quantitative tracer, but might be useful for qualitative analysis given that elevated $\delta^{15}N$ values appear to be indicative of industrial emissions.

Table 5.9: Summary of reported $\delta^{15}N$ values for atmospheric deposition of NO_3^- and NH_4^+ for sites "near" (<30km) the AOSR and "background" (>30km) compiled from Proemse et al. (2013).

	<30km distance		>30km distance	
	$\delta^{15}N\ NO_3^-$	$\delta^{15}N\ NH_4^+$	$\delta^{15}N\ NO_3^-$	$\delta^{15}N\ NH_4^+$
Mean	+0.3‰	-0.2‰	-1.4‰	-1.4‰
S.D.	3.4‰	4.3‰	2.2‰	2.3‰
Min	-4.9‰	-6.3‰	-4.4‰	-4.1‰
Max	+6.3‰	+11.3‰	+2.5‰	+3.3‰

Average total nitrogen contents of lake sediments were 2.8±0.2% (n=18), 2.6±0.5% (n=17), 1.8±0.6% (n=19) and 3.0±0.8% (n=19) for ALE1, SL10W1, SL10W2 and SL10M1, respectively (Figure 5.14). No obvious trends of increased or decreased N contents occur in ALE1 (max=2.8%, min=2.3%), or in SL10W1 (max=3.1%, min=1.1%) and SL10W2 (max=2.7%, min=0.7%), where variations in N contents were not related to depth. The N content of SL10M1 peaks at ~4% at a depth of 21.2 cm, and decreases to around 2% in sediments above and below this point. This depth corresponds to a date of sediment deposition of around 1970, which is concurrent with the start-up of anthropogenic activity in the AOSR. However, given that Proemse et al. (2013) observed higher rates of N-deposition in the vicinity of the AOSR (<30 km) as a result of elevated industrial emissions, it would be unreasonable to attribute the change in SL10M to industrial emissions from the AOSR given that N content decreases in sediments deposited more recently than 1970. Concurrent "peaks" in the Rock-Eval parameters S1, S2 and S3, and in TOC indicate that this may represent a period of higher primary productivity which, based on the decrease in N contents after 1970 despite the increase in activity and industrial emissions from the AOSR, is likely unrelated to these emissions.

Average $\delta^{15}N$ values were 2.0±0.3‰ (n=18), 0.4 ±0.8‰ (n=17), 1.1±0.9‰ (n=19) and 1.3±0.4‰ (n=19) for ALE1, SL10W1, SL10W2 and SL10M1, respectively (Figure 5.14). All three lakes are more than 30km from the AOSR, thus they would be receiving NO_3^- and NH_4^+ with $\delta^{15}N$ values of around -1.4‰

from atmospheric deposition assuming that these have not changed substantially over time from what was measured from 2007-2011 (Proemse et al., 2013). Enrichment factors associated with NO_3^- and NH_4^+ assimilation can be variable, ranging from -27 to 0‰ for either species, depending on the source and abundance of available N (Talbot, 2001). In typical cases, ^{14}N tends to accumulate preferentially in OM during assimilation, and thus it would be expected that in the simplest case, sedimentary OM would have a $\delta^{15}N$ value lower than that of the N in atmospheric deposition (~-1.4‰).

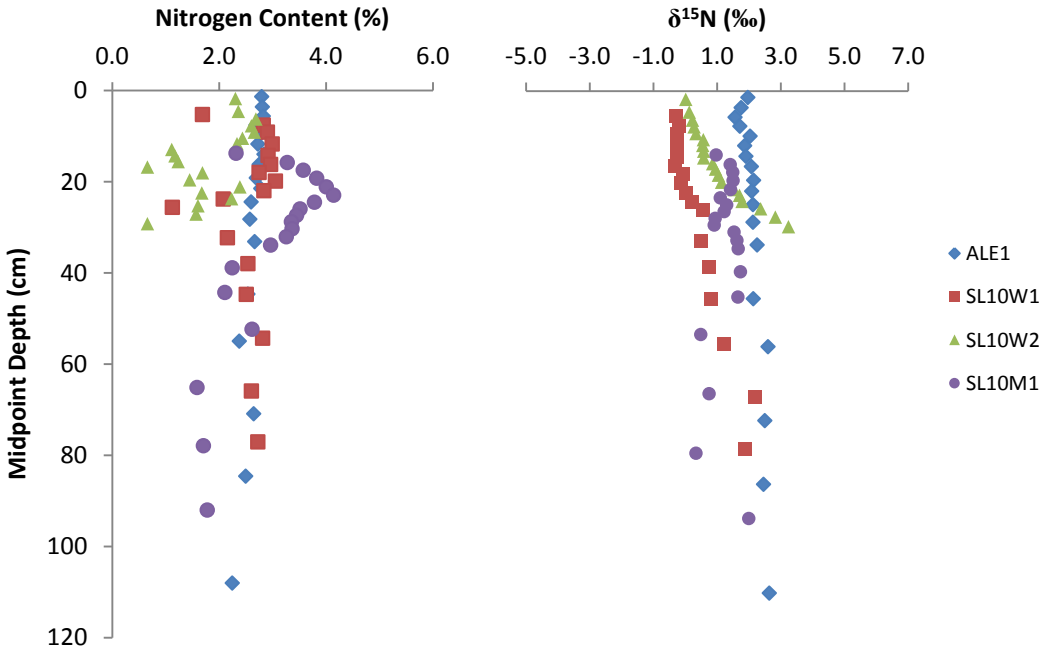

Figure 5.14: Nitrogen contents and $\delta^{15}N$ values by depth for ALE1, SL10W1, SL10W2 and SL10M1.

Because $\delta^{15}N$ values of total sediment N are higher than the -1.4‰ of NO_3^- and NH_4^+ in atmospheric precipitation measured by Proemse et al. (2013) rather than lower as would be predicted were assimilation by phytoplankton the only biochemical process occurring, it is likely that the OM has been microbially altered either during sedimentation or during diagenesis. Gu (2009), Leng et al. (2005)

and Meyers and Teranes (2001) note that the N cycle in lakes is complex, complicating interpretations of $\delta^{15}N$ values, and N-limited lakes which are not impacted by alkalinity and anoxia are most likely to preserve $\delta^{15}N$ values in autochthonous OM which represent the $\delta^{15}N$ of the source N (Jones et al., 2004). Some possible explanations for the discrepancy between $\delta^{15}N$ values which would result from the assimilation of NO_3^- and NH_4^+ in atmospheric deposition having values of -1.4‰ ($\delta^{15}N$ values <-1.4‰), and what is observed in sediment N ($\delta^{15}N$ values >-1‰) include:

- the $\delta^{15}N$ values of NO_3^- and NH_4^+ of atmospheric deposition measured by Proemse et al. (2013) from 2007-2011 are substantially different than the $\delta^{15}N$ values of NO_3^- and NH_4^+ of atmospheric deposition prior to 2007.
- N-fixation by cyanobacteria may be occurring, with an enrichment factor of ~-3 to +4, producing OM with a $\delta^{15}N$ value typically between -3 to +1‰ (Leng et al., 2005; Fogel and Cifuentes, 1993). The relative importance of N-fixation versus N-assimilation can vary from lake to lake (Talbot, 2001; Fogel and Cifuentes, 1993).
- remineralisation of N-containing OM may have modified the $\delta^{15}N$ value of the sediment OM. Typical isotope fractionation effects during remineralisation produce NH_4^+ with a $\delta^{15}N$ value which is ~1‰ lower than the $\delta^{15}N$ of the source OM, while ^{15}N progressively accumulates in the sediment, creating an apparent increase in the $\delta^{15}N$ value of the sediment (Lehmann et al., 2003).
- denitrification tends to remove lighter ^{14}N from the dissolved N-pool, which may escape as N_2 gas. Assimilation of the remaining ^{15}N-enriched NO_3^- where rates of denitrification are high may produce OM which is more enriched in ^{15}N relative to OM produced through assimilation of N from atmospheric deposition (Leng et al., 2005; Heaton, 1986).

An increase of $\delta^{15}N$ values with increasing depth occurs in both cores from SL10W. The increase in SL10W1 occurs between ~77 cm (bottom of the core) and ~16 cm depth (corresponding to an age of ~1860) and represents an increase of around 2.3‰, from ~-0.3 at the top to ~+2‰ at the bottom. In SL10W2, the increase of ~3.3‰ (~0 to ~3.3‰) occurs over the whole ~29cm length of the core. Examination of the plots of N contents and $\delta^{15}N$ values plotted versus age (Figure 5.15) eliminate the possibility that the upward decrease in $\delta^{15}N$ values is a result of impact from industrial emissions from the AOSR. The bulk of the changes in $\delta^{15}N$ values occur prior to ~1860, whereas impact from industrial emissions from the AOSR could only occur after ~1970, and would result in an increase in $\delta^{15}N$ values. Additionally, as ALE is closer to the AOSR and shows no signs of having been impacted by industrial emissions from the AOSR, it is unlikely that the more distant SL10W is significantly impacted.

It is clear from C:N ratio and Rock-Eval pyrolysis data that there has not been a significant change in the relative proportions of autochthonous and allochthonous contributions to sediment OM; the sediment OM in SL10W is derived dominantly from primary "in-lake" production of phytoplankton. A study on controls on $\delta^{15}N$ values of lake sediments by Gu et al. (1996) concluded that $\delta^{15}N$ values are controlled by primary productivity of non-N_2-fixing algae, in lakes where N is not limited, and by fixation of N_2 by cyanobacteria in more eutrophic lakes where DIN is limited by high levels of primary productivity. Further, Gu et al. (1996) reported a decrease in $\delta^{15}N$ values as a lake transitions from eutrophic to hypereutrophic. It is possible that SL10W underwent such a change prior to 1860, resulting in $\delta^{15}N$ values recorded in the sediment, as waters became increasingly N-limited. Rates of productivity appear to have stabilized post-1860, as evidenced by the fairly constant $\delta^{15}N$ values in the top portion of the core.

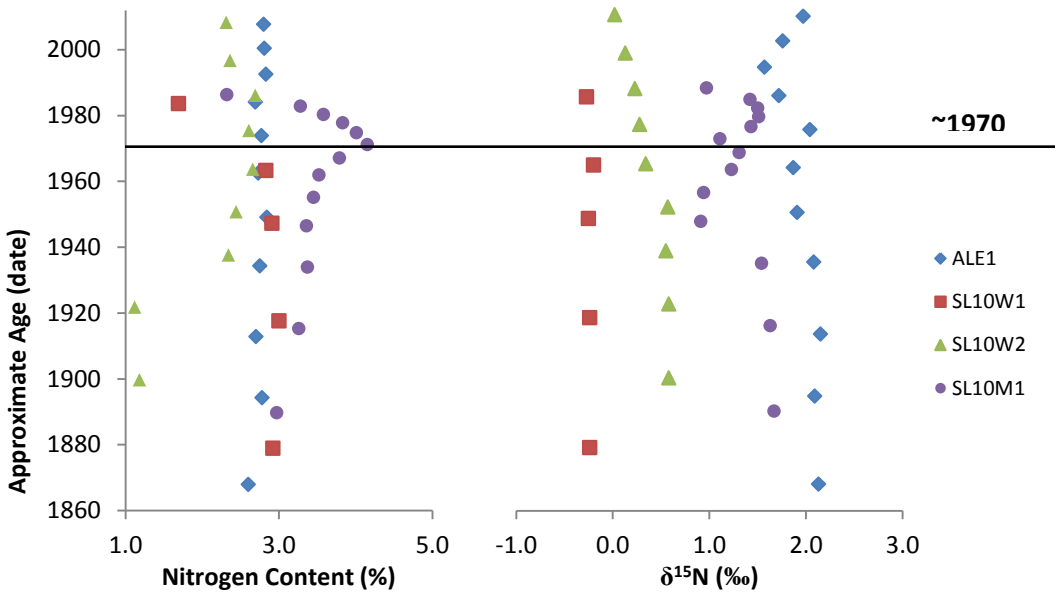

Figure 5.15: Nitrogen contents and $\delta^{15}N$ values of total N in sediments by approximate age for ALE1, SL10W1, SL10W2 and SL10M1.

A study by Holtgrieve et al. (2011) reported a widespread decrease of around 1 to 3‰ in $\delta^{15}N$ values in of remote boreal lake sediments deposited more recently than ~1900, postulated to be a result of the addition of reactive nitrogen (Nr) to the atmosphere by anthropogenic activities throughout the process of industrialization. Lakes ALE and SL10M do not show any trend toward more negative values of $\delta^{15}N$ in the most recently-deposited sediments, though this phenomenon could be considered another possible explanation for the decrease in $\delta^{15}N$ values in SL10W2. However when the ages of sediments are considered (Figure 5.15), the decrease in $\delta^{15}N$ from the bottom of SL10W1 to around 20cm depth does not fit the interpretation proposed by Holtgrieve et al. (2011), as the $\delta^{15}N$ value of sediments deposited more recently than 1900 is approximately constant, and the decrease in $\delta^{15}N$ values occurs in sediments deposited well before 1900. The lakes studied by Holtgrieve et al. (2011) were oligotrophic, in contrast with the lakes in this study whose sediments are largely comprised of OM indicative of a more eutrophic state. Gu and Schelske (2010) reported greater variability in $\delta^{15}N$ values

of particulate OM in eutrophic lakes, thus it is possible that the trend observed by Holtgrieve et al. (2011) is obscured in this study's lake sediments as a result of this study's lakes' more eutrophic state.

CHAPTER SIX: CONCLUSIONS AND FUTURE RESEARCH

6.1 Conclusions

Bulk analyses of sediments comprising 4 cores from 3 lakes, located approximately 97, 132 and 143km east of the Syncrude upgrader taken to be the "center" of anthropogenic activity in the AOSR, using organic petrology, Rock-Eval pyrolysis, C/N ratios and $\delta^{13}C$ values characterized these lake sediments as organic-rich, dominantly composed of OM with an autochthonous origin (in-lake production) with minor contributions from terrigenous sources such as pollen grains, and char produced as a result of frequent forest fires in the area. Lake ALE contained less fresh OM and was primarily derived from primary production by phytoplankton, while SL10W and SL10M contained OM which was very fresh, and partially derived from microbial mats, in addition to phytoplankton. The three lakes had sediments with rather different $\delta^{13}C$ values spanning around 20‰. Of these, SL10M had a $\delta^{13}C$ value which was anomalously high, relative to comparable lakes described in the literature. It can therefore be concluded that there is significant inter-lake variability in the geochemical and isotopic parameters of lake sediment deposits, and interpretations of sedimentary proxy data should not be made without an understanding of the baseline in the respective parameters. This is an important consideration for any future studies using lake sediments in the AOSR.

Dating of lake sediments using the ^{210}Pb method allowed to contrast geochemical and isotopic parameters in sediments deposited before and after 1970, which was taken to be the onset of major anthropogenic activity in the AOSR. While the sediments analyzed represented deposition both pre and post-industrialization, the subsampling of cores was such that only a few data points were available from the period after 1970. This compromised a rigorous statistical evaluation of whether there had been significant trends, indicative of impact from industrial emissions.

Distribution of total sedimentary N and S in the samples from ALE, SL10W and SL10M revealed no compelling evidence to suggest that significant impact from industrial emissions in the AOSR has affected of the lakes since 1970.

The investigated lakes are located more than 30 km from the Syncrude upgrader taken to be the midpoint source of industrial emissions in the AOSR, and thus are not subject to the elevated rates of deposition of S and N reported by Proemse and Mayer (2013). Thus it is likely that the lakes have not been impacted by significant regional industrial N and S emissions.

It is also possible that analyses of $\delta^{15}N$ and $\delta^{34}S$ values in total sedimentary N and S are unsuitable for tracing the fate of industrial emissions from the AOSR. A study using $\delta^{13}C$ values of PAH compounds by Jautzy et al. (2013) indicated that ALE has definitely been impacted by industrial emissions from the AOSR. Thus it may be that industrially-derived emissions of N and S from the AOSR have not yet been sufficient to "overwhelm" the $\delta^{15}N$ and $\delta^{34}S$ signatures and trends produced by natural processes, or that the $\delta^{15}N$ and $\delta^{34}S$ values of industrial emissions are not sufficiently different from background values to produce changes significant enough to be recorded in lake sediments. It appears that PAHs (Jautzy et al., 2013) and stable isotopes of oxygen in NO_3^- and SO_4^{2-} (Proemse et al., 2013; Proemse et al., 2012) are more sensitive proxies for gauging anthropogenic impact in ecosystems in the AOSR. It is also possible that a more detailed study of individual N and S-containing biomarkers and compounds may reveal more conclusive evidence of impact from industrial emissions derived from activity in the AOSR.

6.2 Opportunities for Future Research

Future studies of sediments from lakes in closer proximity to the AOSR where higher levels of atmospheric deposition of N and S does occur (Proemse et al., 2013; Proemse et al., 2012) may be useful

to establish whether N and S isotopes are viable tracers for industrial emissions in lake sediments. Additionally, stable isotope analyses of separate S fractions may offer additional insight into sulfur cycling in boreal lakes in the AOSR. Expansion of the work of Proemse and Mayer (2013) toward the isotopic characterization of industrial emissions will further facilitate the task of tracing their fate in the surrounding terrestrial and aquatic environments.

References

Agency for Toxic Substances & Disease Registry, 2011. Toxic Substances - Polycyclic Aromatic Hydrocarbons. Toxic Substances Portal. URL www.atsdr.cdc.gov/substances/toxsubstance.asp?toxid=25. Accessed August 2013.

Alberta Energy, 2013a. Facts and Statistics. About Oil Sands. URL http://www.energy.alberta.ca/OilSands/791.asp. Accessed August 2013.

Alberta Energy, 2013b. Recover. Oil Sands 101. URL http://www.energy.gov.ab.ca/OilSands/1719.asp. Accessed August 2013.

Alberta Energy, 2013c. Upgrading. Oil Sands 101. URL http://www.energy.alberta.ca/OilSands/791.asp. Accessed August 2013.

Alberta Environment, 2008. Alberta Air Emissions Trends and Projections. Edmonton, AB. 21 pp.

Alberta Government, 2010. Agroclimatic Atlas of Alberta: Map. Agroclimatic Atlas of Alberta. URL http://www1.agric.gov.ab.ca/$department/deptdocs.nsf/all/sag7019. Accessed August 2013.

Alberta Government, 2013a. About the Resource. Alberta's Oil Sands. URL http://www.oilsands.alberta.ca/resource.html. Accessed August 2013.

Alberta Government 2013b. Economic Benefits. Alberta's Oil Sands. URL http://www.oilsands.alberta.ca/economicinvestment.html. Accessed August 2013.

Alberta Government, 2013c. Air. Alberta's Oil Sands. URL http://www.oilsands.alberta.ca/air.html. Accessed August 2013.

Allen, E., 2004. Effects of nitrogen deposition on forests and peatlands: a literature review and discussion of the potential impacts of nitrogen deposition in the Alberta oil sands region. Fort McMurray, Alberta. 114 pp.

Appleby, P.G., 2001. Chronostratigraphic techniques in recent sediments, in: Last, W.M., Smol, J.P. (Eds.), Tracking Environmental Change Using Lake Sediments. Volume 1: Basin Analysis, Coring, and Chronological Techniques. Kluwer Academic Publishers, Dordrecht, The Netherlands, pp. 171–203.

Ariztegui, D., Farrimond, P., McKenzie, J.A., 1996. Compositional variations in sedimentary lacustrine organic matter and their implications for high Alpine Holocene environmental changes: Lake St. Moritz, Switzerland. Organic Geochemistry 24, 453–461.

ATDSR, 2011. Polyciclic Aromatic Hydrocarbons (PAHs). Toxic Substances Portal. URL http://www.atsdr.cdc.gov/substances/toxsubstance.asp?toxid=25. Accessed August 2013.

Bade, D.L., Carpenter, S.R., Cole, J.J., Hanson, P.C., Hesslein, R.H., 2004. Controls of $\delta^{13}C$ -DIC in lakes: geochemistry, lake metabolism and morphometry. Limnology and Oceanography 49, 1160–1172.

Battarbee, R.W., 1990. The causes of lake acidification with special reference to the role of acid deposition (and discussion). Philosophical Transactions of the Royal Society of London. Series B, Biological 327, 339–347.

Bernasconi, S.M., Barbieri, A., Simona, M., 1997. Carbon and nitrogen isotope variations in sedimenting organic matter in Lake Lugano. Limnology and Oceanography 42, 1755–1765.

Berner, R.A., 1984. Sedimentary pyrite formation : an update. Geochimica et Cosmochimica Acta 48, 605–615.

Böhm, C.O., Corkery, M.T., Creaser, R.A., 2004. Preliminary Sm-Nd isotope results from granitoid samples from the Nejanilini granulite domain , north of Seal River , Manitoba (NTS 64P). Manitoba Geological Survey Report of Activites 2004, pp 209-215.

Brenner, M., Whitmore, T.J., Curtis, J.H., Hodell, D.A., Schelske, C.L., 1999. Stable isotope ($\delta^{13}C$ and $\delta^{15}N$) signatures of sedimented organic matter as indicators of historic lake trophic state. Journal of Paleolimnology 22, 205–221.

Carignan, R., Lorrain, S., Lum, K., 1994. A 50-yr Record of Pollution by Nutrients , Trace Metals , and Organic Chemicals in the St . Lawrence River. Canadian Journal of Fisheries and Aquatic Sciences 51, 1088–1100.

Carrie, J., Sanei, H., Goodarzi, F., Stern, G., Wang, F., 2009. Characterization of organic matter in surface sediments of the Mackenzie River Basin, Canada. International Journal of Coal Geology 77, 416–423.

Carrie, J., Sanei, H., Stern, G., 2012. Standardisation of Rock–Eval pyrolysis for the analysis of recent sediments and soils. Organic Geochemistry 46, 38–53.

Carroll, J.J., Mather, A.E., 1992. The system carbon dioxide-water and the Krichevsky-Kasarnovsky equation. Journal of Solution Chemistry 21, 607–621.

CASA, 2003. Sulphur Dioxide Comparison. CASA Data Warehouse. URL http://www.casadata.org/comparison/sulphurdioxide.asp. Accessed August 2013.

CASA, 2013. Data Reports. CASA Data Warehouse. URL http://www.casadata.org/Reports/SelectCategory.asp. Accessed August 2013.

Cheung, K., Klassen, P., Mayer, B., Goodarzi, F., Aravena, R., 2010. Major ion and isotope geochemistry of fluids and gases from coalbed methane and shallow groundwater wells in Alberta, Canada. Applied Geochemistry 25, 1307–1329.

Cook, R.B., Kelly, C.A., 1992. Sulphur cycling and fluxes in temperate dimictic lakes. SCOPE 48 - Sulphur Cycling on the Continents. URL http://www.scopenvironment.org/downloadpubs/scope48/chapter07.html. Accessed August 2013.

Dale, J., 2006a. Glaciation. The Encyclopedia of Saskatchewan. URL http://esask.uregina.ca/entry/glaciation.html. Accessed August 2013.

Dale, J., 2006b. Proglacial lakes. The Encyclopedia of Saskatchewan. URL http://esask.uregina.ca/entry/proglacial_lakes.html. Accessed August 2013.

David, M.B., Mitchell, M.J., 1985. Sulfur constituents and cycling in waters, seston, and sediments of an oligotrophic lake. Limnology and Oceanography 30, 1196–1207.

Dawson, T.E., Mambelli, S., Plamboeck, A.H., Templer, P.H., Tu, K.P., 2002. Stable Isotopes in Plant Ecology. Annual Review of Ecology and Systematics 33, 507–559.

Dean, W.E., 1999. The carbon cycle and biogeochemical dynamics in lake sediments. Journal of Paleolimnology 21, 375–393.

Disnar, J.R., Guillet, B., Keravis, D., Di-Giovanni, C., Sebag, D., 2003. Soil organic matter (SOM) characterization by Rock-Eval pyrolysis: scope and limitations. Organic Geochemistry 34, 327–343.

Donahue, W.F., Allen, E.W., Schindler, D.W., 2006. Impacts of Coal-Fired Power Plants on Trace Metals and Polycyclic Aromatic Hydrocarbons (PAHs) in Lake Sediments in Central Alberta, Canada. Journal of Paleolimnology 35, 111–128.

EHRC, 2005. Name That Pollen or Spore: Bisaccate Grains. Name That Pollen or Spore. URL http://origins.swau.edu/fossil/pollen/bisaccate/bisaccate.html. Accessed August 2013.

Einsiedl, F., Mayer, B., Schäfer, T., 2008. Evidence for incorporation of H_2S in groundwater fulvic acids from stable isotope ratios and sulfur K-edge X-ray absorption near edge structure spectroscopy. Environmental Science & Technology 42, 2439–44.

Environment Canada, 2013. Canadian Climate Normals 1971-2000 Station Data. URL http://climate.weather.gc.ca/climate_normals/results_e.html?stnID=2519&autofwd=1. Accessed 2013.

ERCB, 2013. ST98-2013: Alberta's Energy Reserves 2012 and Supply/Demand Outlook 2013-2022. Calgary, Alberta. 282 pp.

Espitalie, J., Deroo, G., Marquis, F., 1985. La pyrolyse Rock-Eval et ses applications, premiere, deuxieme et troisieme parties. Revue De L'Institut Francais Du Petrole 40 and 41, 563–579, 755–784, 73–89.

Evans, R.D., Rigler, F.H., 1980. Measurement of whole lake sediment accumulation and phosphorus retention using lead-210 dating. Canadian Journal of Fisheries and Aquatic Sciences 37, 817–822.

Farquhar, G.D., Ehleringer, J.R., Hubick, K.T., 1989. Carbon isotope discrimination and photosynthesis. Annual Reviews Plant Physiology Plant Molecular Biology 40, 503–537.

Fenton, M.M., Schreiner, B.T., Nielsen, E., Pawlowicz, J.G., 1994. Quaternary Geology of the Western Plains, in: Geological Atlas of the Western Canada Sedimentary Basin, G.D. Mossop and I. Shetsen (comp.), Canadian Society of Petroleum Geologists and Alberta Research Council, URL: http://www.ags.gov.ab.ca/publications/wcsb_atlas/a_ch26/ch_26.html. Accessed August 2013.

Flett, R., 2013. Understanding Lead-210. Flett Research. URL http://www.flettresearch.ca/UnderstandingPb210.html

Flynn, W.W., 1968. The determination of low levels of polonium-210 in environmental materials. Analytica Chimica Acta 43, 221–227.

Fogel, M.L., Cifuentes, L.A., 1993. Isotope fractionation during primary production, in: Engel, M.H., Macko, S.A. (Eds.), Organic Geochemistry: Principles and Applications. Springer, New York, pp. 73–89.

Frey, D.G., 1988. What is paleolimnology? Journal of Paleolimnology 1, 5–8.

Galimov, E.M., 1980. C13/C12 in kerogen, in: Durand, B. (Ed.), Kerogen--Insoluble Organic Matter from Sedimentary Rocks. Editions Technip, Paris, pp. 271–299.

Ghashghaie, J., Badeck, F.-W., Lanigan, G., Nogu, S., Cornic, G., Griffiths, H., Del, E., 2003. Carbon isotope fractionation during dark respiration and photorespiration in C3 plants. Phytochemistry Reviews 2, 145–161.

Giesemann, A., Jäger, H.-J., Norman, A.L., Krouse, H.R., Brand, W.A., 1994. On-Line Sulfur-Isotope Determination Using an Elemental Analyzer Coupled to a Mass Spectrometer. Analytical Chemistry 66, 2816–2819.

Goossens, H., Dliren, R.R., DeLeeuw, J.W., Schenck, P.A., 1989. Lipids and their mode of occurrence in bacteria and sediments--ll . Lipids in the sediment of a stratified, freshwater lake. Organic Geochemistry 14, 27–41.

Government of Saskatchewan, 2012. Historical Fire Activity. About Environment. URL http://www.environment.gov.sk.ca/Default.aspx?DN=e3b65a62-d11c-4a21-bd82-5247414d0f7d. Accessed August 2013.

Gu, B., 2009. Variations and controls of nitrogen stable isotopes in particulate organic matter of lakes. Oecologia 160, 421–31.

Gu, B., Schelske, C.L., Brenner, M., 1996. Relationship between sediment and plankton isotope ratios ($\delta^{13}C$ and $\delta^{15}N$) and primary productivity in Florida lakes. Canadian Journal of Fisheries and Aquatic Sciences 53, 875–883.

Habicht, K.S., Canfield, D.E., 1996. Sulphur isotope fractionation in modern microbial mats and the evolution of the sulphur cycle. Nature 382, 342–343.

Harrison, A.G., Thode, H.G., 1958. Mechanism of the bacterial reduction of sulphate from isotope fractionation studies. Transactions of the Faraday Society 54, 84–92.

Harrison, R.M., 1990. Chemistry of the Troposphere, in: Harrison, R.M. (Ed.), Pollution: Causes, Effects and Control. CRC Press, Boca Raton, FL, pp. 157–180.

Hassan, K.M., Swinehart, J.B., Spalding, R.F., 1997. Evidence for Holocene environmental change from C / N ratios , and $\delta^{13}C$ and $\delta^{15}N$ values in Swan Lake sediments, western Sand Hills, Nebraska. Journal of Paleolimnology 18, 121–130.

Hayes, B.J.R., Christopher, J.E., Rosenthal, L., Los, G., McKercher, B., Minken, D., Tremblay, Y.M., Fennell, J., Smith, D.G., 1994. Cretaceous Mannville Group of the Western Canada Sedimentary Basin, in: Geological Atlas of the Western Canada Sedimentary Basin, G.D. Mossop and I. Shetsen (comp.), Canadian Society of Petroleum Geologists and Alberta Research Council, URL: http://www.ags.gov.ab.ca/publications/wcsb_atlas/a_ch19/ch_19.html. Accessed August 2013.

Heaton, T.H.E., 1986. Isotopic studies of nitrogen pollution in the hydrosphere and atmosphere: a review. Chemical Geology 59, 87–102.

Hodell, D.A., Schelske, C.L., 1991. Production , sedimentation , and isotopic composition of organic matter in Lake Ontario. Limnology and Oceanography 43, 200–214.

Hoefs, J., 2009. Isotope fractionation processes of selected elements, in: Stable Isotope Geochemistry. Springer-Verlag, Berlin, pp. 35–92.

Holdren Jr., G.R., Brunelle, T.M., Matisoff, G., Wahlen, M., 1984. Timing the increase in atmospheric sulfur deposition in the Adirondack mountains. Nature 311, 245–248.

Holmer, M., Storkholm, P., 2001. Sulphate reduction and sulphur cycling in lake sediments: a review. Freshwater Biology 46, 431–451.

Holtgrieve, G.W., Schindler, D.E., Hobbs, W.O., Leavitt, P.R., Ward, E.J., Bunting, L., Chen, G., Finney, B.P., Gregory-Eaves, I., Holmgren, S., Lisac, M.J., Lisi, P.J., Nydick, K., Rogers, L.A., Saros, J.E., Selbie, D.T., Shapley, M.D., Walsh, P.B., Wolfe, A.P., 2011. A coherent signature of anthropogenic nitrogen deposition to remote watersheds of the northern hemisphere. Science 334, 1545–1548.

Hurley, J.P., Armstrong, D.E., 1991. Pigment preservation in lake sediments: a comparison of sedimentary environments in Trout Lake, Wisconsin. Canadian Journal of Fisheries and Aquatic Sciences 48, 472-486.

Hurley, J.P., Armstrong, D.E., 1990. Fluxes and transformations of aquatic pigments in Lake Mendota, Wisconsin. Limnology and Oceanography 35, 384-398.

Ingvorsen, K., Zeikus, J.G., Brock, T.D., 1981. Dynamics of bacterial sulfate reduction in a eutrophic lake. Applied Environmental Microbiology 42, 1029–1036.

Jacob, D.J., 1999. Geochemical cycles, in: Introduction to Atmospheric Chemistry. Princeton University Press, Princeton, NJ, pp. 83–104.

Jaques, D.R., Legge, A.H., 2013. Ecological analogues for biomonitoring industrial sulfur emissions in the Athabasca oil sands region, Alberta, Canada, in: Percy, K.E., Krupa, S.V. (Eds.), Alberta Oil Sands: Energy, Industry and the Environment. Elsevier Ltd., Kidlington, Oxford, pp. 219–242.

Jautzy, J., Ahad, J.M.E., Gobeil, C., Savard, M.M., 2013. Century-long source apportionment of PAHs in Athabasca oil sands region lakes using diagnostic ratios and compound-specific carbon isotope signatures. Environmental Science & Technology 47, 6155–6163.

Jones, R.I., King, L., Dent, M., Maberly, C., Gibson, C.E., 2004. Nitrogen stable isotope ratios in surface sediments, epilithon and macrophytes from upland lakes with differing nutrient status. Freshwater Biology 49, 382-391.

Kaplan, I.R., Rittenberg, S.C., 1964. Microbial fractionation of sulphur isotopes. Journal of General Microbiology 34, 195–212.

Keeley, J.E., Sandquist, D.R., 1992. Carbon: freshwater plants. Plant, Cell and Environment 15, 1021–1035.

Kelly, E.N., Short, J.W., Schindler, D.W., Hodson, P. V., Ma, M., Kwan, A.K., Fortin, B.L., 2009. Oil sands development contributes polycyclic aromatic compounds to the Athabasca River and its tributaries. Proceedings of the National Academy of Sciences of the United States of America 106, 22346–22351.

Kelly, T.J., Stedman, D.H., Ritter, J.A., Harvey, R.B., 1980. Measurements of oxides of nitrogen and nitric acid in clean air. Journal of Geophysical Research 85, 7417–7425.

Kemp, A.L.., Thode, H.G., 1968. The mechanism of bacterial reduction of sulphate and of sulphite from isotope fractionation studies. Geochimica et Cosmochimica Acta 32, 297–331.

Kendall, C., 1998. Tracing nitrogen sources and cycling in catchments, in: Kendall, C., McDonnell, J.J. (Eds.), Isotope Tracers in Catchment Hydrology. Elsevier Science B.V., Amsterdam, pp. 519–576.

Kreitler, C.W., 1975. Determining the sources of nitrate in groundwater by nitrogen isotope studies. Austin, Texas. : Report of Investments #83, University of Texas at Austin, Bureau of Economic Geology, 57 pp

Kreitler, C.W., 1979. Nitrogen-isotope ratio studies of soils and groundwater nitrate from alluvial fan aquifers in Texas. Journal of Hydrology 42, 142–170.

Krishnamurthy, R.V., Bhattacharya, S., Kusumgar, S., 1986. Palaeoclimatic changes deduced from $^{13}C/^{12}C$ and C/N ratios of Karewa lake sediments, India. Nature 323, 150–152.

Krouse, H.R., 1980. Sulphur isotopes in our environment, in: Fritz, P. and Fontes, J. (Eds.), Isotope Geochemistry, Volume 1. The Terrestrial Environments. Elsevier, Amsterdam, pp. 435-471.

Krouse, H.R., Coplen, T.B., 1997. Reporting of relative sulfur isotope-ratio data. Pure and Applied Chemistry 69, 293–295.

Kurek, J., Kirk, J.L., Muir, D.C.G., Wang, X., Evans, M.S., Smol, J.P., 2013. Legacy of a half century of Athabasca oil sands development recorded by lake ecosystems. Proceedings of the National Academy of Sciences of the United States of America 110, 1761–1766.

Lafargue, E., Marquis, F., Pillot, D., 1998. Rock-Eval 6 applications in hydrocarbon exploration, production, and soil contamination studies. Revue De L'Institut Francais Du Petrole 53, 421–437.

Landis, M.S., Pancras, J.P., Graney, J.R., Stevens, R.K., Percy, K.E., Krupa, S.V., 2013. Receptor modeling of epiphytic lichens to elucidate the sources and spatial distribution of inorganic air pollution in the Athabasca oil sands region, in: Percy, K.E., Krupa, S.V. (Eds.), Alberta Oil Sands: Energy, Industry and the Environment. Elsevier Ltd., Kidlington, Oxford, pp. 427–468.

Lane, C.S., Horn, S.P., Taylor, Z.P., Mora, C.I., 2009. Assessing the scale of prehistoric human impact in the neotropics using stable carbon isotope analyses of lake sediments: a test case from Costa Rica. Latin American Antiquity 20, 120–133.

Laws, E.A., Popp, B.N., Bidigare, R.R., Kennicutt, M.C., Macko, S.A., 1995. Dependence of phytoplankton carbon isotopic composition on growth rate and $[CO_2]$aq : theoretical considerations and experimental results. Geochimica et Cosmochimica Acta 59, 1131–1138.

Leavitt, P.R., Carpenter, S.R., 1990. Aphotic pigment degradation in the hypolimnion: implications for sedimentation studies and paleolimnology. Limnology and Oceanography 35, 520-535.

Lehmann, M.F., Reichert, P., Bernasconi, S.M., Barbieri, A., McKenzie, J. a., 2003. Modelling nitrogen and oxygen isotope fractionation during denitrification in a lacustrine redox-transition zone. Geochimica et Cosmochimica Acta 67, 2529–2542.

Leng, M.J., Lamb, A.L., Heaton, T.H.E., Marshall, J.D., Wolfe, B.B., Jones, M.D., Holmes, J.A., Arrowsmith, C., 2005. Isotopes in lake sediments, in: Leng, M.J. (Ed.), Isotopes in Palaeoenvironmental Research. Springer, Dordrecht, The Netherlands, pp. 147–184.

Leng, M.J., Marshall, J.D., 2004. Palaeoclimate interpretation of stable isotope data from lake sediment archives. Quaternary Science Reviews 23, 811–831.

Lin, G., Ehleringer, J.R., 1997. Carbon isotopic fractionation does not occur during dark respiration in C3 and C4 plants. Plant Physiology 114, 391–394.

Macdonald, R., 2006. Geology. The Encyclopedia of Saskatchewan. URL http://esask.uregina.ca/entry/geology.html. Accessed August 2013.

Macko, S.A., Engel, M.H., Parker, P.L., 1993. Early diagenesis of organic matter in sediments: assessment of mechanisms and preservation by the use of isotopic molecular approaches, in: Engel, M.H., Macko, S.A. (Eds.), Organic Geochemistry: Principles and Applications. Springer, New York, pp. 211–224.

Mariotti, A., Germon, J.C., Hubert, P., Kaiser, P., Letolle, R., Tardieux, A., Tardieux, P., 1981. Experimental determination of nitrogen kinetic isotope fractionation: some principles; illustration for the denitrification and nitrification processes. Plant and Soil 62, 413–430.

Mayer, B., Alpay, S., Gould, W.D., Lortie, L., Rosa, F., 2007. The onset of anthropogenic activity recorded in lake sediments in the vicinity of the Horne smelter in Quebec, Canada: sulfur isotope evidence. Applied Geochemistry 22, 397–414.

Meyers, P.A., 1994. Preservation of elemental and isotopic source identification of sedimentary organic matter. Chemical Geology 114, 289–302.

Meyers, P.A., 1997. Organic geochemical proxies of paleoceanographic, paleolimnologic, and paleoclimatic processes. Organic Geochemistry 27, 213–250.

Meyers, P.A., Ishiwatari, R., 1993. Lacustrine organic geochemistry--an overview of indicators of organic matter sources and diagenesis in lake sediments. Organic Geochemistry 20, 867–900.

Meyers, P.A., Lallier-Vergès, E., 1999. Lacustrine sedimentary organic matter records of Late Quaternary paleoclimates. Journal of Paleolimnology 21, 345–372.

Meyers, P.A., Teranes, J.L., 2001. Sediment Organic Matter, in: Last, W.M., Smol, J.P. (Eds.), Tracking Environmental Change Using Lake Sediments. Volume 2: Physical and Geochemical Methods. Kluwer Academic Publishers, Dordrecht, The Netherlands, pp. 239–269.

Mitchell, M.J., David, M.B., Harrison, R.B., 1992. Sulphur dynamics of forest ecosystems. SCOPE 48 - Sulphur Cycling on the Continents. URL http://www.scopenvironment.org/downloadpubs/scope48/chapter09.html. Accessed August 2013.

Mook, W.G., Bommerson, J.C., Staverman, W.H., 1974. Carbon isotope fractionation between dissolved bicarbonate and gaseous carbon dioxide. Earth and Planetary Science Letters 22, 169–176.

Mossop, G.D., Shetsen, I., 1994. Introduction to the Geological Atlas of the Western Canada Sedimentary Basin, in: Geological Atlas of the Western Canada Sedimentary Basin, G.D. Mossop and I. Shetsen (comp.), Canadian Society of Petroleum Geologists and Alberta Research Council, URL: http://www.ags.gov.ab.ca/publications/wcsb_atlas/a_ch01/ch_01.html. Accessed August 2013.

Nagpal, N.K., 1993. Occurrence in the Environment. Ambient Water Quality Criteria For Polycyclic Aromatic Hydrocarbons (PAHs). URL http://www.env.gov.bc.ca/wat/wq/BCguidelines/pahs/pahs-03.htm#P890_30513. Accessed August 2013.

Nakai, N., Jensen, M.L., 1964. The kinetic isotope effect in the bacterial reduction and oxidation of sulfur. Geochimica et Cosmochimica Acta 28, 1893–1912.

Nielsen, H., 1974. Isotopic composition of the major contributors to atmospheric sulfur. Tellus 26.

Nissenbaum, A., 1972. The organic geochemistry of marine and terrestrial humic substances: implications of carbon and hydrogen isotope studies, in: Tissot, B., Bienner, F. (Eds.), Advances in Organic Geochemistry. Editions Technip, Paris, pp. 39–52.

Nissenbaum, A., Presley, B.J., Kaplan, I.R., 1972. Early diagenesis in a reducing fjord, Saanich Inlet, British Columbia-- I. Cemical and isotopic changes in major components of interstitial water. Geochimica et Cosmochimica Acta 36, 1007–1027.

Nriagu, J.O., Coker, R.D., 1983. Sulphur in sediments chronicles past changes in lake acidification. Nature 303, 692–694.

Nriagu, J.O., Soon, Y.K., 1985. Distribution and isotopic composition of sulfur in lake sediments of northern Ontario. Geochimica et Cosmochimica Acta 49, 823–834.

O'Leary, M.H., 1988. Carbon isotopes in photosynthesis. Bioscience 38, 328–336.

Outridge, P.M., Sanei, H., 2010. Does organic matter degradation affect the reconstruction of pre-industrial atmospheric mercury deposition rates from peat cores? — A test of the hypothesis using a permafrost peat deposit in northern Canada. International Journal of Coal Geology 83, 73–81.

Owens, N.J.P., 1987. Natural variations in ^{15}N in the marine environment. Advances in Marine Biology 24, 389–451.

Pawlowicz, J.G., Fenton, M.M., 1995. Drift thickness of Alberta, Alberta Geological Survey. URL http://www.ags.gov.ab.ca/publications/abstracts/MAP_227.html. Accessed August 2013.

Peterson, B.J., Fry, B., 1987. Stable isotopes in ecosystem studies. Annual Review of Ecology and Systematics 18, 293–320.

Proemse, B.C., Mayer, B., 2013. Tracing industrial nitrogen and sulfur emissions in the Athabasca oil sands region using stable isotopes, in: Percy, K.E., Krupa, S.V. (Eds.), Alberta Oil Sands: Energy, Industry and the Environment. Elsevier Ltd., Kidlington, Oxford, pp. 243–266.

Proemse, B.C., Mayer, B., Fenn, M.E., 2012. Tracing industrial sulfur contributions to atmospheric sulfate deposition in the Athabasca oil sands region, Alberta, Canada. Applied Geochemistry 27, 2425–2434.

Proemse, B.C., Mayer, B., Fenn, M.E., Ross, C.S., 2013. A multi-isotope approach for estimating industrial contributions to atmospheric nitrogen deposition in the Athabasca oil sands region in Alberta, Canada. Environmental Pollution 182, 80-91.

Reyes, J., Goodarzi, F., Sanei, H., Stasiuk, L.D., Duncan, W., 2006. Petrographic and geochemical characteristics of organic matter associated with stream sediments in Trail area British Columbia, Canada. International Journal of Coal Geology 65, 146–157.

Romanek, C.S., Grossman, E.L., Morse, J.W., 1992. Carbon isotopic fractionation in synthetic aragonite and calcite: Effects of temperature and precipitation rate. Geochimica et Cosmochimica Acta 56, 419–430.

Rudd, J.W.M., Kelly, C.A., Furutani, A., 1986. The role of sulfate reduction in long term accumulation of organic and inorganic sulfur in lake sediments. Limnology and Oceanography 31, 1281–1291.

Runesson, U.T., 2011. Boreal forests of the world. borealforest.org. URL http://www.borealforest.org/index.php?category=world_boreal_forest&page=overview. Accessed August 2013.

Sanei, H., Goodarzi, F., 2006. Relationship between organic matter and mercury in recent lake sediment: The physical–geochemical aspects. Applied Geochemistry 21, 1900–1912.

Sanei, H., Goodarzi, F., Snowdon, L.R., Stasiuk, L.D., Van Der Flier-Keller, E., 2000. Characterizing the recent sediments from Pigeon Lake, Alberta as related to anthropogenic and natural fluxes. Environmental Geosciences 7, 177–189.

Sanei, H., Stasiuk, L.D., Goodarzi, F., 2005. Petrological changes occurring in organic matter from recent lacustrine sediments during thermal alteration by Rock-Eval pyrolysis. Organic Geochemistry 36, 1190–1203.

Sarazin, G., Michard, G., Al Gharib, I., Bernat, M., 1992. Sedimentation rate and early diagenesis of particulate organic nitrogen and carbon in Aydat Lake (Puy de Dome, France). Chemical Geology 98, 307–316.

Schidlowski, M., Matzigkeit, U., Krumbein, W.E., 1984. Superheavy organic carbon from hypersaline microbial mats. Naturwissenschaften 71, 303–308.

Schnurrenberger, D., Russell, J., Kelts, K., 2003. Classification of lacustrine sediments based on sedimentary components. Journal of Paleolimnology 29, 141–154.

Schwalb, A., Burns, S.J., Kelts, K., 1999. Holocene environments from stable isotope stratigraphy of ostracods and authigenic carbonate in Chilean Altiplano lakes. Palaeogeography, Palaeoclimatology, Palaeoecology 148, 153–168.

Sebag, D., Disnar, J.R., Guillet, B., Di Giovanni, C., Verrecchia, E.P., Durand, A., 2006. Monitoring organic matter dynamics in soil profiles by “Rock-Eval pyrolysis”: bulk characterization and quantification of degradation. European Journal of Soil Science 57, 344–355.

Siegfriedt, R.K., Wiberley, J.S., Moore, R.W., 1951. Determination of sulfur after combustion in a small oxygen bomb. Analytical Chemistry 23, 1008–1011.

Smith, V.H., Tilman, G.D., Nekola, J.C., 1999. Eutrophication: impacts of excess nutrient inputs on freshwater, marine, and terrestrial ecosystems. Environmental Pollution 100, 179–196.

Stewart, R.E., Leighton, H.G., Marsh, P., Moore, G.W.K., Ritchie, H., Rouse, W.R., Soulis, E.D., Strong, G.S., Crawford, R.W., Kochtubajda, B., 1998. The Mackenzie GEWEX study: the water and energy cycles of a major North American river basin. Bulletin of the American Meteorological Society 79, 2665–2683.

Suncor, 2013. About Us. URL http://www.suncor.com/en/about/164.aspx. Accessed August 2013.

Takahashi, K., Yoshioka, T., Wada, E., Sakamoto, M., 1990. Temporal variations in carbon isotope ratio of phytoplankton in a eutrophic lake. Journal of Plankton Research 12, 799–808.

Talbot, M.R., 2001. Nitrogen isotopes in palaeolimnology, in: Last, W.M., Smol, J.P. (Eds.), Tracking Environmental Change Using Lake Sediments. Volume 2: Physical and Geochemical Methods. Kluwer Academic Publishers, Dordrecht, The Netherlands, pp. 401–439.

Talbot, M.R., Livingstone, D.A., 1989. Hydrogen index and carbon isotopes of lacustrine organic matter as lake level indicators. Palaeogeography, Palaeoclimatology, Palaeoecology 70, 121–137.

Treissman, D., Guigard, S., Kindzierski, W., Schulz, J., Guigard, E., 2003. Sulphur dioxide: environmental effects, fate and behaviour. Science and Standards Branch, Alberta Environment, Edmonton, AB. 61 pp.

Turner, J. V., 1982. Kinetic fractionation of carbon-13 during calcium carbonate precipitation. Geochimica et Cosmochimica Acta 46, 1183–1191.

United States Environmental Protection Agency, 2008. Polycyclic Aromatic Hydrocarbons (PAHs). URL http://www.epa.gov/osw/hazard/wastemin/minimize/factshts/pahs.pdf. Accessed August 2013.

Van der Meer, M.T.J., Schouten, S., de Leeuw, J.W., Ward, D.M., 2000. Autotrophy of green non-sulphur bacteria in hot spring microbial mats: biological explanations for isotopically heavy organic carbon in the geological record. Environmental Microbiology 2, 428–435.

Van der Meer, M.T.J., Schouten, S., Sinninghe Damste, J.S., de Leeuw, J.W., Ward, D.M., 2003. Compound-specific isotopic fractionation patterns suggest different carbon metabolisms among Chloroflexus-like bacteria in hot-spring microbial mats. Applied and Environmental Microbiology 69, 6000–6006.

Van Metre, P.C., Mahler, B.J., 2005. Trends in hydrophobic organic contaminants in urban and reference lake sediments across the United States , 1970 - 2001. Environmental Science & Technology 39, 5567–5574.

Vitousek, P.M., Aber, J.D., Howarth, R.W., Likens, G.E., Matson, P.A., Schindler, D.W., Schlesinger, W.H., Tilman, D.G., 1997. Human alteration of the global nitrogen cycle: sources and consequences. Ecological Applications 7, 737–750.

Whiticar, M.J., 1999. Carbon and hydrogen isotope systematics of bacterial formation and oxidation of methane. Chemical Geology 161, 291–314.

Yamamuro, M., Kayanne, H., 1995. Rapid direct determination of organic carbon and nitrogen in carbonate-bearing sediments with a Yanaco MT-5 CHN analyzer. Limnology and Oceanography 40, 1001–1005.

Zhang, R., Lei, W., Tie, X., Hess, P., 2004. Industrial emissions cause extreme urban ozone diurnal variability. Proceedings of the National Academy of Sciences of the United States of America 101, 6346–6350.